QCD Correlation Functions of Light Quarkonium and Strangeonium Hybrids

A Thesis Submitted to the

College of Graduate Studies and Research

in Partial Fulfillment of the Requirements

for the degree of Master of Science

in the Department of Physics and Engineering Physics

University of Saskatchewan

Saskatoon

By

Ryan Berg

Permission to Use

In presenting this thesis in partial fulfilment of the requirements for a Postgraduate degree from the University of Saskatchewan, I agree that the Libraries of this University may make it freely available for inspection. I further agree that permission for copying of this thesis in any manner, in whole or in part, for scholarly purposes may be granted by the professor or professors who supervised my thesis work or, in their absence, by the Head of the Department or the Dean of the College in which my thesis work was done. It is understood that any copying or publication or use of this thesis or parts thereof for financial gain shall not be allowed without my written permission. It is also understood that due recognition shall be given to me and to the University of Saskatchewan in any scholarly use which may be made of any material in my thesis.

Requests for permission to copy or to make other use of material in this thesis in whole or part should be addressed to:

Head of the Department of Physics and Engineering Physircs
116 Science Place
University of Saskatchewan
Saskatoon, Saskatchewan
Canada
S7N 5E2

Abstract

The correlation function is the critical ingredient for Quantum Chromodynamics (QCD) sum-rule methods that are used to predict hadronic properties. Thus, in order to perform a sum-rule analysis of hybrids, we need to compute a correlation function involving an operator that probes hybrid states composed of a quark-antiquark pair with a gluonic excitation. Using particular combinations of quark and gluon fields and Dirac matrices, we construct currents that probe hybrid states with various J^{PC} quantum numbers. We compute the correlation function to order g_s^3 in QCD, obtaining both perturbative and condensate contributions.

The focus here is on light quarkonium and strangeonium hybrids, which involve quark masses small compared to the external momentum scale ($m_q^2 \ll Q^2$). While for light quarkonium the calculations are performed in the massless limit, for strangeonium we include a strange quark mass correction to the perturbative result. While the details of the calculations outlined throughout this thesis are outlined for $J^{PC} = 0^{+-}$ and 1^{--} due to interest in the exotic quantum numbers 0^{+-}, ultimately the correlation function is computed for all J^{PC} values with $J = 0, 1$. Comparison with existing results for a subset of these J^{PC} quantum numbers provides a validation of our calculations.

Acknowledgements

I'd like to thank both Dr. Tom Steele and Dr. Derek Harnett, for if it weren't for their help, I certainly wouldn't be where I am today, and I'd be a whole lot worse off for it. I feel that the support that I've received through my work here has been well above what was necessary, and for that I am very grateful. I am truly appreciative of not only the opportunity, but the flexibility of making it work.

I'd also like to thank my family for their support and their putting up with me, when I have been both far and close to home. I wouldn't be here without you.

I would also like to thank my friends that have kept me company through this experience. In particular, I'd like to thank Dr. Robin Kleiv helping to make sure that I was taking care of myself, going beyond what was necessary to make sure I knew I wasn't alone far away from home, and showing me the ropes; and Charlie Watson, for making sure that "I think I understand" isn't good enough, and there are always more interesting questions just behind the corner.

To everyone that challenges me to do better.

Contents

List of Tables

List of Figures

List of Abbreviations

QFT	Quantum Field Theory
QCD	Quantum Chromodynamics
VEV	Vacuum Expectation Value
OPE	Operator Product Expansion
LO	Leading Order
NLO	Next-To-Leading Order
RHS	Right Hand Side
LOF	List of Figures
LOT	List of Tables

Chapter 1

Introduction

1.1 Particle Physics and Hybrids

The quark model has been widely successful in classifying the observed hadronic matter of the universe. The quarks, consisting of the up, down, strange, charm, bottom and top quark flavours, listed in order of increasing mass, are a family of spin $\frac{1}{2}$ fermions, which are the constituents of the baryonic and mesonic (hadronic) matter we observe. The quarks all have fractional electric charges; the up, charm and top having charge of $Q = +\frac{2}{3}e$, while the down, strange and bottom quarks have charge $Q = -\frac{1}{3}e$. Combinations of these, in bound systems, can form the integer charges that we see in nature. The lightest three quarks, the up, down and strange, due to their similar light mass, form an approximate flavour symmetry group, which has been very successful in classifying the lightest baryons and mesons.

While the constituent quark model [2, 3] is successful in classifying mesons and baryons, it does not describe the underlying dynamics of the quarks involved. The theory that describes the quark dynamics is *Quantum Chromodynamics (QCD)*. Originally introduced in order to obtain the correct statistics for a bound system of fermions, the concept of a *colour charge* was introduced as a property of all quarks [4]. Thus, QCD is separate from the quark model, and the two together form our modern theory of hadrons. From experiment, the number of unique colours can be inferred to be three [5]; however, this net colour charge is never observed in nature, and so all bound systems of quarks, known as hadrons, must be colour neutral, or *colourless* (ie. colour singlets).

Baryons are described within the quark model as bound systems of three quarks. While the most common hadrons, protons and neutrons, are constructed from collections of up and down quarks, bound systems involving heavier quarks are also well described by the quark

model. As baryonic systems are composed of three spin $\frac{1}{2}$ constituent particles, the baryons are fermions. Throughout this thesis, however, our focus will be on mesons.

In the constituent quark model, mesons are described by a bound quark-antiquark pair. As quarks are spin-$\frac{1}{2}$ fermions, a bound system of two quarks has either spin-0 or spin-1. The total angular momentum of a bound system is then described by the vector sum of the intrinsic spin $\vec{S}$ and the relative orbital angular momentum $\vec{L}$:

$$\vec{J} = \vec{S} + \vec{L}. \tag{1.1}$$

The ground state for a given hadron is then given by the $|\vec{L}| = L = 0$ condition; radially excited bound states correspond to increased orbital angular momentum, in integer steps (ie. for $L^2 = l(l+1)$, $l = 0, 1, 2, \ldots$).

There are two other quantum numbers that are particularly useful in classifying particles. The first of these is parity (P), which is given for mesons by

$$P = (-1)^{L+1}, \tag{1.2}$$

and describes how the mirror image of the particle is described. The second of these is charge conjugation (C), which for mesons is given by

$$C = (-1)^{L+S}, \tag{1.3}$$

which describes how the particle changes under exchange of particles with their corresponding anti-particles.

Both of these quantities depend on the relative orbital angular momentum of the bound quarks (for baryons) or quark-antiquark pairs (mesons), and thus excited states may have different P and C values relative to their ground state. The charge conjugation quantum number depends on the spin angular momentum even for zero orbital angular momentum.

We can combine the total angular momentum, parity and charge conjugation quantum numbers to classify mesons; collectively, this is referred to as a particle's J^{PC} values. Combining (1.1), (1.2) and (1.3), we can generate all possible J^{PC} values that can be constructed via the constituent quark model for mesons:

$$J^{PC} \in \left\{0^{-+}, 0^{++}, 1^{--}, 1^{+-}, 1^{++}, 2^{--}, \ldots\right\}. \tag{1.4}$$

Here, $(\ldots)$ signifies that further terms in this set increase in the value of J, such that we have listed all possible combinations involving $J = 0, 1$. However, the set in (1.4) does not contain all possible values of J^{PC}, as there is no way to construct those values with a bound two quark system. In particular, the J^{PC} values

$$J^{PC} \in \left\{0^{+-}, 0^{--}, 1^{-+}\right\} \tag{1.5}$$

do not match up with any possible meson that could be constructed in the quark model. The J^{PC} values in (1.5) are referred to as *exotic* quantum numbers. Should a particle be discovered with quantum numbers from (1.5), this would constitute a particle outside of the quark model.

A proposed type of particle not described by the quark model is known as a *hybrid*. These are particles with an excited gluonic degree of freedom. As our central restriction for bound systems being able to exist is that observable states be colourless, hybrids are not explicitly ruled out by QCD, because the colour-octet gluons can combine with a quark-antiquark pair to form a colour singlet. As such, information about the existence of hybrids is beneficial whether they are observed or not; if hybrids are observed, then we can infer that colourless states beyond the quark model are possible, while if they are not observed, we can infer that we are missing information for a full description of hadrons, and colour confinement is not the whole picture.

While a concrete identification of hybrids could provide insight into whether or not bound systems beyond the quark model mesons and baryons are possible, due to the strength of the strong force, it is difficult to infer the content of a hadron that may have a complicated substructure. Though a hybrid may look very much like an ordinary hadron most of the time, a scenario that would signal the identification of something new would be the identification of something with the exotic quantum numbers outlined above. The additional gluonic degree of freedom in a hybrid allows the construction of a bound system with exotic quantum numbers, and so any meson-like particles with exotic quantum numbers is open to a hybrid interpretation.

In the near future, there are experiments that will be coming online with the intent of searching explicitly for particles that may lie outside of the quark model. These include the

GlueX facility [6], housed at the Thomas Jefferson National Accelerator Facility in Virginia, USA, which will search for exotic hadrons, and the PANDA experiment [7], located at the Facility for Antiproton and Ion Research in Darmstadt, Germany, which amongst other research, will be searching for exotic signals as well. A sum-rule analysis that yields predictions of the masses of hybrids can be used to determine in what energy range should the search for hybrid signals be focused on, and the data that these facilities generate can possibly be used to infer the existence of exotic hybrid particles. As a hybrid correlation function is used as the main input in a sum-rules analysis, the calculations in this thesis serve as a basis for further sum-rules work.

In this thesis, we set out to investigate hybrids in the context of the quantum field theory of QCD, with a focus on a comprehensive analysis of both exotic and non-exotic J^{PC} for $J = 0, 1$. The hybrid systems being investigated involve closed flavour systems only, involving up, down and strange quarks. The first two are referred to as light quarkonium, and systems involving strange quarks are referred to as strangeonium. As these quarks are light compared to the external momentum, we perform series expansions in the relevant quark masses. For the strange hybrid system, we obtain a strange quark mass correction to the perturbative calculation stemming from the larger mass of the strange quark relative to the up and down quarks. While the calculations are illustrated for $J^{PC} = 0^{+-}$ (exotic) and $J^{PC} = 1^{--}$ (non-exotic), the calculations are mostly agnostic to the particular choice of quantum numbers. As such, in the conclusion we list the results for all possible $J = 0$ and $J = 1$ quantum numbers. This calculation is a natural complement to a recent study of all possible $J = 0, 1$ charmonium hybrids [8].

1.2 Quantum Chromodynamics

The full motivation and details for the construction of quantum chromodynamics (QCD) as a non-Abelian gauge theory are outlined in several places (see, eg., [9, 10], amongst many others); therefore, we simply aim to outline the most important and necessary details required for use in calculations of correlation functions of operators containing quark and gluon fields.

In a concise form, the Lagrangian for QCD is

$$\mathcal{L}(x) = -\frac{1}{4}\left(G^n_{\mu\nu}(x)\right)^2 + \sum_A \overline{\psi}^A(x)\left(i\not{D} - m_A\right)\psi^A(x). \tag{1.6}$$

In this expression, $\psi^A(x)$ denotes a quark field for an index A, where A denotes the flavour of the quark field. Here, we have used the Feynman slash notation, where

$$\not{D} = \gamma^\mu D_\mu. \tag{1.7}$$

Here, γ^μ denotes a Dirac γ matrix (see Appendix A for conventions related to γ matrices). The gluon field strength tensor $G^n_{\mu\nu}(x)$ is constructed from the gluon field $B^n_\nu(x)$, and is defined as

$$G^n_{\mu\nu}(x) = \partial_\mu B^n_\nu(x) - \partial_\nu B^n_\mu(x) + g f^{nml} B^m_\mu(x) B^l_\nu(x). \tag{1.8}$$

Here, the indices n,m,$l \in \{1, \ldots, 8\}$, where the range is over the 8 generators of the $SU(3)$ gauge group for QCD, and the structure constants f^{nml} are antisymmetric under the exchange of any two indices n, m, l; the Greek indices μ and ν are Lorentz indices, running from 0 to 3. Finally, g is the gauge coupling strength.

The covariant derivative D_μ is defined as

$$D^{ab}_\mu(x) \equiv \partial^{(x)}_\mu \delta^{ab} - ig\, t^{ab}_m\, B^m_\mu(x), \tag{1.9}$$

where the t^{ab}_m are the fundamental representation generators of the $SU(3)$ group for $m \in \{1, \ldots, 8\}$ and $a, b \in \{1, 2, 3\}$, defined by $[t_n, t_m]_{ab} = i f_{nml}\,(t_l)_{ab}$. Using for the gluon field

$$B_\mu(x) = igt^n B^n_\mu(x), \tag{1.10}$$

we can compress (1.9) to

$$D_\mu = I\partial_\mu - B_\mu(x). \tag{1.11}$$

With (1.10), we have for the gluon field strength tensor,

$$G_{\mu\nu}(x) = igt^n G^n_{\mu\nu}(x). \tag{1.12}$$

Note that with definitions (1.10) and (1.11), $G_{\mu\nu}(x)$ can be constructed via

$$G_{\mu\nu} = -\left[D_\mu, D_\nu\right]. \tag{1.13}$$

With these definitions, we can expand (1.6) in order to separate out the free Lagrangian terms from the interacting terms:

$$\begin{aligned}\mathcal{L}(x) = &-\frac{1}{4}\Big[\partial_\mu B^a_\nu(x) - \partial_\nu B^a_\mu(x)\Big]\Big[\partial^\mu B^\nu_a(x) - \partial^\nu B^\mu_a(x)\Big] + \overline{\psi}^A_a(x)\left(i\partial\!\!\!/ - m_A\right)\psi^A_a(x) \\ &+ g\,\overline{\psi}^A_a(x) t^n_{ab}\gamma^\mu\psi^A_b(x)B^\mu_n(x) - \frac{1}{2}gf_{abc}\Big[\partial_\mu B^a_\nu(x) - \partial_\nu B^a_\mu(x)\Big]B^\mu_b(x)B^\nu_c(x) \\ &- \frac{1}{4}\,g^2 f_{abc}f_{ade}B^b_\mu(x)B^c_\nu(x)B^\mu_d(x)B^\nu_e(x)\end{aligned} \tag{1.14}$$

The first two terms describe the free gluon and fermion lagrangians, respectively. The remaining terms each describe a type of interaction, which are quark-quark-gluon, three-gluon and four-gluon interactions, respectively. As the interaction terms are important in the evaluation of Green's functions of fields, we can assign a label to each interaction term:

$$\mathcal{L}^{(1)}_{\text{int}}(x) = \frac{1}{2}\,g\,\overline{\psi}^A_a(x)\lambda^n_{ab}\gamma^\mu\psi^A_b(x)B^\mu_n(x), \tag{1.15}$$

$$\mathcal{L}^{(2)}_{\text{int}}(x) = -\frac{1}{2}gf_{abc}\Big[\partial_\mu B^a_\nu(x) - \partial_\nu B^a_\mu(x)\Big]B^\mu_b(x)B^\nu_c(x), \tag{1.16}$$

$$\mathcal{L}^{(3)}_{\text{int}}(x) = -\frac{1}{4}\,g^2 f_{abc}f_{ade}B^b_\mu(x)B^c_\nu(x)B^\mu_d(x)B^\nu_e(x). \tag{1.17}$$

The additional factor of g in (1.17) plays an important role in determining what types of interactions are possible at a given order in perturbation theory.

To simplify some of the notation, we can introduce

$$\underline{G}^n_{\mu\nu}(x) = \partial_\mu B^n_\nu(x) - \partial_\nu B^n_\mu(x) \tag{1.18}$$

This notation is chosen to mimic the electromagnetic field strength tensor. With it, the gluon field strength tensor can be split into two terms,

$$G^n_{\mu\nu}(x) = \underline{G}^n_{\mu\nu}(x) + gf^{nml}B^m_\mu(x)B^l_\nu(x) \tag{1.19}$$

The first term is just that in (1.18), while the second arises purely from the non-Abelian nature of $SU(3)$. This split is useful in perturbative calculations, as the non-Abelian term is proportional to g, and so enters at a higher order in perturbation theory.

In the application of perturbation theory, we require the use of two-point Green's functions of fields, or propagators, from free field theory. A full treatment of the derivation of these propagators is standard, and can be found in many quantum field theory textbooks ([9, 10, 11]). The full machinery will not be reviewed here. For the fields in the definitions of the propagators, it should be noted that these are implicitly interaction picture fields.

The quark propagator $S_{ij}^{ab}(x-y)$ is defined by

$$\begin{aligned}\left\langle 0|T\left\{\psi_i^a(x)\,\overline{\psi}_j^b(y)\right\}|0\right\rangle &= i\,S_{ij}^{ab}(x-y)\\ &= i\delta^{ab}\int\frac{d^4k}{(2\pi)^4}\frac{(\not{k}+m)_{ij}}{k^2-m^2+i\eta}e^{-ik(x-y)}.\end{aligned}\tag{1.20}$$

Here i,j denote Dirac indices, while a,b denote colour indices; in the integrand, k denotes momentum, with $\not{k} = k_\mu\gamma^\mu$, while m is the appropriate quark mass. The $i\eta$ is inserted to avoid the singularities in the integrand; η is a small real number, chosen to enforce a particular pole prescription, and is to be taken to zero after the integration is performed. This is a convention in the denominators of all integrands of propagators, and will be omitted in the expressions that follow, but its presence is implied. The propagator is defined only for quark fields of the same flavour; each quark flavour has a similar propagator, the only difference being the quark mass involved.

For perturbative calculations, it is often more convenient to work with the Fourier transform of the propagator, and so we define

$$\widetilde{S}_{ij}^{ab}(k) = \delta^{ab}\frac{(\not{k}+m)_{ij}}{k^2-m^2}\tag{1.21}$$

to be the momentum space representation of the fermion propagator. Thus, we have

$$S_{ij}^{ab}(x-y) = \int\frac{d^4k}{(2\pi)^4}\widetilde{S}_{ij}^{ab}(k)e^{-ik(x-y)}.\tag{1.22}$$

Throughout, a tilde will be used to denote momentum space propagators.

In the Feynman gauge, the gluon propagator $D^{nm}_{\mu\nu}(x-y)$ is defined by

$$\begin{aligned}\left\langle 0|T\left\{B^n_\mu(x)B^m_\nu(y)\right\}|0\right\rangle &= i\,D^{nm}_{\mu\nu}(x-y)\\ &= i\delta^{nm}\int\frac{d^4k}{(2\pi)^4}\frac{-g_{\mu\nu}}{k^2}e^{-ik(x-y)}.\end{aligned}\tag{1.23}$$

Here, $g_{\mu\nu}$ is the metric tensor in flat spacetime (see Appendix A for conventions), n, m denote colour indices, and μ, ν denote Lorentz indices. It is in this gauge that the gluon propagator is most simply expressed for performing perturbation theory. In the same way as the fermion propagator, we can introduce the Fourier transform of the gluon field propagator $D^{nm}_{\mu\nu}(x-y)$ as

$$\widetilde{D}^{nm}_{\mu\nu}(k) = \delta^{nm}\frac{-g_{\mu\nu}}{k^2},\tag{1.24}$$

such that $\widetilde{D}^{nm}_{\mu\nu}(k)$ is the momentum space representation of the propagator.

While performing perturbation theory, it may be the case that expressions involve the gluon field strength tensor $G_{\mu\nu}(x)$, rather than the gluon fields themselves. In such cases, it is not necessary to reduce expressions involving $G_{\mu\nu}(x)$ to those involving $B_\mu(x)$ if we instead define a propagator for $G_{\mu\nu}(x)$. To do this, we can construct a propagator

$$\left\langle 0|T\left\{G^n_{\mu\nu}(x)G^m_{\rho\sigma}(y)\right\}|0\right\rangle\tag{1.25}$$

by using the propagator for the gluon fields. However, the non-Abelian terms arising in (1.19) carry an extra factor of g, meaning that they contribute to higher order perturbation theory; with this in mind, we can generate the lowest order term for this expression via

$$\left\langle 0|T\left\{G^n_{\mu\nu}(x)G^m_{\rho\sigma}(y)\right\}|0\right\rangle = \left\langle 0|T\left\{\underline{G}^n_{\mu\nu}(x)\underline{G}^m_{\rho\sigma}(y)\right\}|0\right\rangle + O(g).\tag{1.26}$$

The higher order terms in g involve a greater number of fields, and so are better handled by breaking down $G_{\mu\nu}(x)$ into its component gluon fields for calculations involving higher order corrections in perturbation theory.

To evaluate the first term on the right hand side of (1.26), we can break $\underline{G}^n_{\mu\nu}(x)$ into its gluon fields:

$$\begin{aligned}\left\langle 0|T\left\{\underline{G}^n_{\mu\nu}(x)\underline{G}^m_{\rho\sigma}(y)\right\}|0\right\rangle &= \langle 0|T\left\{\partial_\mu B^n_\nu(x)\partial_\rho B^m_\sigma(y)\right\}|0\rangle - \left\langle 0|T\left\{\partial_\mu B^n_\nu(x)\partial_\sigma B^m_\rho(y)\right\}|0\right\rangle\\ &\quad - \left\langle 0|T\left\{\partial_\nu B^n_\mu(x)\partial_\rho B^m_\sigma(y)\right\}|0\right\rangle + \left\langle 0|T\left\{\partial_\nu B^n_\mu(x)\partial_\sigma B^m_\rho(y)\right\}|0\right\rangle.\end{aligned}\tag{1.27}$$

By extracting the derivatives acting on the appropriate spacetime variables from each of the time-ordered products on the right hand side of (1.27), we have derivatives acting on gluon field propagators. We can then define the propagator $H^{nm}_{\mu\nu\rho\sigma}(x-y)$ of (1.27) via

$$\begin{aligned}\left\langle 0|T\left\{\underline{G}^n_{\mu\nu}(x)\underline{G}^m_{\rho\sigma}(y)\right\}|0\right\rangle &= iH^{nm}_{\mu\nu\rho\sigma}(x-y),\\ &= i\int\frac{d^4k}{(2\pi)^4}\,\widetilde{H}^{nm}_{\mu\nu\rho\sigma}(k)\,e^{-ik(x-y)}.\end{aligned} \tag{1.28}$$

The derivatives have a simple behaviour in the momentum space representation, as they simply bring down factors of momentum, yielding

$$\widetilde{H}^{nm}_{\mu\nu\rho\sigma}(k) = -\,\delta^{nm}\frac{1}{k^2}\Big(g_{\nu\sigma}k_\mu k_\rho - g_{\nu\rho}k_\mu k_\sigma - g_{\mu\sigma}k_\nu k_\rho + g_{\mu\rho}k_\nu k_\sigma\Big). \tag{1.29}$$

1.3 Operator Product Expansion

In order to extract information about the product of non-local composite operators $\mathcal{O}(x)\mathcal{O}(0)$ in the $x\to 0$ limit, we need to be careful about how this limit is approached. Due to the fact that $(\mathcal{O}(0))^2$ contains divergences (ie. in the $x\to 0$ limit, $\mathcal{O}(x)\mathcal{O}(0)\propto\frac{1}{x}$), the straightforward $x\to 0$ limit does not exist. The *operator product expansion* (OPE) is a method of decomposing non-local products of composite operators as complex number functions multiplied by entirely local operators [12]:

$$\mathcal{O}(x)\mathcal{O}(0) \;=\; \sum_n C^n(x)\mathcal{O}_n(0). \tag{1.30}$$

The operators $\mathcal{O}_n(0)$ are local, gauge and Lorentz invariant composite operators that have the same symmetries as $\mathcal{O}(x)\mathcal{O}(0)$. The $C^n(x)$, known as Wilson coefficients, are complex number expressions that have dimensions which ensure that the product $C^n(x)\mathcal{O}_n(0)$ has the same dimensions as $\mathcal{O}(x)\mathcal{O}(0)$, and contain the singular structure of the $x\to 0$ limit. With this expansion, time-ordered products of fields can be expressed as

$$\langle\Omega|T\left\{\mathcal{O}(x)\mathcal{O}(0)\right\}|\Omega\rangle = \sum_n C^n(x)\left\langle\Omega\right|:\mathcal{O}_n(0):\left|\Omega\right\rangle, \tag{1.31}$$

where $|\Omega\rangle$ denotes the vacuum state in QCD, and $:\mathcal{O}_n(0):$ is the normal-ordered product of $\mathcal{O}_n(0)$, which is defined in detail in Section 1.4.

The lowest dimension operator in this expansion is simply the unit operator,

$$\mathcal{O}_1 = 1, \tag{1.32}$$

and so $C^1(x)$ corresponds directly to the perturbative evaluation of the time-ordered product. The higher order terms in this series correspond to nonzero values for the vacuum expectation value (VEV) of composite fields. Through these terms, the behaviour of the QCD vacuum can be parameterized in the low energy limit.

The nonzero nature of the vacuum expectation values of fields in (1.31) has several ramifications. In particular, in QCD in the limit of massless quarks, the nonvanishing VEV of a combination of quark fields known as the quark condensate,

$$\langle \Omega | : \overline{q}(0) q(0) : | \Omega \rangle \neq 0, \tag{1.33}$$

suggests a broken chiral symmetry. By the Nambu-Goldstone theorem [13, 14, 15], each broken symmetry implies that there exist a massless boson with quantum numbers that are related to the operators associated with the broken symmetry. However, as the quarks are not massless, neither are the Nambu-Goldstone bosons that correspond to the broken symmetry. However, the pions are relatively light mesons with quantum numbers corresponding to the pseudoscalar operators underlying (1.33), and permit an interpretation of them as the Nambu-Goldstone bosons corresponding to the broken chiral symmetry imposed by the nonzero VEV of the quark-antiquark pair of fields in QCD.

The nonzero VEVs that appear in the operator product expansion are known as *condensates*, the quark condensate in (1.33) is simply one example. Compared to (1.33), the consequences of these others are less physically obvious. However, higher dimension condensates in the series (1.30) can sometimes be related approximately to lower dimensional ones [16]. The coefficients $C^n(x)$ (or in momentum space, $C^n(q)$) scale in the short distance (or high energy) in such a way that the higher order terms in the series (1.30) yield contributions to the sum decreasing in magnitude. This would allow us to terminate the sum at a given order to obtain an approximation for the full expression.

The coefficients $C^n(x)$ that correspond to a particular VEV can be computed perturbatively, but the condensates themselves cannot yet be calculated within the framework of QCD. Rather, the condensate values are determined phenomenologically.

1.4 Wick's Theorem

In considering time-ordered products of fields, we can exchange field operators in the Heisenberg picture for those in the *interaction picture* (where time evolution is described by the free Hamiltonian) with the introduction of the interaction lagrangian via

$$\langle\Omega|T\left\{\phi(x)\phi(y)\right\}|\Omega\rangle = \frac{\langle 0|T\left\{\phi_I(x)\phi_I(y)\exp\left(i\int d^4z\,\mathcal{L}_I(z)\right)\right\}|0\rangle}{\langle 0|T\left\{\exp\left(i\int d^4z\,\mathcal{L}_I(z)\right)\right\}|0\rangle}. \tag{1.34}$$

Here, $|\Omega\rangle$ denotes the ground state (vacuum) of the fully interacting theory, while $|0\rangle$ denotes the ground state (vacuum) of the free field theory. The subscript I indicates that the fields on the right hand side of (1.34) are interaction picture fields; that is,

$$\phi_I(x) = e^{iH_0(t-t_0)}\phi(\vec{x},t_0)e^{-iH_0(t-t_0)} \tag{1.35}$$

where H_0 is the free-field Hamiltonian. $\mathcal{L}_I(z)$ contains all terms in the lagrangian that depend on the couplings, and all fields involved are interaction-picture fields. The factor in the denominator is a normalization which eliminates vacuum bubble diagrams that arise in the evaluation of the time-ordered products.

Expression (1.34) allows the use of the non-interacting fields and vacuum in calculations, and enables a perturbative expansion by considering the series expansion of the exponential

$$\begin{aligned}\langle 0|T\left\{\phi_I(x)\phi_I(y)\exp\left(i\int d^4z\,\mathcal{L}_I(z)\right)\right\}|0\rangle \\ = \langle 0|T\left\{\phi_I(x)\phi_I(y)\right\}|0\rangle + i\int d^4z\,\langle 0|T\left\{\phi_I(x)\phi_I(y)\mathcal{L}_I(z)\right\}|0\rangle + \dots .\end{aligned} \tag{1.36}$$

To evaluate interaction-picture time-ordered products (in the following, we drop the subscript I denoting interaction-picture fields under the assumption that all fields under consideration are interaction-picture fields), we invoke Wick's Theorem as outlined in [9]:

$$T\left\{\phi(x_1)\dots\phi(x_n)\right\} =: \phi(x_1)\dots\phi(x_n) + (\text{all possible contractions}) : . \tag{1.37}$$

Here : (any number of fields) : is known as a *normal-ordered product*. It moves all positive frequencies of fields (annihilation operators) to the right, and negative frequencies (creation operators) to the left, such that normal-ordered products have zero free-field vacuum expectation value.

A contraction between two interaction-picture fields is written

$$\underbrace{\phi(x)\phi}(y) \equiv \langle 0|T\left\{\phi(x)\phi(y)\right\}|0\rangle\,, \tag{1.38}$$

and is a c-number function. In the application of Wick's Theorem, it is assumed that the fields involved are all interaction-picture fields, and the subscript I denoting this is dropped. This definition creates a connection between the two-point Green's functions, defined as propagators in Section 1.2, and time-ordered products of multiple fields. For example, for four scalar fields at four distinct spacetime points, application of Wick's Theorem yields

$$\begin{aligned} T\left\{\phi(x_1)\phi(x_2)\phi(x_3)\phi(x_4)\right\} = &\underbrace{\phi(x_1)\phi}(x_2)\underbrace{\phi(x_3)\phi}(x_4) + (\text{permutations of } x_1,\ldots,x_4) \\ &+ \underbrace{\phi(x_1)\phi}(x_2) : \phi(x_3)\phi(x_4) : + (\text{permutations of } x_1,\ldots,x_4) \\ &+ : \phi(x_1)\phi(x_2)\phi(x_3)\phi(x_4) : . \end{aligned} \tag{1.39}$$

While the above was defined using scalar fields which commute with one another, the same expressions hold with anti-commuting fields; the commutation relations of the fields keep track of the minus signs that arise, and the overall Wick's Theorem expression remains the same. This also holds for expressions involving more complicated fields and combinations thereof.

In a more general context, when applying Wick's Theorem to composite operators,

$$T\left\{\mathcal{O}_1(x)\mathcal{O}_2(0)\right\} = : \mathcal{O}_1(x)\mathcal{O}_2(0) : + : (\text{all possible contractions}) : . \tag{1.40}$$

To obtain nonzero fully connected diagrams, contractions must occur between different spacetime points for the individual operators that are part of the composite ones. The application of Wick's Theorem then generates a term which is as fully contracted as possible (that is, given the individual fields of the composite operators, the maximum number of possible contractions between the fields has been performed), plus a series of terms with various combinations of normal-ordered products multiplied by terms with contractions.

While the fully contracted terms in (1.40) contribute to the traditional perturbative expansion, we can assign further importance to the remaining normal-ordered products. By the definition of the vacuum of the free-field Hamiltonian, normal-ordered products of operators

vanish under vacuum to vacuum transitions,

$$\langle 0| : (\text{any number of fields}) : |0\rangle = 0. \tag{1.41}$$

However, for the fully interacting QCD vacuum, this condition does not necessarily need to hold; that is,

$$\langle \Omega| : (\text{any number of fields}) : |\Omega\rangle \neq 0. \tag{1.42}$$

In the expansion (1.40), if we can extract the spacetime dependence of the normal-ordered products, we have a series that looks very similar to that of the operator product expansion (1.31). Those factors that are the field contractions, multiplied by the extracted spacetime dependence of the normal-ordered products of fields, corresponds to $C^n(x)$ for a given local operator. Thus, through this connection, we have a method of calculating the coefficients $C^n(x)$; for the terms with normal-ordered products arising from the application of Wick's Theorem, apply the usual perturbative Feynman diagram analysis on the contractions with the appropriate fields uncontracted that correspond to a condensate structure in the OPE.

1.5 Outline of Thesis

The basic ingredient in a sum-rule analysis is the correlation function, defined by

$$\Pi^{\mu\nu}(q) = i \int d^4x \, e^{iq\cdot x} \, \langle \Omega | \, T\{J^\mu(x) J^\nu(0)\} | \Omega \rangle \, . \tag{1.43}$$

Here, $J^\mu(x)$ is a composite operator (also called a *current*) constructed to probe an appropriate state. Throughout this thesis, we focus our attention on operators $J^\mu(x)$ that probe hybrid states; with different choices for the structure of $J^\mu(x)$, we can construct operators that probe all possible J^{PC} values for $J = 0, 1$.

A sum-rule analysis uses the correlation function as the key input to extract a prediction of the mass that the operator $J^\mu(x)$ is probing [16]. This is done by analyzing scalar quantities constructed out of (1.43), and relating them to a phenomenelogical model.

In particular, we focus on $J^\mu(x)$ constructed out of light and strange quark fields, which are light in comparison to the external momentum scale. Thus, in the calculation of the

hybrid correlation functions, we can perform a series expansion in $\frac{m^2}{q^2}$, where q^2 is the external momentum and m^2 is the quark mass. For the light quarkonium hybrids, we retain only the leading order term in this expansion, and for the strangeonium hybrids we keep the next-to-leading order mass correction terms as well.

This thesis is focused on the evaluation of (1.43) for a current that probes hybrids. This is done via the application of the operator product expansion. The Wilson coefficients are calculated perturbatively. The first operator in the operator product expansion of (1.43) is simply the unit operator; the first calculation outlined in this thesis is the leading order (LO) perturbative result.

Through the application of Wick's Theorem to the correlation function (1.43), we can obtain a connection to additional terms appearing in the operator product expansion. The terms in which not all of the fields are contracted can be identified with terms from the operator product expansion, after care is taken to extract the spatial dependence, as well as the colour, Dirac and Lorentz structure from the terms that remain in the normal-ordered products. These contributions to a correlation function (1.43) are called *condensates*, and will be further outlined throughout this thesis. These condensate contributions form the bulk of the calculation of the correlation function, and there are various types, corresponding to different field operator contents.

The calculation of both the perturbative and condensate contributions to the correlator are very similar to one another, regardless of the choice of J^{PC} according to which we create our hybrid current. Due to this, we can calculate the correlator for all J^{PC} choices for $J = 0, 1$. In the conclusion, we collect these results for use in a future sum-rule analysis.

Chapter 2

Hybrid Correlation Functions

2.1 Correlation Functions

To construct a current that probes a hybrid particle, we are subject to a few constraints: the hybrid current operator must be a composite operator constructed out of fields that describe the quark and gluon degrees of freedom, the operator must be a colour singlet, and the operator's structure must correspond to the choice of the J^{PC} values appropriate to the hybrid particle of interest. These constraints are satisfied by a current of the form

$$J^{\mu}(x) = g_s \, \overline{\psi}^a(x) \, \Gamma^{\nu} \, t^n_{ab} \, \overline{G}^n_{\mu\nu}(x) \, \psi^b(x) \tag{2.1}$$

as in [17], where $\overline{\psi}^a(x)$ and $\psi^b(x)$ are quark and antiquark field operators, Γ^{ν} is the appropriate Dirac matrix that describes the J^{PC} values of the hybrid under investigation, $t^n_{ab} = \frac{\lambda^n_{ab}}{2}$ (where λ^n_{ab} are the Gell-Mann matrices, see Appendix A for some of their properties), and $\overline{G}^n_{\mu\nu}(x)$ is either the gluon field strength tensor or its dual (defined as $\frac{1}{2}\epsilon^{\mu\nu\rho\sigma} G^n_{\rho\sigma}(x)$), depending on the properties of the hybrid we wish to investigate. We can parameterize this choice in terms of the gluon field strength tensor by writing

$$\overline{G}^n_{\mu\nu}(x) = \Delta_{\mu\nu\rho\sigma} G^{\rho\sigma,\,n}(x), \tag{2.2}$$

where we define

$$\Delta^{(1)}_{\mu\nu\rho\sigma} = g_{\mu\rho} \, g_{\nu\sigma}, \tag{2.3}$$

$$\Delta^{(2)}_{\mu\nu\rho\sigma} = \frac{1}{2}\epsilon_{\mu\nu\rho\sigma}. \tag{2.4}$$

For what we use for Γ_μ, we have either

$$\Gamma_\mu^{(1)} = \gamma_\mu, \tag{2.5}$$

$$\Gamma_\mu^{(2)} = \gamma_\mu\gamma_5. \tag{2.6}$$

The properties of these Dirac matrices are discussed in Section A.2. The choice of the various combinations of $\Delta^{(1)}_{\mu\nu\rho\sigma}$, $\Delta^{(2)}_{\mu\nu\rho\sigma}$, $\Gamma^{(1)}_\mu$ and $\Gamma^{(2)}_\mu$ permit the construction of a current that allows us to probe various J^{PC} values for any P and C.

With the above, we can write a hybrid current for arbitrary choice of J^{PC} as

$$J^\mu(x) = g_s\Delta_{\mu\nu\rho\sigma}\,\overline{\psi}^a(x)\,\Gamma^\nu\,\frac{\lambda^n_{ab}}{2}\,G^{\rho\sigma,\,n}(x)\,\psi^b(x). \tag{2.7}$$

With appropriate choices for Δ and Γ, (2.7) can be used to probe 8 distinct J^{PC} combinations. The identification of which currents are related to which quantum numbers is illustrated in Table 2.1.

Current	Scalar Projection	Vector Projection
$\overline{\psi}^a_i\,t^n_{ab}\,\gamma^\nu_{ij}\,G^n_{\mu\nu}\,\psi^b_j$	0^{++}	1^{-+}
$\overline{\psi}^a_i\,t^n_{ab}\,(\gamma^\nu\gamma^5)_{ij}\,G^n_{\mu\nu}\,\psi^b_k$	0^{--}	1^{+-}
$\frac{1}{2}\epsilon_{\mu\nu\rho\sigma}\,\overline{\psi}^a_i\,t^n_{ab}\,\gamma^\nu_{ij}\,G^n_{\rho\sigma}\,\psi^b_j$	0^{-+}	1^{++}
$\frac{1}{2}\epsilon_{\mu\nu\rho\sigma}\,\overline{\psi}^a_i\,t^n_{ab}\,(\gamma^\nu\gamma^5)_{ij}\,G^n_{\rho\sigma}\,\psi^b_j$	0^{+-}	1^{--}

Table 2.1: The J^{PC} values that correspond to a given current that can be extracted via projecting out the desired state.

We can define the correlation function (or correlator) of our currents as

$$\Pi^{\mu\nu}(q) = i\int d^4x\,e^{iq\cdot x}\,\langle\Omega|\,T\{J^\mu(x)J^\nu(0)\}|\Omega\rangle\,, \tag{2.8}$$

where $J^\mu(x)$ is defined as in (2.7). From how the current couples to hadronic states, we can break the correlation function down into pieces that describe both $J = 0$ and $J = 1$ particles via

$$\Pi^{\mu\nu}(q) = \frac{q^\mu q^\nu}{q^2}\Pi_S(q^2) + \frac{(q^\mu q^\nu - q^2 g^{\mu\nu})}{q^2}\Pi_V(q^2). \tag{2.9}$$

To extract the pieces that correspond to each spin, we apply projection operators to (2.8):

$$\Pi_S(q^2) = \frac{q_\mu q_\nu}{q^2}\Pi^{\mu\nu}(q), \tag{2.10}$$

$$\Pi_V(q^2) = \frac{1}{D-1}\left(\frac{q_\mu q_\nu}{q^2} - g_{\mu\nu}\right)\Pi^{\mu\nu}(q). \tag{2.11}$$

The J^{PC} values we will present in detail are 0^{+-} and 1^{--}, which correspond to the spin projections of (2.8) with the use of $\Gamma^{(2)}_\mu$ and $\Delta^{(2)}_{\mu\nu\rho\sigma}$. However, the current is defined in such a way that calculations depend little on the choice of Γ and Δ. This allows for computation of $\Pi_S(q^2)$ and $\Pi_V(q^2)$ for all of the previously mentioned choices of J^{PC} via the same method. Thus, although analysis is focused on 0^{+-} and 1^{--}, we will ultimately present results for all possible $J = 0, 1$ values of J^{PC}.

Inserting the current (2.7) into (2.8) yields

$$\begin{aligned}\Pi^{\mu\nu}(q) = \frac{i}{4}\, g_s^2\, \Delta^{\mu\rho\omega_1\omega_2}\Delta^{\nu\sigma\omega_3\omega_4}\lambda^n_{\alpha\beta}\lambda^m_{\gamma\delta}(\Gamma_\rho)_{ij}(\Gamma_\sigma)_{kl}\int d^4x\, e^{iq\cdot x} \\ \times \left\langle\Omega\right| T\left\{\overline{\psi}_\alpha(x)\psi_\beta(x)\overline{\psi}_\gamma(0)\psi_\delta(0)G^{\omega_1\omega_2,\,n}(x)G^{\omega_3\omega_4,\,m}(0)\right\}\left|\Omega\right\rangle .\end{aligned} \tag{2.12}$$

During the calculations outlined in this thesis, we leave Δ and Γ unspecified as often as possible in the expressions they appear. However, to evaluate the correlation function for the specific choice of $J^{PC} = 0^{+-}$ and 1^{--}, we use $\Delta^{(2)}$ and $\Gamma^{(2)}$ where necessary, and in the conclusion collect the results for all J^{PC} values.

2.2 Wick's Theorem for Correlators

To compute the correlation function (2.12), we need to calculate the time-ordered product of the fields. We do this via an application of Wick's Theorem. To first order (that is, without

yet introducing interaction terms from the QCD Lagrangian), this yields

$$
\begin{aligned}
T\left\{\overline{\psi}_\alpha(x)\psi_\beta(x)\overline{\psi}_\gamma(0)\psi_\delta(0)G^n_{\omega_1\omega_2}(x)G^m_{\omega_3\omega_4}(0)\right\} = \\
&: \overline{\psi}_\alpha(x)\psi_\beta(x)\overline{\psi}_\gamma(0)\psi_\delta(0)G^n_{\omega_1\omega_2}(x)G^m_{\omega_3\omega_4}(0) : \\
&+ : \overline{\psi}_\alpha(x)\psi_\beta(x)\overline{\psi}_\gamma(0)\psi_\delta(0)G^n_{\omega_1\omega_2}(x)G^m_{\omega_3\omega_4}(0) : \\
&+ : \overline{\psi}_\alpha(x)\psi_\beta(x)\overline{\psi}_\gamma(0)\psi_\delta(0)G^n_{\omega_1\omega_2}(x)G^m_{\omega_3\omega_4}(0) : \\
&+ : \overline{\psi}_\alpha(x)\psi_\beta(x)\overline{\psi}_\gamma(0)\psi_\delta(0)G^n_{\omega_1\omega_2}(x)G^m_{\omega_3\omega_4}(0) : \\
&+ : \overline{\psi}_\alpha(x)\psi_\beta(x)\overline{\psi}_\gamma(0)\psi_\delta(0)G^n_{\omega_1\omega_2}(x)G^m_{\omega_3\omega_4}(0) : \\
&+ : \overline{\psi}_\alpha(x)\psi_\beta(x)\overline{\psi}_\gamma(0)\psi_\delta(0)G^n_{\omega_1\omega_2}(x)G^m_{\omega_3\omega_4}(0) : \\
&+ : \overline{\psi}_\alpha(x)\psi_\beta(x)\overline{\psi}_\gamma(0)\psi_\delta(0)G^n_{\omega_1\omega_2}(x)G^m_{\omega_3\omega_4}(0) : \\
&+ : \overline{\psi}_\alpha(x)\psi_\beta(x)\overline{\psi}_\gamma(0)\psi_\delta(0)G^n_{\omega_1\omega_2}(x)G^m_{\omega_3\omega_4}(0) : . \qquad (2.13)
\end{aligned}
$$

The first term in this expression has every field contracted. It is this term that we call the *perturbative* contribution to the correlator; it does not contribute to any of the condensate terms. The other terms that arise from the application of Wick's Theorem are contributions to the condensate terms in the operator product expansion.

The fields that remain uncontracted in (2.13) are indicative to which condensate from the OPE that the term contributes. The terms in (2.13) which have only quark fields uncontracted contribute to the quark condensate, while terms with only gluon field strength tensors uncontracted contribute to condensates including gluon fields.

We can organize the terms of (2.13) to match up with the operator product expansion of the time-ordered product of the currents. Schematically, the operator product expansion

looks like

$$\begin{aligned}\langle\Omega|T\{J_\mu(x)J_\nu(0)\}|\Omega\rangle = & C_{\mu\nu}^{\ 1}(x) \\ & + C_{\mu\nu}^{\ \overline{\psi}\psi}(x)\,\langle\Omega|\,:\overline{\psi}\psi(0):\,|\Omega\rangle \\ & + C_{\mu\nu}^{\ G^2}(x)\,\langle\Omega|\,:(G^a_{\alpha\beta})^2(0):\,|\Omega\rangle \\ & + C_{\mu\nu}^{\ \overline{\psi}G\psi}(x)\,\langle\Omega|\,:\overline{\psi}\sigma\cdot G\psi(0):\,|\Omega\rangle \\ & + C_{\mu\nu}^{\ \overline{\psi}\psi\overline{\psi}\psi}(x)\,\langle\Omega|\,:\overline{\psi}\psi\overline{\psi}\psi(0):\,|\Omega\rangle \\ & + C_{\mu\nu}^{\ G^3}(x)\,\langle\Omega|\,:g^3 f_{abc}G^a_{\alpha\beta}G^b_{\beta\gamma}G^c_{\gamma\alpha}(0):\,|\Omega\rangle \\ & + \ldots \end{aligned} \tag{2.14}$$

where the coefficients $C_{\mu\nu}$ carry all of the spatial information, while the condensates are local, gauge invariant, Lorentz scalars and colour singlets.

The QCD Lagrangian must be of dimension $[\text{length}]^{-4}$ in order for the action to be dimensionless. However, through dimensional analysis with $\hbar = c = 1$, we can relate dimensions of length and mass by $[\text{length}] = [\text{mass}]^{-1}$. Due to this, we are free to commit to considering all quantities as having dimensions of mass to some power (positive or negative). This freedom, along with the restriction on the dimension of the Lagrangian, allows us to identify the mass dimension of the quark and gluon fields:

$$\begin{aligned}[\psi] &= +\frac{3}{2}, \\ [B^\mu] &= +1, \\ [G^{\mu\nu}] &= +2. \end{aligned} \tag{2.15}$$

With the above, we can talk about the dimension of a product of fields; to determine a dimension of a product of fields, simply sum the the dimensions of each of the fields in the product. We use the notation "nD" to denote the dimension n of a product of fields and adopt the same convention when discussing condensates.

In considering the terms on the right hand side (RHS) of (2.14), we name the condensates (the VEV of the normal-ordered product of fields in (2.14)) according to their dimension. In Section (1.3) we defined the first of these, the quark condensate. However, with the position dependence extracted, we define $\langle\Omega|\,:\overline{\psi}\psi(0):\,|\Omega\rangle \equiv \left\langle\overline{\psi}\psi\right\rangle$ as the 4D quark condensate. For

light quarks, the mass times the quark condensate takes on the value

$$m_q \langle \overline{q} q \rangle = -\frac{1}{2} f_\pi^2 m_\pi^2, \tag{2.16}$$

given in [18]. Here, $f_\pi = 0.093\text{GeV}$, and $m_\pi = 0.139\text{GeV}$, both taken from [19]. For strange quarks, we can relate the 4D strange quark condensate to the 4D light quark condensate via

$$\langle \overline{s} s \rangle \approx 0.7 \langle \overline{u} u \rangle , \tag{2.17}$$

which is taken from [20]. $\langle \Omega | : \overline{\psi} \sigma \cdot G \psi(0) : | \Omega \rangle \equiv \left\langle \overline{\psi} \sigma G \psi \right\rangle$ is known as the mixed condensate; for the mixed condensate with light quarks, we have from [21]

$$m \langle \overline{q} \sigma G q \rangle = M_0^2 \, m \langle \overline{q} q \rangle . \tag{2.18}$$

Here, $M_0^2 = (0.8 \pm 0.1)\text{GeV}^2$, which is pulled from [21]. This, along with (2.17), allows us to calculate the mixed condensate with strange quarks as well. $\langle \Omega | : \overline{\psi} \psi \overline{\psi} \psi(0) : | \Omega \rangle$ ($\equiv \left\langle \overline{\psi} \psi \right\rangle^2$) after the application of the vacuum saturation hypothesis [16]) is known as the 6D quark condensate, and when combined with the strong coupling constant has the value

$$\alpha \langle \overline{q} q \rangle^2 = (5.8 \pm 0.9) \times 10^{-4} \text{GeV}^6. \tag{2.19}$$

This is pulled from [22]. Next, $\langle \Omega | : (G^a_{\alpha\beta})^2(0) : | \Omega \rangle \equiv \langle \alpha G^2 \rangle$ is referred to as the 4D gluon condensate. When paired with the strong coupling constant α_s, it takes on the value

$$\left\langle \alpha G^2 \right\rangle = (7.5 \pm 2.0) \times 10^{-2} \text{GeV}^4, \tag{2.20}$$

which is taken from [23]. Finally, $\langle \Omega | : g^3 f_{abc} G^a_{\alpha\beta} G^b_{\beta\gamma} G^c_{\gamma\alpha}(0) : | \Omega \rangle \equiv \langle g^3 G^3 \rangle$ is known as the 6D gluon condensate, and has the value

$$\left\langle g^3 G^3 \right\rangle = (8.2 \pm 1.0)\text{GeV}^2 \left\langle \alpha G^2 \right\rangle , \tag{2.21}$$

which is also taken from [23].

We can rearrange the terms in (2.13) to generate an expression of the form (2.14). This is done by extracting the spatial dependence, tensor and spinor structure from the uncontracted fields in (2.13). Once this has been performed, each term can be calculated via ordinary perturbation theory techniques, and can be put into correspondence with a representative

Feynman diagram. This is done in Figure 2.1. Each distinct topology corresponds to an inequivalent combination of contracted fields from the application of Wick's Theorem to the correlation function.

This process, however, is non-trivial. In extracting the spatial dependence from the uncontracted fields, we generate contributions to condensates such that the original dimensions of the expressions remain the same. Thus, the process of extracting the spatial, Lorentz and colour structure from (2.13) is complicated by potential mixing of higher order condensate contributions.

The process of relating the operator product expansion in (2.14) to terms generated by (2.13) yields terms of up to order $O(g^3)$, but not all of the possible ones. To obtain all terms of $O(g^3)$, we need to consider the next order term in the expansion of (2.12), that is, the insertion of the interaction terms of the QCD Lagrangian that generate contributions of $O(g^3)$. The two that do this are the interactions (1.15) and (1.16). Therefore we need also consider

$$i\int d^4z\, T\left\{\overline{\psi}_\alpha(x)\psi_\beta(x)\overline{\psi}_\gamma(0)\psi_\delta(0)G^n_{\omega_1\omega_2}(x)G^m_{\omega_3\omega_4}(0)\mathcal{L}^{(1)}_{\rm int}(z)\right\} \tag{2.22}$$

and

$$i\int d^4z\, T\left\{\overline{\psi}_\alpha(x)\psi_\beta(x)\overline{\psi}_\gamma(0)\psi_\delta(0)G^n_{\omega_1\omega_2}(x)G^m_{\omega_3\omega_4}(0)\mathcal{L}^{(2)}_{\rm int}(z)\right\} \tag{2.23}$$

as next-to-leading order (NLO) corrections to the correlation function; these reduce to

$$\Pi^{\mu\nu}_{(\text{Int. }1)}(q) = -\frac{g^3}{8}\Delta_{\mu\rho\omega_1\omega_2}\Delta_{\nu\sigma\omega_3\omega_4}(\Gamma^\rho)_{ij}(\Gamma^\sigma)_{kl}(\gamma^\xi)_{rs}(\lambda^n)_{ab}(\lambda^m)_{cd}(\lambda^p)_{ef}\int d^4x\, d^4z\, e^{iqx}$$
$$\left\langle\Omega\right|T\left\{\overline{\psi}^a_i(x)\psi^b_j(x)\overline{\psi}^c_k(0)\psi^d_l(0)\overline{\psi}^e_r(z)\psi^f_s(z)G^n_{\omega_1\omega_2}(x)G^m_{\omega_3\omega_4}(0)B^p_\xi(z)\right\}\left|\Omega\right\rangle \tag{2.24}$$

for the inclusion of the QCD interaction term (1.15) and

$$\Pi^{\mu\nu}_{(\text{Int. }2)}(q) = \frac{g^3}{8}\Delta_{\mu\rho\omega_1\omega_2}\Delta_{\nu\sigma\omega_3\omega_4}(\Gamma^\rho)_{ij}(\Gamma^\sigma)_{kl}(\lambda^n)_{ab}(\lambda^m)_{cd}f_{rst}\int d^4x\, d^4z\, e^{iqx}$$
$$\left\langle\Omega\right|T\left\{\overline{\psi}^a_i(x)\psi^b_j(x)\overline{\psi}^c_k(0)\psi^d_l(0)G^n_{\omega_1\omega_2}(x)G^m_{\omega_3\omega_4}(0)G^r_{\eta\xi}(z)B^\eta_s(z)B^\xi_t(z)\right\}\left|\Omega\right\rangle \tag{2.25}$$

for the inclusion of the QCD interaction term (1.16).

The number of terms that arise from these time-ordered products becomes unwieldly, yet each term can be put into one-to-one correspondence with a representative Feynman

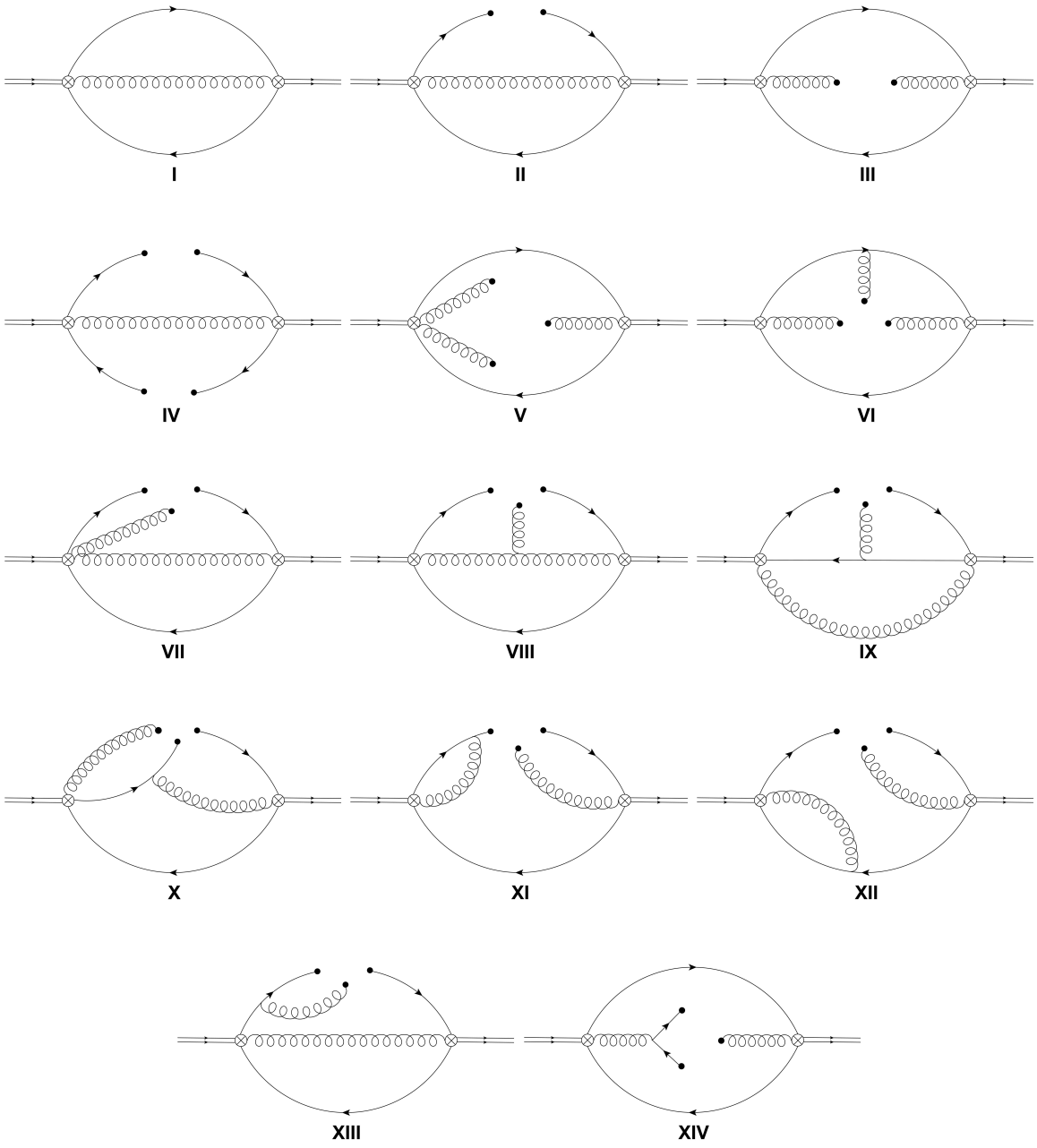

Figure 2.1: All order g^2 and g^3 contributions to $\Pi^{\mu\nu}(q)$. The Roman numerals labelling the various types of Feynman diagram topology that arise from the application of Wick's Theorem to the correlation function, and follows the same convention used in [1], and will be used throughout the thesis. All Feynman diagrams were produced using the program JaxoDraw [24, 25].

diagram. Many of these terms are, in fact, identical under a change in momentum variables; thus, multiple terms can correspond to the same Feynman diagram topology.

2.3 Perturbation Theory

At leading order (LO), there is only one fully contracted term that arises from the application of Wick's Theorem to the correlator as there exists only one possible contraction for each field in the time-ordered product. This fully contracted term is thus the only contribution to perturbation theory, and can be represented by Fig. 2.2.

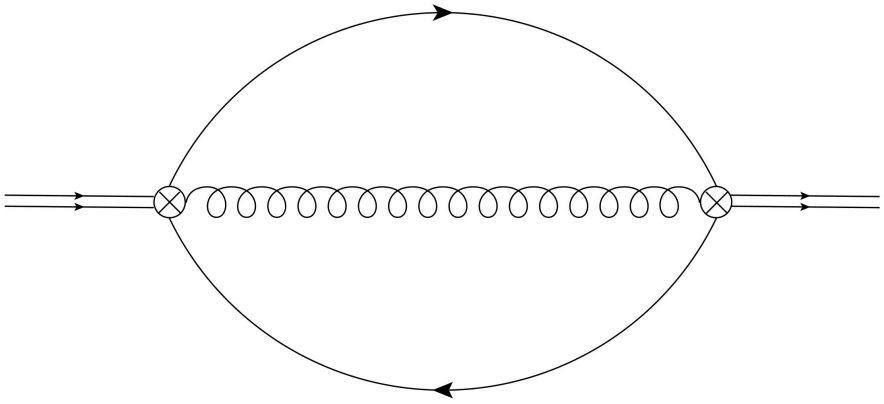

Figure 2.2: Diagram I: The only diagram that contributes at leading order to the perturbation theory calculation.

A key challenge is to evaluate the two loop integrals that arise from the calculation of this diagram.

2.3.1 Leading Order Perturbative Calculation

Applying Wick's Theorem to 2.12 yields the fully contracted perturbative result (see Fig. 2.2)

$$\Pi^{\mu\nu(i)}(q) = \frac{i}{4}\, g_s^2\, \Delta^{\mu\rho\omega_1\omega_2}\Delta^{\nu\sigma\omega_3\omega_4}\lambda^n_{ab}\lambda^m_{cd}(\Gamma_\rho)_{ij}(\Gamma_\sigma)_{kl}\int d^4x\, e^{iq\cdot x}$$
$$\times \left\langle\Omega\right| N\big\{\overline{\psi}^a_i(x)\psi^b_j(x)\overline{\psi}^c_k(0)\psi^d_l(0)G^n_{\omega_1\omega_2}(x)G^m_{\omega_3\omega_4}(0)\big\}\left|\Omega\right\rangle . \tag{2.26}$$

Throughout this thesis, we denote the contribution to the correlation function of a particular diagram labelled by a Roman numeral M, which denotes a type of Feynman diagram topology in Figure 2.1, by $\Pi^{\mu\nu(M)}(q)$ (we use lowercase letters when decorating $\Pi^{\mu\nu}$ to avoid confusion between a vector projection V and a Roman numeral 5 later). Equation (2.26) can be written in terms of position space propagators:

$$\Pi^{\mu\nu(i)}(q) = \frac{i}{4}\, g_s^2\, \Delta^{\mu\rho\omega_1\omega_2}\Delta^{\nu\sigma\omega_3\omega_4}\lambda^n_{ab}\lambda^m_{cd}(\Gamma_\rho)_{ij}(\Gamma_\sigma)_{kl}\int d^4x\, e^{iq\cdot x} \\ \times\Big[-iS^{ad}_{li}(-x)\Big]\Big[iS^{bc}_{jk}(x)\Big]\Big[i\delta^{nm}H_{\omega_1\omega_2\omega_3\omega_4}(x)\Big]. \tag{2.27}$$

The propagators each have their own momentum space representations, and we can use these to perform the spatial integral. Also, we can arrange the colour and Dirac matrices into traces using the delta functions for the colour and Dirac indices from the propagators. The colour trace are handled according to the trace rules outlined in Appendix A.2, yielding the expression

$$\Pi^{\mu\nu(i)}(q) = -16\pi\alpha_s\, i\ \Delta^{\mu\rho\omega_1\omega_2}\Delta^{\nu\sigma\omega_3\omega_4}\int\frac{d^4k_1}{(2\pi)^4}\frac{d^4k_2}{(2\pi)^4}\widetilde{H}_{\omega_1\omega_2\omega_3\omega_4}(k_2-k_1) \\ \times\mathrm{Tr}\Big(\Gamma_\rho\widetilde{S}(k_1;m)\Gamma_\sigma\widetilde{S}(k_2-q;m)\Big). \tag{2.28}$$

The Dirac trace is more easily performed after expanding the fermion propagators in the quark mass.

2.3.2 Mass Expansion for Fermion Propagators

For mass expansions of fermion propagators, we have

$$S(k;m) = \sum_{n=0}^{\infty}\frac{1}{n!}\,m^n\left(\frac{\partial^n}{\partial m^n}S(k;m)\right)\Bigg|_{m=0}. \tag{2.29}$$

However, we have

$$\frac{\partial}{\partial m}S(k;m) = S(k;m)^2, \tag{2.30}$$

which is easily generalized to

$$\frac{\partial^n}{\partial m^n}S(k;m) = n!\,S(k;m)^{n+1}. \tag{2.31}$$

This gives us a nice expression for the series expansion of fermion propagators in mass,

$$S(k;m) = \sum_{n=0}^{\infty} m^n S(k;0)^{n+1}. \tag{2.32}$$

Setting $m = 0$ in the numerator of the fermion propagator leaves the numerator proportional to a Dirac matrix. Thus, the n^{th} term in (2.32) has $n+1$ Dirac matrices.

2.3.3 Perturbative Diagram Mass Expansion

In this calculation, we separate

$$\Pi^{\mu\nu(i)}(q) = \Pi^{\mu\nu(i)}_{O(1)}(q) + \Pi^{\mu\nu(i)}_{O(m^2)}(q), \tag{2.33}$$

where this diagram is the sum of the first order term plus the first mass correction. This is convenient because the Dirac structure of the mass correction is much more complicated than that of the leading order mass term. The first order term in the mass expansion for $\Pi^{\mu\nu}(q)$ allows us to simply set the masses in the fermion propagators to zero, yielding an expression of the form

$$\begin{aligned}\Pi^{\mu\nu(i)}_{O(1)}(q) = -16\pi\alpha_s\, i\, \Delta^{\mu\rho\omega_1\omega_2}\Delta^{\nu\sigma\omega_3\omega_4} \int \frac{d^4k_1}{(2\pi)^4}\frac{d^4k_2}{(2\pi)^4}\widetilde{H}_{\omega_1\omega_2\omega_3\omega_4}(k_2-k_1) \\ \times \mathrm{Tr}\Big(\Gamma_\rho \widetilde{S}(k_1;0)\Gamma_\sigma \widetilde{S}(k_2-q;0)\Big).\end{aligned} \tag{2.34}$$

In terms of the explicit Dirac structure, this expression is

$$\begin{aligned}\Pi^{\mu\nu(i)}_{O(1)}(q) = -16\pi\alpha_s\, i\, \Delta^{\mu\rho\omega_1\omega_2}\Delta^{\nu\sigma\omega_3\omega_4} \int \frac{d^4k_1}{(2\pi)^4}\frac{d^4k_2}{(2\pi)^4}\widetilde{H}_{\omega_1\omega_2\omega_3\omega_4}(k_2-k_1) \\ \times \frac{1}{k_1^2(k_2-q)^2}\mathrm{Tr}\big(\Gamma_\rho \not{k}_1 \Gamma_\sigma(\not{k}_2 - \not{q})\big).\end{aligned} \tag{2.35}$$

Due to the introduction of an additional Dirac matrix from the mass expansion (2.32), the $O(m)$ correction to $\Pi^{\mu\nu}(q)$ is zero. This is due to the fact that for either choice of Γ_μ, there are an overall odd number of γ-matrices, the trace of which is zero, as outlined in Appendix A.2.

The next non-zero term in the series shows up at $O(m^2)$, and using (2.32) for the fermion propagators yields

$$\begin{aligned}\Pi^{\mu\nu(i)}_{O(m^2)}(q) = -16\pi\alpha_s m^2\, i\, \Delta^{\mu\rho\omega_1\omega_2}\Delta^{\nu\sigma\omega_3\omega_4}\int \frac{d^4k_1}{(2\pi)^4}\frac{d^4k_2}{(2\pi)^4}\widetilde{H}_{\omega_1\omega_2\omega_3\omega_4}(k_2-k_1)\\ \times \mathrm{Tr}\Big(\Gamma_\rho \widetilde{S}(k_1;0)^3\Gamma_\sigma\widetilde{S}(k_2-q;0) + \Gamma_\rho\widetilde{S}(k_1;0)^2\Gamma_\sigma\widetilde{S}(k_2-q;0)^2\\ + \Gamma_\rho\widetilde{S}(k_1;0)\Gamma_\sigma\widetilde{S}(k_2-q;0)^3\Big).\end{aligned} \tag{2.36}$$

Writing this explicitly in terms of the Dirac structure, we have

$$\begin{aligned}\Pi^{\mu\nu(i)}_{O(m^2)}(q) = -16\pi\alpha_s m^2\, i\, \Delta^{\mu\rho\omega_1\omega_2}\Delta^{\nu\sigma\omega_3\omega_4}\int \frac{d^4k_1}{(2\pi)^4}\frac{d^4k_2}{(2\pi)^4}\widetilde{H}_{\omega_1\omega_2\omega_3\omega_4}(k_2-k_1)\\ \times\Bigg(\frac{1}{(k_1)^6(k_2-q)^2}\mathrm{Tr}\big(\Gamma_\rho \not{k}_1^{\,3}\Gamma_\sigma(\not{k}_2-\not{q})\big)\\ + \frac{1}{(k_1)^4(k_2-q)^4}\mathrm{Tr}\big(\Gamma_\rho \not{k}_1^{\,2}\Gamma_\sigma(\not{k}_2-\not{q})^2\big)\\ + \frac{1}{(k_1)^2(k_2-q)^6}\mathrm{Tr}\big(\Gamma_\rho \not{k}_1\Gamma_\sigma(\not{k}_2-\not{q})^3\big)\Bigg).\end{aligned} \tag{2.37}$$

This second order contribution is only relevant when the quark mass is large compared to the external scale. For light quarks, the mass is small enough that the first order expression is sufficient, but heavier quarks (like strange) require higher order corrections. For a sense of scale, the masses under consideration as listed in [19] are

$$m_u \approx 2.3\,\mathrm{MeV} \tag{2.38}$$

$$m_d \approx 4.8\,\mathrm{MeV} \tag{2.39}$$

$$m_s \approx 95\,\mathrm{MeV} \tag{2.40}$$

The much larger strange quark mass in comparison to the light up and down quarks forces us to include an $O(m_s^2)$ mass correction to perturbation theory.

Both of the leading order and $O(m^2)$ terms must have their traces taken before the integrals over the momenta can be performed. It is at this point that Γ_μ must be specified as the trace depends on its form. In anticipation of handling the integrals via dimensional regularization, the trace identities are computed in d, rather than 4, dimensions.

To perform the integrals that arise throughout this thesis, we use dimensional regularization [26, 27] to handle divergences. This technique is established in many quantum field theory textbooks such as [9] and [28], and will only briefly be outlined here.

For integrals over momentum, we generalize from 4 dimensions to d dimensions through the replacement

$$\int \frac{d^4k}{(2\pi)^4} \to \frac{1}{(\nu^2)^{\frac{d-4}{2}}} \int \frac{d^dk}{(2\pi)^d} \tag{2.41}$$

where ν is a renormalization scale, with the dimensions of momentum. This factor of ν appears later in our final results in dimensionless ratios with the external momentum, as an argument of a logarithm. Thus, our correlation functions will be functions of this scale.

The use of dimensional regularization allows us to extract divergent behaviour in the limit $d \to 4$, by letting $d = 4 + 2\epsilon$, expanding the results of the integrals in powers of ϵ, and letting $\epsilon \to 0$. This convention is in line with [10]. While explicit divergent structure in the form of $\frac{1}{\epsilon}$ arises from the evaluation of several of the integrals throughout this thesis, we can take care to eliminate it in order to extract physical quantities that we are interested in.

Although tensor integrals can be computed, it is simpler to perform scalar integrals. Thus, at this point, we project out the spin one and spin zero components of $\Pi^{\mu\nu}(q)$ using (2.10) and (2.11) to yield a fully contracted expression. Upon specifying $\Delta_{\mu\nu\rho\sigma}$ and Γ_μ, this procedure generates our eight different expressions, corresponding to eight different choices of quantum numbers, containing scalar integrals that can be performed.

2.3.4 TARCER

The integrals that are needed to sum the diagrams of Fig. 2.1 are complicated by their loop structure, and can be difficult to perform. The method developed in [29, 30] can be used to reduce the number of integrals that must be evaluated for any diagram with two or fewer loops by exchanging complicated momentum dependence in the numerators for different weights of factors appearing in the denominators. This is done by modifying the dimension of the integrals, and relating changes in dimension to changes in the powers of the denominators of various types of integrands. This, in turn, generates a collection of recursion relations that can be used to simplify integrals that come from loop diagrams.

This method is implemented via the Mathematica package TARCER, developed by R. Mertig and R. Scharf, outlined in [31]. As the integrals generated in these hybrid correlation function calculations are complicated and numerous, it us beneficial to compare the final

results of calculations performed by hand previously to those that TARCER computes. As hybrid correlator calculations for $J^{PC} = 1^{-+}, 0^{--}$ have been performed by hand in [1], we can use TARCER to benchmark results for these quantum numbers as a consistency check. We list the final results of the correlation function calculation in the conclusion, where we will see that this is the case.

The process of using the recursion relations on the integrals from the perturbation theory analyis reduces the complicated structure to combinations of the following simple forms:

$$\text{TJI}\left[d, q^2, \{\{\nu_1, m_1\}, \{\nu_2, m_2\}, \{\nu_3, m_3\}\}\right] = \tag{2.42}$$

$$\frac{1}{\pi^d} \int \frac{d^d k_1 d^d k_2}{(k_1^2 - m_1^2)^{\nu_1}((k_1 - k_2)^2 - m_2^2)^{\nu_2}((k_2 - q)^2 - m_3^2)^{\nu_3}}, \tag{2.43}$$

$$\text{TBI}\left[d, q^2, \{\{\nu_1, m_1\}, \{\nu_2, m_2\}\}\right] = \frac{1}{\pi^{\frac{d}{2}}} \int \frac{d^d k_1}{(k_1^2 - m_1^2)^{\nu_1}((k_1 - q)^2 - m_2^2)^{\nu_2}}, \tag{2.44}$$

$$\text{TAI}\left[d, q^2, \{\{\nu_1, m_1\}\}\right] = \frac{1}{\pi^{\frac{d}{2}}} \int \frac{d^d k_1}{(k_1^2 - m_1^2)^{\nu_1}}. \tag{2.45}$$

(The notation used here is the same as is used in [31].) Therefore, these are the only integrals that need to be evaluated to yield final results.

To simplify calculations of the integrals generated by the application of perturbation theory, it is useful to automate most of the process. In Appendix B, I outline the code I wrote in order to perform traces over Dirac indices involving an arbitrary number of Dirac matrices, as well as an interface to convert the integrands produced upon completion of the traces into inputs that TARCER uses. With these, little no human intervention is required between specifying what trace needs to be performed and the evaluation of any of the loop integrals that arise.

2.3.5 Integral Substitutions

Since TARCER outputs TJI, TBI, and TAI integrals, we need final expressions for these integrals with various weights for the factors in the denominators. The massless integral cases are much simpler than the full expressions and are listed for arbitrary weights of the

denominators in [10]:

$$\text{TJI}\left[d, q^2, \{\{\nu_1, 0\}, \{\nu_2, 0\}, \{\nu_3, 0\}\}\right] = -\frac{(-q^2)^{d-4}}{(q^2)^{\nu_1+\nu_2+\nu_3-4}} \times \frac{\Gamma(\nu_1+\nu_2+\nu_3-d)\Gamma(\frac{d}{2}-\nu_3)\Gamma(\frac{d}{2}-\nu_2)\Gamma(\frac{d}{2}-\nu_1)}{\Gamma(\nu_1)\Gamma(\nu_2)\Gamma(\nu_3)\Gamma(\frac{3}{2}d-\nu_1-\nu_2-\nu_3)}, \tag{2.46}$$

$$\text{TBI}\left[d, q^2, \{\{\nu_1, 0\}, \{\nu_2, 0\}\}\right] = i\frac{(-q^2)^{\frac{d}{2}-2}}{(q^2)^{\nu_1+\nu_2-2}} \frac{\Gamma(\frac{d}{2}-\nu_1)\Gamma(\frac{d}{2}-\nu_2)\Gamma(\nu_1+\nu_2-\frac{d}{2})}{\Gamma(\nu_1)\Gamma(\nu_2)\Gamma(d-\nu_1-\nu_2)}. \tag{2.47}$$

The massless TAI integral, however, corresponds to a massless tadpole diagram. Since all of the integrals being performed are done in the massless limit, any result that yields an integral of the form of the TAI is automatically zero and does not need to be considered [28]. Thus,

$$\text{TAI}\left[d, q^2, \{\{\nu_1, 0\}\}\right] = 0. \tag{2.48}$$

The TJI and TBI integrals correspond to two loop and one loop diagrams respectively. As the perturbative diagram is two loop, TARCER reduces the integrals needed for the evaluation of $\Pi^{\mu\nu}(q)$ to the TJI form.

2.3.6 Final Result

Applying the TARCER recursion relations to the expressions in (2.35) and (2.37), we generate integrals of the forms outlined in Section 2.3.4, which evaluate to the expressions outlined in Section 2.3.5. We are interested in the $d \to 4$ limit of the expressions that arise from this process; we expand around $\epsilon = 0$ in the process outlined in Section 2.3.3.

In applying this procedure, we obtain a divergent $\frac{1}{\epsilon}$ term, plus additional finite terms in the $\epsilon \to 0$ limit. As a representative result of this process, we can consider the scalar projection of the massless perturbative result with the choice of $\Delta^{(2)}_{\mu\nu\rho\sigma}$ and $\Gamma^{(2)}_{\mu}$:

$$\begin{aligned}\Pi^{(i)}_S(q^2) = &-\frac{\alpha_s}{960\pi^3\epsilon}q^6 + \frac{\alpha_s}{19200\pi^3}q^6\left(57 + 40(\log(4\pi)-\gamma_E) - 40\log\left(\frac{-q^2}{\nu^2}\right)\right) \\ &+ \frac{\alpha_s}{32\pi^3\epsilon}m^2q^4 - \frac{\alpha_s}{384\pi^3}m^2q^4\left(31 + 24(\log(4\pi)-\gamma_E) - 24\log\left(\frac{-q^2}{\nu^2}\right)\right).\end{aligned} \tag{2.49}$$

Here, the terms of $O(\epsilon)$ and higher are left off, as they are zero in the $\epsilon \to 0$ limit. We have also defined the strong coupling constant $\alpha_s = \frac{g_s^2}{4\pi}$. It is important to note that both m and α_s are also implicit functions of the renormalization scale ν. However, a representative value of α_s, evaluated at the scale $M_\tau^2 \approx (1.776)^2\,\mathrm{GeV}^2$ is given in [19] as

$$\alpha_s(M_\tau^2) \approx 0.330. \tag{2.50}$$

As the factors of $\log(4\pi)$ and γ_E always appear in these calculations in this way, we can discard them under the following rescaling scheme

$$\nu^2 \to 4\pi e^{-\gamma_E}\nu^2 \tag{2.51}$$

wherever the renormalization scale appears. With this, we have our final result for the scalar projection,

$$\begin{aligned}\Pi_S^{(i)}(q^2) = &-\frac{\alpha_s}{960\pi^3\epsilon}q^6 + \frac{19\alpha_s}{6400\pi^3}q^6 + \frac{\alpha_s}{480\pi^3}q^6\log\left(\frac{-q^2}{\nu^2}\right)\\ &+\frac{\alpha_s}{32\pi^3\epsilon}m^2q^4 - \frac{31\alpha_s}{384\pi^3}m^2q^4 + \frac{\alpha_s}{16\pi^3}m^2q^4\log\left(\frac{-q^2}{\nu^2}\right)\end{aligned} \tag{2.52}$$

Along with this, we can consider the vector projection of the same perturbative result, which yields

$$\begin{aligned}\Pi_V^{(i)}(q^2) = &-\frac{\alpha_s}{480\pi^3\epsilon}q^6 + \frac{77\alpha_s}{9600\pi^3}q^6 - \frac{\alpha_s}{240\pi^3}q^6\log\left(\frac{-q^2}{\nu^2}\right)\\ &+\frac{5\alpha_s}{96\pi^3\epsilon}m^2q^4 - \frac{23\alpha_s}{128\pi^3}m^2q^4 + \frac{5\alpha_s}{48\pi^3}m^2q^4\log\left(\frac{-q^2}{\nu^2}\right).\end{aligned} \tag{2.53}$$

In the above expressions, the logarithmic terms are those that we are interested in, yet there remain additional terms. The terms proportional to $\frac{1}{\epsilon}$ are divergent, and need to be handled with care; in a sum-rules analysis, a transform is applied which eliminates terms that are polynomial in q^2, terms with this type of divergent structure. This transform, known as the Borel transform [16], eliminates the non-logarithmic terms in both (2.52) and (2.53) as they are both polynomial in q^2. While these terms are thus irrelevant to a sum-rules analysis, it is still convenient to record these terms as a consistency check. Throughout this thesis, the terms that are proportional to neither the divergent terms nor the logarithmic terms in the correlation function are refererred to as *finite* contributions, in contrast with the divergent $(\frac{1}{\epsilon})$ and logarithmic contributions.

In the condensate calculations that follow, the factors of q^2 always appear in the numerator. As the dimension of the condensates increase, the power of the momentum prefactor decreases. As we consider condensates only up to dimension six, the lowest exponent of momentum appearing in prefactors is zero. Thus, we never obtain a term proportional to $\frac{1}{q^2}$, and the Borel transform can eliminate all of the divergent terms that appear in the correlation function calculations.

Lastly, although (2.52) and (2.53) are the results listed for the choice of $\Delta^{(2)}_{\mu\nu\rho\sigma}$ and $\Gamma^{(2)}_{\mu}$, similar results are obtained for the other choices of $\Delta_{\mu\nu\rho\sigma}$ and Γ_{μ}. While throughout this thesis we continue to list the results specifically for the choice $\Delta^{(2)}_{\mu\nu\rho\sigma}$ and $\Gamma^{(2)}_{\mu}$, in the conclusion we collect the contributions for all possible quantum numbers. This allows for a simple consistency check with investigations of other quantum numbers, most notably with the 0^{--} and 1^{-+} results given in [1].

2.4 Condensate Technicalities

To extract the spatial dependence of the uncontracted fields resulting from the application of Wick's Theorem, we can apply a Talyor expansion. This process generates normal-ordered products of local operators but introduces derivatives that break the gauge invariance of the condensate expressions. To extract gauge invariant information, we can exchange ordinary derivatives of the fields for gauge covariant ones. This then restores gauge invariance in expressions involving a normal-ordered product of fields but introduces higher dimensional condensate terms simply on dimensional grounds.

For both the gluon and quark fields, we need a set of rules for the exchange of ordinary derivatives for gauge covariant ones. This is most easily achieved using a specific gauge condition; once the exchange rules are specified, we can then extract the spinor and tensor structure from the VEVs.

2.4.1 Fixed Point Gauge

For calculations of Wilson coefficients, it is easiest to work with the following gauge condition, known as the *fixed point gauge* [32, 33]:

$$x_\mu B^\mu(x) = 0. \tag{2.54}$$

This gauge has the property that expressions involving derivatives of (2.54) are simplified,

$$\partial_\nu \left[x^\mu B^a_\mu(x)\right] = 0 \Rightarrow x^\mu \partial_\nu B^a_\mu(x) = -B^a_\nu(x). \tag{2.55}$$

The strength of this identity comes from being able to use it to exchange gauge dependent quantities for gauge invariant ones. For measurable quantities, gauge fields and ordinary derivatives need to be exchanged for field strength tensors and covariant derivatives, respectively, to form gauge invariant expressions.

The choice of this gauge in the condensate calculations could, in principle, interfere with the choice of the Feynman-'t Hooft gauge used to define the propagators. However, in [34], this is shown not to be the case, at least in the calculation of gauge invariant quantities. Thus, we are free to exploit the fixed point gauge in the calculation of the condensates while using the standard Feynman-'t Hooft gauge for the gluon propagators that arise in the following calculations.

To eliminate gauge fields, condition (2.55) allows the gauge field B^a_μ to be expressed as an integral of the field strength tensor $G^a_{\nu\mu}$ via

$$B^a_\mu(x) = \int_0^1 \mathrm{d}\alpha\, \alpha\, G^a_{\nu\mu}(\alpha x)\, x^\nu. \tag{2.56}$$

Equation (2.56) allows for a Taylor series expansion of the gauge fields in terms of the field strength

$$B^a_\mu(x) = \sum_{n=0}^{\infty} \frac{1}{n!\,(n+2)} x^\nu x^{\alpha_1} \cdots x^{\alpha_n} \left(\partial_{\alpha_1} \cdots \partial_{\alpha_n} G^a_{\nu\mu}(x)\right)\Big|_{x=0}. \tag{2.57}$$

However, the derivatives in this expansion are not gauge covariant, and so need to be replaced. However, direct substitution of gauge covariant derivatives for ordinary ones does

not yield a gauge invariant quantity, but the following arrangement does:

$$B_\mu(x) = \sum_{n=0}^{\infty} \frac{1}{n!\,(n+2)} x^\nu x^{\alpha_1} \cdots x^{\alpha_n} \left(\left[D_{\alpha_1}, \left[D_{\alpha_2}, \left[\cdots \left[D_{\alpha_n}, G_{\nu\mu}(x) \right] \right] \right] \right] \right) \Big|_{x=0}. \tag{2.58}$$

To see that this is the case, we can generalize (2.55) for an arbitrary number of derivatives,

$$x^{\alpha_1} \cdots x^{\alpha_n} \partial_{\alpha_1} \cdots \partial_{\alpha_{n-1}} B_{\alpha_n}(x) = -n\, x^{\alpha_1} \cdots x^{\alpha_{n-1}} \partial_{\alpha_1} \cdots \partial_{\alpha_{n-2}} B_{\alpha_{n-1}}(x). \tag{2.59}$$

As this is recursive, we can apply the same procedure repeatedly to the right hand side of (2.59) which yields

$$x^{\alpha_1} \cdots x^{\alpha_n} \partial_{\alpha_1} \cdots \partial_{\alpha_{n-1}} B_{\alpha_n}(x) = (-1)^m\, m!\, x^\alpha B_\alpha(x). \tag{2.60}$$

However,the fixed point gauge condition (2.54) sets the above to zero, leaving

$$x^{\alpha_1} \cdots x^{\alpha_n} \partial_{\alpha_1} \cdots \partial_{\alpha_{n-1}} B_{\alpha_n}(x) = 0. \tag{2.61}$$

Equation (2.61) implies that any number of derivatives acting on a gauge field, with each index contracted against a spacetime variable x, is zero. The implications of this are far reaching in terms of how we can construct gauge invariant expressions with covariant derivatives. Often, the replacement of ordinary derivatives with covariant ones generates terms with derivatives that act on the gauge fields, but (2.61) implies that all of these terms are zero.

For expressions involving quark fields, we have the ordinary Taylor series expansion

$$\psi(x) = \sum_{n=0}^{\infty} \frac{1}{n!} x^{\alpha_1} \cdots x^{\alpha_n} \left(\partial_{\alpha_1} \cdots \partial_{\alpha_n} \psi(x) \right) \Big|_{x=0}; \tag{2.62}$$

however, we would like to exchange the ordinary derivatives in (2.62) for covariant ones. In this case, we can simply make the replacement directly:

$$\psi(x) = \sum_{n=0}^{\infty} \frac{1}{n!} x^{\alpha_1} \cdots x^{\alpha_n} \left(D_{\alpha_1} \cdots D_{\alpha_n} \psi(x) \right) \Big|_{x=0}. \tag{2.63}$$

We obtain a similar expression

$$\overline{\psi}(x) = \sum_{n=0}^{\infty} \frac{1}{n!} x^{\alpha_1} \cdots x^{\alpha_n} \left(\overline{\psi}(x) D^\dagger_{\alpha_1} \cdots D^\dagger_{\alpha_n} \right) \Big|_{x=0}, \tag{2.64}$$

where we have

$$\overline{\psi}(x) \partial^\dagger_\mu \equiv \partial_\mu \overline{\psi}(x). \tag{2.65}$$

2.4.2 Expansion of VEVs

Using the fixed point gauge condition, we can apply a series expansion to the normal-ordered products of uncontracted fields in (2.13) to extract gauge invariant information. As a particular example, we can extract the spatial dependence of the normal-ordered product of the fourth term in (2.13) as follows:

$$\begin{aligned} :G^n_{\mu\nu}(x)G^m_{\rho\sigma}(0): = {} & :G^n_{\mu\nu}(0)G^m_{\rho\sigma}(0): + x^\alpha :[D_\alpha, G^n_{\mu\nu}](0)G^m_{\rho\sigma}(0): \\ & + \frac{1}{2}x^\beta x^\alpha :[D_\beta,[D_\alpha, G^n_{\mu\nu}]](0)G^m_{\rho\sigma}(0): + \dots . \end{aligned} \tag{2.66}$$

From this expansion, we can see that the first term directly corresponds to the third term of (2.14). For the higher order terms, it is less apparent what contribution they make to the OPE.

The extraction of the tensor structure (as there is no spinor structure in this expression) from each term in (2.66) yields a combinatoric factor involving the necessary Lorentz indices times a scalar VEV, which we have identified as a condensate, and will match a term in the OPE for the correlation function. In the case of (2.66), the tensor structure must respect the symmetries of the gluon fields involved in the series expansion. However, since the scale x has been extracted from the gluon fields via Taylor series expansion, the only structures we have available to construct a tensor are metric tensors $g_{\mu\nu}$.

Looking at the second term on the RHS of (2.66), there are an odd number of Lorentz indices. As the only tensors we can form are made of metric tensors, which have an even number of indices, there is no tensor that we can construct that respects the symmetries of the normal-ordered product. Thus, this term must be zero. The same goes for all terms in this series with an odd number of Lorentz indices, by the same argument.

Thus, this expansion only includes every other term, leaving

$$\left\langle :G^n_{\mu\nu}(x)G^m_{\rho\sigma}(0):\right\rangle = \left\langle :G^n_{\mu\nu}(0)G^m_{\rho\sigma}(0):\right\rangle + \frac{1}{2}x^\beta x^\alpha \left\langle :[D_\beta,[D_\alpha, G^n_{\mu\nu}]](0)G^m_{\rho\sigma}(0):\right\rangle + \dots \tag{2.67}$$

We want to extract all of the colour and tensor structure from (2.67). For the first term,

we can write

$$\left\langle :G^n_{\mu\nu}(0)G^m_{\rho\sigma}(0):\right\rangle \;=\; Y_{1\,\mu\nu\rho\sigma}^{\;\;nm}\left\langle :(G^a_{\alpha\beta})^2(0):\right\rangle$$

$$\equiv Y_{1\,\mu\nu\rho\sigma}^{\;\;nm}\left\langle G^2\right\rangle . \tag{2.68}$$

Here, we have defined

$$Y_{1\,\mu\nu\rho\sigma}^{\;\;nm} = \frac{1}{8\,d(d-1)}\delta^{nm}(g_{\mu\rho}g_{\nu\sigma} - g_{\mu\sigma}g_{\nu\rho}), \tag{2.69}$$

where d is the dimension of spacetime. The tensor decomposition of this condensate, as well as several others (including others that appear in this thesis) can be found in [35, 16, 36]. The second term in (2.67) has a much more involved tensor decomposition; however, on dimensional grounds, this term cannot contribute to the 4D gluon condensate, so we postpone its analysis Section 2.6.

Similarly, we can apply (2.63) and (2.64) to the vacuum expectation values of the normal ordered products of the uncontracted fields in the second and third terms respectively of (2.13) to obtain

$$\left\langle :\overline{\psi}_{\gamma,k}(x)\psi_{\beta,j}(0):\right\rangle \;=\; \left\langle :\overline{\psi}_{\gamma,k}(0)\psi_{\beta,j}(0):\right\rangle + \;x^\xi\left\langle :(\overline{\psi}_{\gamma,k}D^\dagger_\xi)(0)\psi_{\beta,j}(0):\right\rangle + \ldots \tag{2.70}$$

$$\left\langle :\overline{\psi}_{\alpha,i}(0)\psi_{\delta,l}(x):\right\rangle \;=\; \left\langle :\overline{\psi}_{\alpha,i}(0)\psi_{\delta,l}(0):\right\rangle + \;x^\xi\left\langle :\overline{\psi}_{\alpha,i}(D_\xi\psi_{\delta,l})(0):\right\rangle + \ldots . \tag{2.71}$$

As in (2.67), we obtain a series with VEVs of increasing dimension. However, the structure of the VEVs is richer in this case as there is not only Lorentz structure, but Dirac structure as well. Though the complexity of the VEVs increases for each additional term in the series expansion, the first term in both (2.70) and (2.71) has a particularly simple tensor structure:

$$\left\langle :\overline{\psi}^\alpha_i(0)\psi^\beta_j(0):\right\rangle = Y_{2\,ij}^{\;\;\alpha\beta}\left\langle :\overline{\psi}^\xi_k(0)\psi^\xi_k(0):\right\rangle$$

$$\equiv Y_{2\,ij}^{\;\;\alpha\beta}\left\langle \overline{\psi}\psi\right\rangle . \tag{2.72}$$

Here, we have defined

$$Y_{2\,ij}^{\;\;\alpha\beta} = \frac{1}{12}\delta_{ij}\delta^{\alpha\beta}. \tag{2.73}$$

For the next order terms in the series (2.70) and (2.71), we eliminate the derivative inside of the normal-ordered product via the use of the equation of motion for the fermion fields

$$\gamma^\mu D_\mu \psi(x) = -im\psi(x) \tag{2.74}$$

to obtain the following decomposition:

$$\left\langle : \overline{\psi}_i^\alpha (D_\mu \psi_j^\beta)(0) : \right\rangle = Y_{3\mu,ij}^{\alpha\beta} \left\langle \overline{\psi}\psi \right\rangle . \tag{2.75}$$

Here, we define

$$Y_{3\mu,ij}^{\alpha\beta} = -\frac{im}{12d}(\gamma_\mu)_{ji}\delta^{\alpha\beta}. \tag{2.76}$$

To analyze the term with $D^\dagger$, we can invoke *translation invariance*. Translation invariance simply states that the local VEVs are position independent, and thus

$$\begin{aligned} \partial_\mu \left\langle : \overline{\psi}\psi : \right\rangle &= 0 \\ &= \left\langle : (\partial_\mu \overline{\psi})\psi : \right\rangle + \left\langle : \overline{\psi}(\partial_\mu \psi) : \right\rangle . \end{aligned} \tag{2.77}$$

The first equality arises from the fact that the VEV is a scalar, while the second is just application of the product rule to the fields. We can upgrade the derivatives on these terms to covariant ones via (2.63) and (2.64) to obtain

$$\left\langle : (\overline{\psi} D_\mu^\dagger)\psi : \right\rangle = - \left\langle : \overline{\psi}(D_\mu \psi) : \right\rangle . \tag{2.78}$$

Again, these condensates can be found in [35], amongst others. Thus, we can apply the result from (2.75) to (2.70) with the introduction of a minus sign for the second term in the series expansion. With this, we can rewrite (2.70) and (2.71):

$$\left\langle : \overline{\psi}_{\gamma,k}(x)\psi_{\beta,j}(0) : \right\rangle \; = \; (Y_{2jk}^{\gamma\beta} - x^\xi Y_{3\xi,jk}^{\gamma\beta}) \left\langle \overline{\psi}\psi \right\rangle + \ldots \tag{2.79}$$

$$\left\langle : \overline{\psi}_{\alpha,i}(0)\psi_{\delta,l}(x) : \right\rangle \; = \; (Y_{2li}^{\alpha\delta} + x^\xi Y_{3\xi,li}^{\alpha\delta}) \left\langle \overline{\psi}\psi \right\rangle + \ldots \tag{2.80}$$

Both (2.79) and (2.80) appear in [35], but the use of Y_2 and Y_3 is my own convention. Of note in the expansions (2.79) and (2.80) is the Dirac structure.

In calculating the condensate contributions to the correlation function, there is always a Dirac trace that needs to be performed. In the massless limit (when performing the small mass expansion), (2.32) tells us that each fermion propagator is proportional to a gamma matrix, while the definition of the current supplies an even number of of gamma matrices (two of either γ^μ or $\gamma^\mu\gamma^5$). This allows us to easily identify which terms inside of a trace over the Dirac structure will yield zero, knowing the Dirac matrix structure of Y_2 and Y_3; for condensates with an odd dimension, this always conspires to pair the condensate with a factor of the quark mass, to obtain an expression with an even dimension.

Having extracted Lorentz and colour structure from the first term of (2.67), we can identify this as a contribution to the 4D gluon condensate. Similarly, with the extraction of the Lorentz, Dirac and colour structure from the first two terms of (2.70) and (2.71) as in (2.79) and (2.80), we can identify these as contributions to the 4D quark condensate in the OPE.

The term of next highest dimension product of fields remaining in a normal-ordered product in (2.13) is the fifth, with only the gluon field tensors contracted. Using the covariant series expansion of the fields, we obtain the following expression for the normal-ordered product:

$$:\overline{\psi}_i^\alpha(x)\psi_j^\beta(x)\overline{\psi}_k^\gamma(0)\psi_l^\delta(0):=:\overline{\psi}_i^\alpha(0)\psi_j^\beta(0)\overline{\psi}_k^\gamma(0)\psi_l^\delta(0):+\ldots. \tag{2.81}$$

The higher order terms in this expansion involve covariant derivatives of the quark fields; however, on dimensional grounds, as position space derivatives have dimensions of mass, each higher order term in this series is related to a combination of fields of higher dimension by the application of the equations of motion of the fields. This, in turn, can cause different condensate contributions to contribute at higher order in the expansion in x. If we restrict our attention to condensates of dimension six and lower, then the higher order terms in this series are irrelevant.

In order to extract the spinor and colour structure, we look at the VEV of the RHS of (2.81). In order to simplify this expression, we can invoke an approximation known as the vacuum saturation hypothesis [16], which allows us to write the 6D condensate as a product

of two 3D ones:

$$\left\langle : \overline{\psi}_i^\alpha(0)\psi_j^\beta(0)\overline{\psi}_k^\gamma(0)\psi_l^\delta(0) : \right\rangle = \left\langle : \overline{\psi}_i^\alpha(0)\psi_j^\beta(0) : \right\rangle \left\langle : \overline{\psi}_k^\gamma(0)\psi_l^\delta(0) : \right\rangle - \left\langle : \overline{\psi}_i^\alpha(0)\psi_l^\delta(0) : \right\rangle \left\langle : \overline{\psi}_k^\gamma(0)\psi_j^\beta(0) : \right\rangle . \tag{2.82}$$

For each of the individual condensates remaining, we can apply (2.72), which yields

$$\left\langle : \overline{\psi}_i^\alpha(0)\psi_j^\beta(0)\overline{\psi}_k^\gamma(0)\psi_l^\delta(0) : \right\rangle = Y_{4_{ijkl}}^{\alpha\beta\gamma\delta} \left\langle : \overline{\psi}(0)\psi(0) : \right\rangle \left\langle : \overline{\psi}(0)\psi(0) : \right\rangle \equiv Y_{4_{ijkl}}^{\alpha\beta\gamma\delta} \left\langle \overline{\psi}\psi \right\rangle^2 . \tag{2.83}$$

Here, we have defined

$$Y_{4_{ijkl}}^{\alpha\beta\gamma\delta} = -\frac{1}{144}(\delta_{il}\delta_{jk}\delta^{\alpha\delta}\delta^{\beta\gamma} - \delta_{ij}\delta_{kl}\delta^{\alpha\beta}\delta^{\gamma\delta}). \tag{2.84}$$

The remaining higher dimensional condensates are more complicated. Both the higher order terms coming from the series expansions (2.67), (2.70) and (2.71) and terms arising from the insertion of the interactions from the QCD Lagrangian to the higher dimensional condensates. However, having accounted for all of the lowest dimension condensate terms, we can calculate these condensate contributions immediately.

This section has layed out all of the technicalities needed for computation of the simplest condensate contributions to the correlator. The process of extracting the Dirac, colour, Lorentz and spacetime structure of these VEV expressions can be found in more detail in [35]. However, in the context used here, most of the condensates have a much simpler form, as we only consider one nonzero spacetime point x, which simplifies the condensate expressions considerably.

2.5 Lowest Dimensional Condensates

We can apply the first order results from (2.67), (2.70), (2.71) and (2.81) to the normal-ordered products contained in the Wick's Theorem expansion of the currents (2.13). On dimensional grounds, considering only those products of operators which are at most dimension six, we only evaluate terms two through five of (2.13); the first term contributes only to the perturbative expression while the others all contribute to condensate terms.

Throughout the rest of this thesis, there will be many contributions to the correlator that have the same value. This occurs when at least one contribution is related to another by a linear shift in the momentum variable in an integral; equivalently, this occurs when their Feynman diagram representations are identical. Due to this equivalence, in most cases we are free to calculate one of the contributions to the correlator, and simply multiply this result by the number of equivalent contributions.

In the calculations that follow, we use the general term *diagram* to be the sum of all the contributions with identical propagator structure. Equivalently, the term *diagram* is used to denote the sum of all topologically identical Feynman diagrams of a given type. Each calculation then has a representative contribution, which is then multiplied by the number of equivalent contractions at the end of the calculation. The number of identical contributions is what is referred to as the *multiplicity* of any given diagram.

2.5.1 Diagram II

For the condensate calculations, we denote each section by "Diagram M", where M is a Roman numeral corresponding to the diagram labelled by M in Figure 2.1. In what follows in this thesis, we calculate each Feynman diagram topology in Figure 2.1 in increasing Roman numeral value, and identify each diagram with its appropriate condensate.

From 2.4, we see that both the second and third terms of (2.13) contribute to the 4D quark condensate. From the correlator (2.12), we see that both terms in (2.13) share the same overall coefficient; thus, we define

$$\begin{aligned}\Pi^{\mu\nu(ii)}(q) = \frac{i}{4}\, g_s^2\, \Delta^{\mu\rho\omega_1\omega_2}\Delta^{\nu\sigma\omega_3\omega_4}\lambda^n_{ab}\lambda^m_{cd}(\Gamma_\rho)_{ij}(\Gamma_\sigma)_{kl}\int d^4x\, e^{iq\cdot x} \\ \Big(\langle : \overline{\psi}^a_i(x)\psi^b_j(x)\overline{\psi}^c_k(0)\psi^d_l(0)G^n_{\omega_1\omega_2}(x)G^m_{\omega_3\omega_4}(0) : \rangle \\ + \langle : \overline{\psi}^a_i(x)\psi^b_j(x)\overline{\psi}^c_k(0)\psi^d_l(0)G^n_{\omega_1\omega_2}(x)G^m_{\omega_3\omega_4}(0) : \rangle \Big).\end{aligned} \tag{2.85}$$

The two terms in this expression have nearly identical Feynman diagram representations; Figure 2.3 is the representative diagram for this contribution, and represents (2.85).

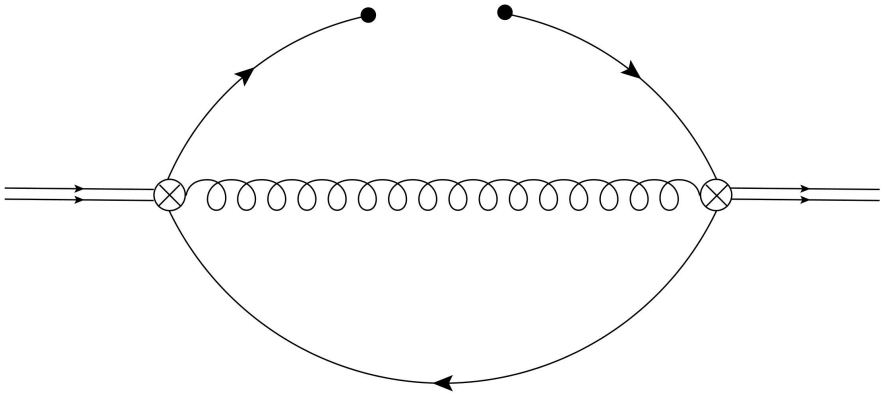

Figure 2.3: Diagram II: A representative diagram for the 4D quark condensate, of which there are two identical contributions.

Using (2.79) and (2.80), we rewrite this in terms of the 4D quark condensate,

$$\begin{aligned}\Pi^{\mu\nu(ii)}(q) = \frac{i}{4}\, g_s^2\, \Delta^{\mu\rho\omega_1\omega_2}\Delta^{\nu\sigma\omega_3\omega_4}\lambda^n_{ab}\lambda^m_{cd}(\Gamma_\rho)_{ij}(\Gamma_\sigma)_{kl}\int d^4x\, e^{iq\cdot x} \\ \times\Big(-\Big[-iS^{da}_{li}(-x)\Big]\Big[i\delta^{nm}H_{\omega_1\omega_2\omega_3\omega_4}(x)\Big]\Big[(Y^{\,bc}_{2\,kj}+x^\xi Y^{\,bc}_{3\,\xi,kj})\Big] \\ +\Big[iS^{bc}_{jk}(x)\Big]\Big[i\delta^{nm}H_{\omega_1\omega_2\omega_3\omega_4}(x)\Big]\Big[(Y^{\,ad}_{2\,il}-x^\xi Y^{\,ad}_{3\,\xi,il})\Big]\Big)\left\langle\overline{\psi}\psi\right\rangle. \end{aligned} \tag{2.86}$$

In order to evaluate the position space integral, the factor of x^ξ needs to be managed. How this is done is shown in the following example. To evaluate

$$I = \int d^4x \int \frac{d^4k_1}{(2\pi)^4}\frac{d^4k_2}{(2\pi)^4}\, e^{ix\cdot(q-k_1-k_2)}x^\xi \widetilde{S}_{jk}(k_1)\widetilde{H}_{\omega_1\omega_2\omega_3\omega_4}(k_2), \tag{2.87}$$

we can rewrite this by exchanging the factor of x^ξ for a derivative,

$$I = \int d^4x \int \frac{d^4k_1}{(2\pi)^4}\frac{d^4k_2}{(2\pi)^4}\Big(-i\frac{\partial}{\partial k_{1\xi}}\, e^{ix\cdot(q-k_1-k_2)}\Big)\widetilde{S}_{jk}(k_1)\widetilde{H}_{\omega_1\omega_2\omega_3\omega_4}(k_2), \tag{2.88}$$

and then using integration by parts on the derivative to move it onto the fermion propagator

$$I = i\int d^4x \int \frac{d^4k_1}{(2\pi)^4}\frac{d^4k_2}{(2\pi)^4}\, e^{ix\cdot(q-k_1-k_2)}\Big(\frac{\partial}{\partial k_{1\xi}}\widetilde{S}_{jk}(k_1)\Big)\widetilde{H}_{\omega_1\omega_2\omega_3\omega_4}(k_2). \tag{2.89}$$

For derivatives with respect to fermion propagator momentum, we can use

$$\frac{\partial}{\partial k_\mu}\widetilde{S}_{ij}(k) = -\Big(\widetilde{S}(k)\gamma^\mu\widetilde{S}(k)\Big)_{ij}. \tag{2.90}$$

This identity is quite useful as it provides a scheme for eliminating factors of position variables in integrands in favour of a more complicated Dirac structure.

Thus, using (2.90), we can rewrite (2.89) to obtain

$$I = -i \int d^4x \int \frac{d^4k_1}{(2\pi)^4} \frac{d^4k_2}{(2\pi)^4} \, e^{ix\cdot(q-k_1-k_2)} \Big(\widetilde{S}(k_1)\gamma^\xi \widetilde{S}(k_1) \Big)_{jk} \widetilde{H}_{\omega_1\omega_2\omega_3\omega_4}(k_2). \tag{2.91}$$

With the elimination of x^ξ, the position integral can be done, leaving

$$I = -i \int \frac{d^4k}{(2\pi)^4} \Big(\widetilde{S}(q-k)\gamma^\xi \widetilde{S}(q-k) \Big)_{jk} \widetilde{H}_{\omega_1\omega_2\omega_3\omega_4}(k). \tag{2.92}$$

Using (2.92), we can simplify (2.86) to obtain

$$\begin{aligned} \Pi^{\mu\nu(ii)}(q) = &-\frac{4}{3} \, i\pi\alpha_s \, \Delta^{\mu\rho\omega_1\omega_2} \Delta^{\nu\sigma\omega_3\omega_4} \left\langle \overline{\psi}\psi \right\rangle \int \frac{d^4k}{(2\pi)^4} \Bigg[\mathrm{Tr}\Big(\Gamma_\rho \widetilde{S}(q-k;m) \Gamma_\sigma \Big) \\ &- \frac{m}{d} \mathrm{Tr}\Big(\Gamma_\rho \gamma_\xi \Gamma_\sigma \widetilde{S}(q-k;m) \gamma^\xi \widetilde{S}(q-k;m) \Big) + \mathrm{Tr}\Big(\Gamma_\sigma \widetilde{S}(q-k;m) \Gamma_\rho \Big) \\ &- \frac{m}{d} \mathrm{Tr}\Big(\Gamma_\sigma \gamma_\xi \Gamma_\rho \widetilde{S}(q-k;m) \gamma^\xi \widetilde{S}(q-k;m) \Big) \Bigg] \widetilde{H}_{\omega_1\omega_2\omega_3\omega_4}(k). \end{aligned} \tag{2.93}$$

Then, applying (2.32) to expand the fermion propagators in mass, and keeping the lowest order non zero terms, yields

$$\begin{aligned} \Pi^{\mu\nu(ii)}(q) = &-\frac{4}{3} \, i\pi\alpha_s \, \Delta^{\mu\rho\omega_1\omega_2} \Delta^{\nu\sigma\omega_3\omega_4} m \left\langle \overline{\psi}\psi \right\rangle \int \frac{d^4k}{(2\pi)^4} \Bigg[\mathrm{Tr}\Big(\Gamma_\rho \widetilde{S}(q-k;0)^2 \Gamma_\sigma \Big) \\ &- \frac{1}{d} \mathrm{Tr}\Big(\Gamma_\rho \gamma_\xi \Gamma_\sigma \widetilde{S}(q-k;0) \gamma^\xi \widetilde{S}(q-k;0) \Big) + \mathrm{Tr}\Big(\Gamma_\sigma \widetilde{S}(q-k;0)^2 \Gamma_\rho \Big) \\ &- \frac{1}{d} \mathrm{Tr}\Big(\Gamma_\sigma \gamma_\xi \Gamma_\rho \widetilde{S}(q-k;0) \gamma^\xi \widetilde{S}(q-k;0) \Big) \Bigg] \widetilde{H}_{\omega_1\omega_2\omega_3\omega_4}(k). \end{aligned} \tag{2.94}$$

At this point, the calculation proceeds much as it does for the perturbative diagram. The traces are evaluated, and the spin projections are applied to produce scalar integrals. The integrals are then converted to d dimensional ones, and the TARCER package reduces the integrals that arise in (2.94) to TBI integrals (2.44). These integrals are then evaluated using (2.47), and undergo the substitution $d = 4 + 2\epsilon$. Finally, the results are expanded as a series in ϵ, and the limit as $\epsilon \to 0$ is taken in the finite terms.

This process is repeated for each diagram that is to be evaluated in the rest of this thesis is assumed in the calculations that follow. Once the condensate structure has been established and the mass series expansions performed as in (2.94), the process outlined yields the results of the particular scalar and vector contributions to the correlator, as in (2.52) and (2.53) for the perturbative case. For the 4D quark condensate, this process yields

$$\Pi_S^{(ii)}(q^2) = -\frac{\alpha_s}{3\pi\epsilon} m \left\langle \overline{\psi}\psi \right\rangle q^2 - \frac{\alpha_s}{2\pi} m \left\langle \overline{\psi}\psi \right\rangle q^2 - \frac{\alpha_s}{3\pi} m \left\langle \overline{\psi}\psi \right\rangle q^2 \log\left(\frac{-q^2}{\nu^2} \right), \tag{2.95}$$

$$\Pi_V^{(ii)}(q^2) = -\frac{4\alpha_s}{9\pi\epsilon} m \left\langle \overline{\psi}\psi \right\rangle q^2 - \frac{7\alpha_s}{27\pi} m \left\langle \overline{\psi}\psi \right\rangle q^2 - \frac{12\alpha_s}{27\pi} m \left\langle \overline{\psi}\psi \right\rangle q^2 \log\left(\frac{-q^2}{\nu^2}\right). \tag{2.96}$$

Of note in (2.95) and (2.96) is that the structure that would contribute to a sum-rules analyis is only the logarithmic pieces. The divergent $\frac{1}{\epsilon}$ and finite pieces would not contribute after a Borel transform of the correlator, but are listed for consistency's sake.

2.5.2 Diagram III

For the 4D gluon condensate, only the fourth term of (2.13) can contribute; none of the other terms in (2.13) have the correct normal-ordered product structure, and no QCD interaction terms can lead to a contribution of $O(g_s^2)$. Therefore, we consider only the term

$$\begin{aligned}\Pi^{\mu\nu(iii)}(q) = &\frac{i}{4} g_s^2 \, \Delta^{\mu\rho\omega_1\omega_2} \Delta^{\nu\sigma\omega_3\omega_4} \lambda^n_{ab} \lambda^m_{cd} (\Gamma_\rho)_{ij} (\Gamma_\sigma)_{kl} \int d^4x \, e^{iq\cdot x} \\ &\times \left\langle : \overline{\psi}^a_i(x) \psi^b_j(x) \overline{\psi}^c_k(0) \psi^d_l(0) G^n_{\omega_1\omega_2}(x) G^m_{\omega_3\omega_4}(0) : \right\rangle . \end{aligned} \tag{2.97}$$

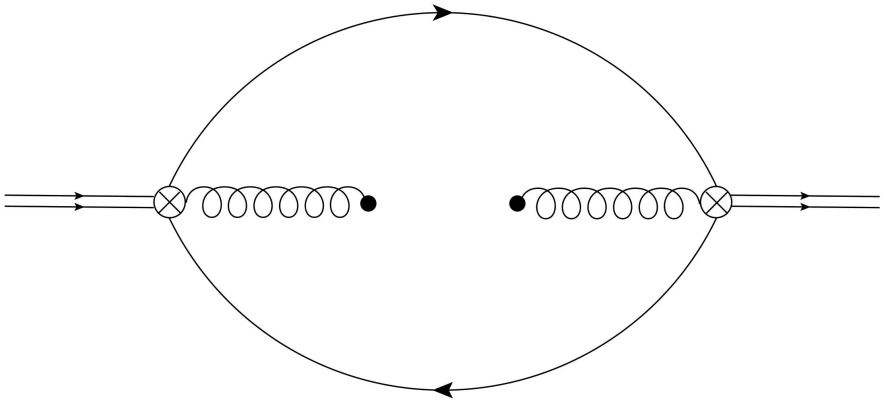

Figure 2.4: Diagram III: the only contribution to the 4D gluon condensate.

Again, higher order terms in the series (2.67), cannot contribute to the 4D gluon condensate either on dimensional grounds. Thus, we have only the one contribution, which has associated diagram Figure 2.4, which is

$$\begin{aligned}\Pi^{\mu\nu(iii)}(q) = &\frac{i}{4} g_s^2 \, \Delta^{\mu\rho\omega_1\omega_2} \Delta^{\nu\sigma\omega_3\omega_4} \lambda^n_{ab} \lambda^m_{cd} (\Gamma_\rho)_{ij} (\Gamma_\sigma)_{kl} \int d^4x \, e^{iq\cdot x} \\ &\times \Big(\Big[iS^{bc}_{jk}(x) \Big] \Big[-iS^{da}_{li}(-x) \Big] \Big[Y_{1\,\omega_1\omega_2\omega_3\omega_4}^{\,nm} \left\langle G^2 \right\rangle \Big] \Big). \end{aligned} \tag{2.98}$$

This expression is considerably simpler than that of the 4D quark condensate, yielding

$$\begin{aligned}\Pi^{\mu\nu(iii)}(q) =& 2\pi i \Delta_{\mu\rho\omega_1\omega_2}\Delta_{\nu\sigma\lambda_1\lambda_2}Y_1^{nn}_{\omega_1\omega_2\omega_3\omega_4}\left\langle \alpha G^2\right\rangle \\ &\times \int \frac{d^dk}{(2\pi)^4}\mathrm{Tr}\left(\Gamma^\rho \widetilde{S}(k;m)\Gamma^\sigma \widetilde{S}(k-q;m)\right).\end{aligned} \tag{2.99}$$

The lowest order term in the mass expansion of the integrand here has an even number of Dirac matrices, and so has a relatively simple form

$$\Pi^{\mu\nu(iii)}(q) = 2\pi i \Delta_{\mu\rho\omega_1\omega_2}\Delta_{\nu\sigma\lambda_1\lambda_2}Y_1^{nn}_{\omega_1\omega_2\omega_3\omega_4}\left\langle \alpha G^2\right\rangle \int \frac{d^4k}{(2\pi)^4}\mathrm{Tr}\left(\Gamma^\rho \widetilde{S}(k;0)\Gamma^\sigma \widetilde{S}(k-q;0)\right). \tag{2.100}$$

The expression (2.100) is then calculated via computer according to the process outlined in Section 2.5.1. The corresponding scalar and vector projections are

$$\Pi_S^{(iii)}(q^2) = -\frac{1}{24\pi\epsilon}\left\langle \alpha G^2\right\rangle q^2 - \frac{5}{144\pi}\left\langle \alpha G^2\right\rangle q^2 - \frac{1}{24\pi}\left\langle \alpha G^2\right\rangle q^2 \log\left(\frac{-q^2}{\nu^2}\right), \tag{2.101}$$

$$\Pi_V^{(iii)}(q^2) = \frac{1}{36\pi\epsilon}\left\langle \alpha G^2\right\rangle q^2 + \frac{7}{216\pi}\left\langle \alpha G^2\right\rangle q^2 + \frac{1}{36\pi}\left\langle \alpha G^2\right\rangle q^2 \log\left(\frac{-q^2}{\nu^2}\right). \tag{2.102}$$

Again, as in Section 2.5.1, only the logarithmic pieces are of physical importance for a sum-rule analysis.

2.5.3 Diagram IV

From the Wick's Theorem expansion (2.13), the fifth term gives a contribution to the 6D quark condensate, so we evaluate the following:

$$\begin{aligned}\Pi^{\mu\nu(iv)}(q) =& \frac{i}{4}g_s^2\,\Delta^{\mu\rho\omega_1\omega_2}\Delta^{\nu\sigma\omega_3\omega_4}\lambda^n_{ab}\lambda^m_{cd}(\Gamma_\rho)_{ij}(\Gamma_\sigma)_{kl}\int d^4x\, e^{iq\cdot x} \\ &\times \left\langle : \overline{\psi}^a_i(x)\psi^b_j(x)\overline{\psi}^c_k(0)\psi^d_l(0)\underbrace{G^n_{\omega_1\omega_2}(x)}G^m_{\omega_3\omega_4}(0) : \right\rangle.\end{aligned} \tag{2.103}$$

However, as the dimension of the normal-ordered product has increased, other terms may contribute to the 6D quark condensate as well. It turns out, however, that all other contributions to the 6D quark condensate contribute at $O(g_s^4)$ (or $O(\alpha_s^2)$), and therefore enter in next-to-leading order corrections in the strong coupling, which we are not considering.

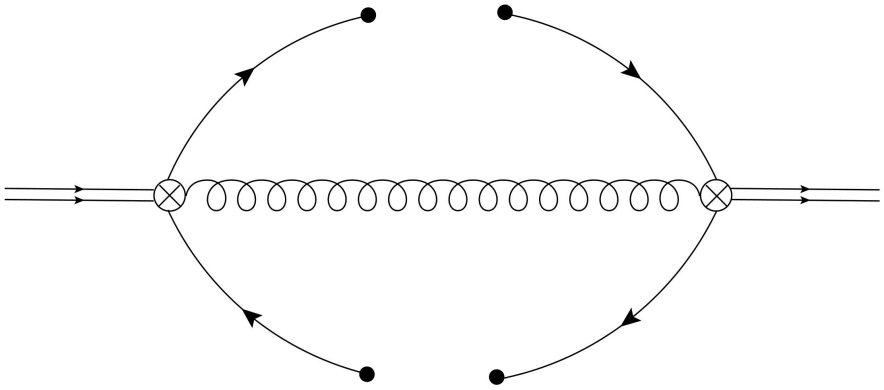

Figure 2.5: Diagram IV: The only contribution to the 6D quark condensate.

The expansion of the VEV in (2.103) then only has one term that contributes to the 6D quark condensate, corresponding to the first term in the expansion (2.81), and has a representative diagram shown in Figure 2.5. This diagram has a particularly simple structure, as there are no loops involved:

$$\Pi^{\mu\nu(iv)}(q) = \frac{i}{4}\, g_s^2\, \Delta^{\mu\rho\omega_1\omega_2}\Delta^{\nu\sigma\omega_3\omega_4}\lambda^n_{ab}\lambda^m_{cd}(\Gamma_\rho)_{ij}(\Gamma_\sigma)_{kl}\int d^4x\, e^{iq\cdot x} \\ \times\Big(\Big[i\delta^{nm}H_{\omega_1\omega_2\omega_3\omega_4}(x)\Big]\Big[Y_4^{abcd}{}_{ijkl}\left\langle\overline{\psi}\psi\right\rangle^2\Big]\Big). \tag{2.104}$$

As there are no loops, there are no undetermined momenta to integrate over, and thus we have a concise expression for the 6D quark condensate contribution

$$\Pi^{\mu\nu(iv)}(q) = \frac{\pi}{9}\alpha_s\,\Delta^{\mu\rho\omega_1\omega_2}\Delta^{\nu\sigma\omega_3\omega_4}\mathrm{Tr}(\Gamma_\rho\Gamma_\sigma)\widetilde{H}_{\omega_1\omega_2\omega_3\omega_4}(q)\left\langle\overline{\psi}\psi\right\rangle^2. \tag{2.105}$$

In this case, the full procedure of performing integrals need not be performed, and we need simply project out the spins, which yields for the scalar and vector pieces respectively

$$\Pi_S^{(iv)}(q^2) = 0, \tag{2.106}$$

$$\Pi_V^{(iv)}(q^2) = \frac{8\pi\alpha_s}{9}\left\langle\overline{\psi}\psi\right\rangle^2. \tag{2.107}$$

There is no significant reason for the vanishing of (2.106); this is not the case for all choices of P and C.

2.6 6D Gluon Condensate

2.6.1 Tensor Decomposition

The 6D gluon condensate is the first to receive contributions from multiple different terms from the Wick's Theorem expansion of the correlator. The QCD interaction terms introduce new possibilities for fields that can remain uncontracted, yielding different VEV structures that can contribute to a 6D gluon condensate.

The first of these is

$$\mathrm{Tr}\Big[\,\langle :[D_\tau,[D_\omega,G_{\mu\nu}]](0)\,G_{\rho\sigma}(0):\rangle\,\Big] \tag{2.108}$$

which arises as the second order term in the series expansion (2.67). The other term we must consider is

$$\big\langle :G^a_{\mu\nu}(0)G^b_{\rho\sigma}(0)G^c_{\omega\tau}(0):\big\rangle\,, \tag{2.109}$$

which arises when considering the correlator with the interaction (1.15). As both of these need to be expressed in terms of the 6D gluon condensate for further calculations, and the fact that their tensor decompositions are not presented in the literature, we show here how these are calculated explicitly.

For both (2.108) and (2.109), the decomposition can only depend on metric tensors and appropriate colour structures; for (2.108), the calculation involving this VEV structure is much easier if the gluon field strength tensors have their colour matrix structure built into the condensate, while (2.109) has no such difficulties. In expressions involving (2.108), this form of VEV arises regardless, and there is no loss in considering the trace form of this VEV. In both cases, the position dependence has already been stripped from the VEVs leaving little for the VEVs to depend on. In the most general sense, these VEVs could depend on an expression with arbitrary combinations of the Lorentz and colour indices; however, the anti-symmetric nature of $G^a_{\mu\nu}$ eliminates most of the freedom of possible index combinations.

For the Lorentz structure, we could simply write down every possible combination of metric tensors and then rule out those which do not have the required symmetry; however,

the number of possible terms generated using this strategy is quite large, and it is easier to simply construct explicitly the possible terms that arise.

For (2.108), the indices μ and ν cannot be paired with one another on the same metric tensor, and the same goes for the indices ρ and σ. This is due to the fact that a pairing of this kind does not respect the symmetries of the gluon field strength tensors in the VEV. With this in mind, we can write down an expression built out of metric tensors that pairs indices that do not both come from the same gluon field strength tensor,

$$g_{\mu\rho}g_{\nu\sigma}g_{\tau\omega}. \tag{2.110}$$

As the VEV is antisymmetric with respect to the exchange of the two indices on any individual gluon field strength tensor, the expression we construct must also respect this symmetry. To reflect this symmetry, we can subtract from the equation above an identical term except for the indices μ and ν swapped:

$$g_{\mu\rho}g_{\nu\sigma}g_{\tau\omega} - g_{\nu\rho}g_{\mu\sigma}g_{\tau\omega}. \tag{2.111}$$

This term is also manifestly antisymmetric under the exchange of indices $\rho \leftrightarrow \sigma$. For (2.108), there is no additional symmetry that needs to be reflected in the tensor decomposition. This is thus one of the terms which (2.108) is dependent on. However, there are additional terms that can be written down with the same logic as (2.110), with different initial pairings of indices. These expressions are then antisymmetrized following the procedure outlined above; as it turns out, there are two other unique combinations that can be constructed in this way. Thus, we must have

$$\begin{aligned}\mathrm{Tr}\Big[\,\langle :[D_\tau,[D_\omega,G_{\mu\nu}]](0)\,G_{\rho\sigma}(0):\rangle\,\Big] \;=\; & A\,g_{\tau\omega}(g_{\mu\rho}g_{\nu\sigma}-g_{\nu\rho}g_{\mu\sigma}) \\ & +B\Big(g_{\omega\sigma}(g_{\mu\tau}g_{\nu\rho}-g_{\nu\tau}g_{\mu\rho})-g_{\omega\rho}(g_{\mu\tau}g_{\nu\sigma}-g_{\nu\tau}g_{\mu\sigma})\Big) \\ & +C\Big(\,g_{\tau\sigma}(g_{\mu\omega}g_{\nu\rho}-g_{\nu\omega}g_{\mu\rho})-g_{\tau\rho}(g_{\mu\omega}g_{\nu\sigma}-g_{\nu\omega}g_{\mu\sigma})\Big).\end{aligned} \tag{2.112}$$

Through this process, we have eliminated a large number of degrees of freedom that this expression could depend upon, leaving only three undetermined constants that need to be solved for. To solve for the constants A, B and C, we can contract on the Lorentz and colour indices in three different ways, by multiplying (2.112) by $g^{\tau\omega}g^{\mu\rho}g^{\nu\sigma}\delta^{ab}$, $g^{\omega\sigma}g^{\mu\tau}g^{\nu\rho}\delta^{ab}$

and $g^{\tau\sigma}g^{\mu\omega}g^{\nu\rho}\delta^{ab}$, and rearranging the derivatives inside the normal-ordered product. Using the Bianchi/Jacobi identity [9, 10],

$$\big[D^{\rho}, G^{\mu\nu}\big] + \big[D^{\mu}, G^{\nu\rho}\big] + \big[D^{\nu}, G^{\rho\mu}\big] = 0, \tag{2.113}$$

the system of three equations can be solved simultaneously, yielding

$$\mathrm{Tr}\Big[\, \langle : [D_{\mu}, [D_{\nu}, G_{\rho\sigma}]] G_{\omega\tau} : \rangle \,\Big] = g^3\, Y_{5\mu\nu\rho\sigma\omega\tau} \left\langle G^3 \right\rangle . \tag{2.114}$$

This can be abbreviated in the same fashion as the other condensates thus far, as

$$\begin{aligned} Y_{5\mu\nu\rho\sigma\omega\tau} = &- \frac{1}{2d(d^2-4)} f^{nmt} \left\langle : G_{\mu}{}^{\nu,n} G_{\nu}{}^{\rho,m} G_{\rho}{}^{\mu,t} : \right\rangle \Big(2g_{\mu\nu}(g_{\rho\omega}g_{\sigma\tau} - g_{\sigma\omega}g_{\rho\tau}) \\ &+ g_{\nu\tau}(g_{\rho\omega}g_{\sigma\mu} - g_{\sigma\omega}g_{\rho\mu}) - g_{\nu\omega}(g_{\rho\tau}g_{\sigma\mu} - g_{\sigma\tau}g_{\rho\mu}) \\ &- \frac{3}{d-1}\big(g_{\mu\tau}(g_{\rho\omega}g_{\sigma\nu} - g_{\sigma\omega}g_{\rho\nu}) - g_{\mu\omega}(g_{\rho\tau}g_{\sigma\nu} - g_{\sigma\tau}g_{\rho\nu})\big)\Big), \end{aligned} \tag{2.115}$$

where

$$f^{nmt} \left\langle : G_{\mu}{}^{\nu,n} G_{\nu}{}^{\rho,m} G_{\rho}{}^{\mu,t} : \right\rangle \equiv \left\langle G^3 \right\rangle . \tag{2.116}$$

The structure of (2.109) can be handled with a similar approach. If we consider the following VEV, related to (2.109), but with the Lorentz indices fully contracted,

$$\left\langle : G^n_{\mu\nu} G^m_{\nu\rho} G^t_{\rho\mu} : \right\rangle , \tag{2.117}$$

and we make the exchange $n \leftrightarrow m$:

$$\begin{aligned} \left\langle : G^m_{\mu\nu} G^n_{\nu\rho} G^t_{\rho\mu} : \right\rangle &= \left\langle : G^n_{\nu\rho} G^m_{\mu\nu} G^t_{\rho\mu} : \right\rangle , \\ &= (-1)^3 \left\langle : G^n_{\rho\nu} G^m_{\nu\mu} G^t_{\mu\rho} : \right\rangle , \\ &= - \left\langle : G^n_{\mu\nu} G^m_{\nu\rho} G^t_{\rho\mu} : \right\rangle . \end{aligned} \tag{2.118}$$

We see that the VEV of (2.109) is antisymmetric under the exchange of two colour indices when the Lorentz indices are contracted, so we need only calculate the antisymmetric projection of this VEV through the use of the structure constants f^{nmt},

$$f^{nmt} \left\langle : G^n_{\mu\nu} G^m_{\rho\sigma} G^t_{\omega\tau} : \right\rangle . \tag{2.119}$$

Using the antisymmetrization procedure outlined above, we generate

$$f^{nmt}\left\langle :G^n_{\mu\nu}G^m_{\rho\sigma}G^t_{\omega\tau}:\right\rangle = \frac{1}{d(d-1)(d-2)} f^{nmt}\left\langle :G_\mu{}^{\nu,n}G_\nu{}^{\rho,m}G_\rho{}^{\mu,t}:\right\rangle \Big(g_{\mu\rho}g_{\nu\omega}g_{\sigma\tau} - g_{\nu\rho}g_{\mu\omega}g_{\sigma\tau} - g_{\mu\sigma}g_{\nu\omega}g_{\rho\tau} + g_{\nu\sigma}g_{\mu\omega}g_{\rho\tau} - g_{\mu\rho}g_{\nu\tau}g_{\sigma\omega} + g_{\nu\rho}g_{\mu\tau}g_{\sigma\omega} + g_{\mu\sigma}g_{\nu\tau}g_{\rho\omega} - g_{\nu\sigma}g_{\mu\tau}g_{\rho\omega}\Big). \tag{2.120}$$

To condense the notation, we can introduce

$$f^{nmt}\left\langle :G^n_{\mu\nu}G^m_{\rho\sigma}G^t_{\omega\tau}:\right\rangle = Y_{6\mu\nu\rho\sigma\omega\tau}\left\langle G^3\right\rangle, \tag{2.121}$$

where we have defined

$$Y_{6\mu\nu\rho\sigma\omega\tau} = \frac{1}{d(d-1)(d-2)}\Big(g_{\mu\rho}g_{\nu\omega}g_{\sigma\tau} - g_{\nu\rho}g_{\mu\omega}g_{\sigma\tau} - g_{\mu\sigma}g_{\nu\omega}g_{\rho\tau} + g_{\nu\sigma}g_{\mu\omega}g_{\rho\tau} - g_{\mu\rho}g_{\nu\tau}g_{\sigma\omega} + g_{\nu\rho}g_{\mu\tau}g_{\sigma\omega} + g_{\mu\sigma}g_{\nu\tau}g_{\rho\omega} - g_{\nu\sigma}g_{\mu\tau}g_{\rho\omega}\Big). \tag{2.122}$$

Note that using the fixed point gauge (2.56), we can rewrite any expression involving the normal-ordered products of B and G entirely in terms of G, as in

$$\left\langle :G^n_{\mu\nu}(x)B^m_\sigma(z)G^t_{\omega\tau}(0):\right\rangle = \int_0^1 d\alpha\,\alpha\,z^\rho\left\langle :G^n_{\mu\nu}(x)G^m_{\rho\sigma}(\alpha z)G^t_{\omega\tau}(0):\right\rangle. \tag{2.123}$$

This allows us to eliminate factors of B inside of normal-ordered products and, in exchanging them for G, obtain a connection to gluon condensate terms, as in (2.24) or (2.25).

2.6.2 Diagram V

The first of the two contributions to the 6D gluon condensate arises from the second order term in the expansion (in x) of

$$\Pi^{\mu\nu(v)} = \frac{i}{4}g^2\Delta_{\mu\rho\omega_1\omega_2}\Delta_{\nu\sigma\omega_3\omega_4}\Gamma^\rho_{ij}\Gamma^\sigma_{kl}\lambda^n_{ab}\lambda^m_{cd}\int d^4x\,e^{iq\cdot x} \times \left\langle :\overline{\psi}^a_i(x)\psi^b_j(x)\overline{\psi}^c_k(0)\psi^d_l(0)G^n_{\omega_1\omega_2}(x)G^m_{\omega_3\omega_4}(0):\right\rangle. \tag{2.124}$$

This expression has an associated diagram, given in Figure 2.6. This diagram is known as an *equation of motion* diagram because it does not arise directly from a term in the Wick's Theorem expansion of the correlator but rather through the series expansion of the normal

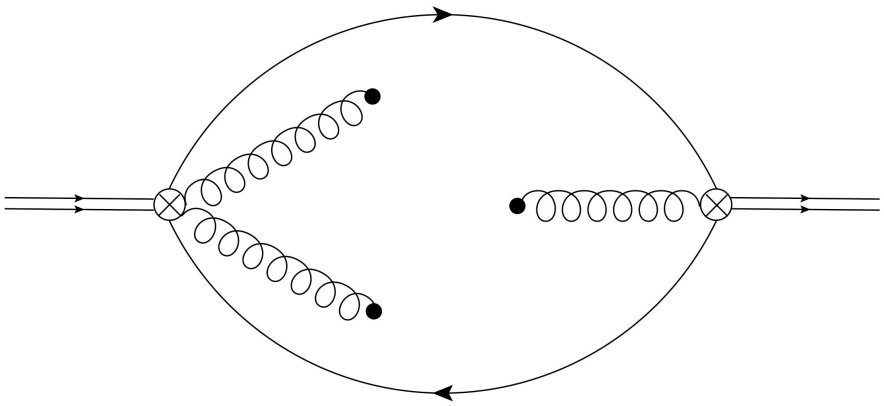

Figure 2.6: Diagram V: The first contribution to 6D gluon condensate. There is only one contribution of this type.

ordered product, which is then simplified through the use of the equations of motion for the fields.

Thus, this diagram only has one contribution given by

$$\Pi^{\mu\nu(v)} = -\frac{i}{2}g^3\Delta_{\mu\rho\omega_1\omega_2}\Delta_{\nu\sigma\omega_3\omega_4}\Gamma^{\rho}_{ij}\Gamma^{\sigma}_{kl}\left\langle G^3\right\rangle {Y_5}_{\alpha\beta}{}^{\omega_1\omega_2\omega_3\omega_4} \times \int d^4x\, e^{iq\cdot x}x^{\alpha}x^{\beta}\Big[S_{jk}(x)\Big]\Big[S_{li}(-x)\Big]. \tag{2.125}$$

We can perform integration by parts to eliminate x^{α} and x^{β}; then, only the lowest order term in the mass expansion of the fermion propagators contributes here, so for this diagram

$$\Pi^{\mu\nu(v)} = -\frac{i}{2}\Delta_{\mu\rho\omega_1\omega_2}\Delta_{\nu\sigma\omega_3\omega_4}g^3\left\langle G^3\right\rangle {Y_5}_{\alpha\beta}{}^{\omega_1\omega_2\omega_3\omega_4} \times \int \frac{d^4k}{(2\pi)^4}\mathrm{Tr}\Big[\Gamma^{\rho}\widetilde{S}(k)\gamma^{\alpha}\widetilde{S}(k)\Gamma^{\sigma}\widetilde{S}(k-q)\gamma^{\beta}\widetilde{S}(k)\Big]. \tag{2.126}$$

This expression is then handed to the computer, and once again, we follow the process outlined in Section 2.5.1. The scalar and vector projections of the correlator for this diagram are, respectively,

$$\Pi^{(v)}_S(q^2) = \frac{1}{64\pi^2\epsilon}\left\langle g^3G^3\right\rangle + \frac{19}{384\pi^2}\left\langle g^3G^3\right\rangle + \frac{1}{64\pi^2}\left\langle g^3G^3\right\rangle \log\left(\frac{-q^2}{\nu^2}\right), \tag{2.127}$$

$$\Pi^{(v)}_V(q^2) = -\frac{1}{64\pi^2\epsilon}\left\langle g^3G^3\right\rangle - \frac{5}{128\pi^2}\left\langle g^3G^3\right\rangle - \frac{1}{64\pi^2}\left\langle g^3G^3\right\rangle \log\left(\frac{-q^2}{\nu^2}\right). \tag{2.128}$$

Of note here is that the logarithmic pieces are nonzero in both of the above cases, in contrast with the 6D quark condensate. This is simply due to the fact that we have loop integrals

here, which can potentially lead to divergences, whereas the first order contribution to the 6D quark condensate has no loops.

2.6.3 Diagram VI

The second contribution to the 6D gluon condensate arise from the consideration of the QCD interaction (2.22); to account for all contributions to the 6D gluon condensate of this type, we need to consider all contractions of the form

$$\Pi^{\mu\nu(vi)} = -\frac{g^3}{8}\Delta_{\mu\rho\omega_1\omega_2}\Delta_{\nu\sigma\omega_3\omega_4}\Gamma^{\rho}_{ij}\Gamma^{\sigma}_{kl}\gamma^{\xi}_{rs}\lambda^{n}_{ab}\lambda^{m}_{cd}\lambda^{p}_{ef}\int d^4x\, d^4z\, e^{iq\cdot x} \\ \langle : \overline{\psi}^a_i(x)\psi^b_j(x)\overline{\psi}^c_k(0)\psi^d_l(0)\overline{\psi}^e_r(z)\psi^f_s(z)G^n_{\omega_1\omega_2}(x)G^m_{\omega_3\omega_4}(0)B^p_\xi(z) : \rangle\,. \quad (2.129)$$

which arise in the application of Wick's Theorem to (2.24). In what follows, we have a through f as Dirac indices, with $a, \ldots, f \in \{1, \ldots, 4\}$. For the colour indices, $r, s \in \{1, 2, 3\}$, and $p \in \{1, \ldots, 8\}$. There are two contractions like this; however, all of the contributions to the 6D gluon condensate are in fact identical, so we only outline one such calculation below. The value of this diagram can then simply be multiplied by two to obtain the final result. In what follows, we use $\Pi^{\mu\nu}_{(\text{rep.})}$ to denote a representative contribution to a given diagram, and drop the subscript (rep.) when denoting the sum of all identical contributions of a given type. The contribution (2.129) has a representative diagram given in Figure 2.7.

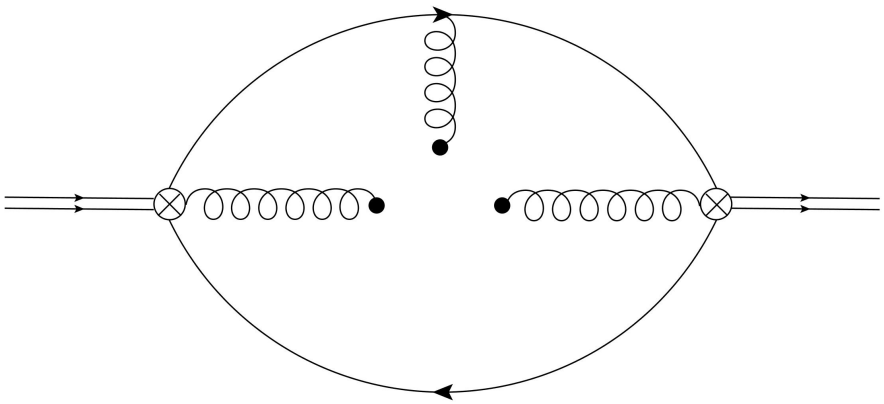

Figure 2.7: Diagram VI: The second contribution to 6D gluon condensate. There are two identical contributions of this type, corresponding to the gluon line being attached to either the top or the bottom quark line.

In terms of the propagators arising from the contraction (2.129), we have

$$\Pi^{\mu\nu(vi)}_{(\text{rep.})} = \frac{1}{8} g^3 \Delta_{\mu\rho\omega_1\omega_2} \Delta_{\nu\sigma\omega_3\omega_4} \Gamma^{\rho}_{ij} \Gamma^{\sigma}_{kl} \gamma^{\xi}_{rs} \int d^4x \, d^4z \, e^{iq\cdot x} z^{\eta} Y_6{}^{\omega_1\omega_2\omega_3\omega_4}{}_{\eta\xi} \left\langle G^3 \right\rangle \times \Big[S_{jk}(x) \Big] \Big[S_{lr}(-z) \Big] \Big[S_{si}(z-x) \Big]. \tag{2.130}$$

As per usual, we can transform the propagators into their momentum space representations to perform the position space integrals, and expand the fermion propagators in the quark mass to obtain

$$\Pi^{\mu\nu(vi)}_{(\text{rep.})} = -\frac{i}{8} \Delta_{\mu\rho\omega_1\omega_2} \Delta_{\nu\sigma\omega_3\omega_4} g^3 \left\langle G^3 \right\rangle Y_6{}^{\omega_1\omega_2\omega_3\omega_4}{}_{\eta\xi} \left\langle G^3 \right\rangle \times \int \frac{d^4k}{(2\pi)^4} \text{Tr} \Big[\Gamma^{\rho} \widetilde{S}(k) \Gamma^{\sigma} \widetilde{S}(k-q) \gamma^{\eta} \widetilde{S}(k-q) \gamma^{\xi} \widetilde{S}(k-q) \Big]. \tag{2.131}$$

Expression (2.131) is then fed into the computer. Multiplying this result by two to take into account the number of contributions with identical topologies, the scalar and vector projections of this expression respectively are

$$\Pi^{(vi)}_{S}(q^2) = -\frac{1}{64\pi^2\epsilon} \left\langle g^3 G^3 \right\rangle - \frac{3}{128\pi^2} \left\langle g^3 G^3 \right\rangle - \frac{1}{64\pi^2} \left\langle g^3 G^3 \right\rangle \log\left(\frac{-q^2}{\nu^2} \right), \tag{2.132}$$

$$\Pi^{(vi)}_{V}(q^2) = \frac{1}{64\pi^2\epsilon} \left\langle g^3 G^3 \right\rangle + \frac{5}{384\pi^2} \left\langle g^3 G^3 \right\rangle + \frac{1}{64\pi^2} \left\langle g^3 G^3 \right\rangle \log\left(\frac{-q^2}{\nu^2} \right). \tag{2.133}$$

Adding the two diagrams, we can sum the scalar ((2.127) and (2.132)) and vector contributions ((2.128) and (2.133)) to obtain

$$\Big(\Pi^{(v)}_{S} + \Pi^{(vi)}_{S} \Big)(q^2) = \frac{5}{192\pi^2} \left\langle g^3 G^3 \right\rangle, \tag{2.134}$$

$$\Big(\Pi^{(v)}_{V} + \Pi^{(vi)}_{V} \Big)(q^2) = -\frac{5}{192\pi^2} \left\langle g^3 G^3 \right\rangle. \tag{2.135}$$

The cancellation of the divergent $\frac{1}{\epsilon}$ piece and the logarithmic piece in this summation holds for all hybrid quantum numbers considered. As the logarithmic terms provide important contributions to a sum-rules analysis, this cancellation is noteworthy.

2.7 Mixed Condensates

The mixed condensate, denoted by

$$\left\langle \overline{\psi}\, \sigma_{\mu\nu} G^{\mu\nu} \psi \right\rangle , \tag{2.136}$$

has eight different contributions, arising from eight different Feynman diagram topologies. However, most of them do not arise from the time-ordered product (2.13), but rather from first order corrections in the perturbative expansion involving QCD interactions (1.15) and (1.16).

The colour structures that arise from the insertion of the QCD interaction terms in the correlator are more complicated than those athat arise from the first order ones. While the first order terms typically resulted in traces over two colour matrices, for the mixed condensate, many more possibilities arise. The algebra of these possibilities is outlined in Appendix A.2, and the details are left off of the individual condensate diagrams.

The number of equivalent topologies that arise from applying Wick's Theorem to (2.24) and (2.25) is much greater than for the first order correlator expansion (2.13). As the number is quite large, an explicit form for the Wick's Theorem expansion will be omitted; however, for each diagram, we outline the multiplicity of each in their respective sections.

Wick's Theorem, when applied to (2.24) and (2.25), gives rise to terms where perturbation theory does not make sense; we encountered one such case in Section 2.6.2. This happens when the Wick's Theorem expansion yields a diagram with a zero momentum propagator. To make sense of these contributions, we can relate them to contributions that arise from the series expansions of the condensates, as was done in Section 2.6.2. How this is done is determined by context, and the details are then outlined in the appropriate sections.

Before directly calculating the diagrams that arise, we work out the details of the mixed condensate structure itself, which simplifies the individual diagram calculations immensely.

2.7.1 Tensor Decomposition

As there are several contributions to the mixed condensate, which arise from contractions of many different types. We set out to outline the forms that the VEVs can take for use

in calculations of various diagrams. First, we consider higher order terms of the quark condensate that arises from the expansion in x of the normal-ordered product of two quark fields,

$$\begin{aligned}\Big\langle :\overline{\psi}_i^{\alpha}(x)\psi_j^{\beta}(0):\Big\rangle = \frac{1}{12}\,\delta^{\alpha\beta}\Bigg[&\bigg(\delta_{ij}\Big(1-\frac{x^2}{8}m^2\Big)\\ &+\frac{i}{d}mx^{\mu}(\gamma_{\mu})_{ji}\Big(1-\frac{x^2}{12}m^2\Big)\bigg)\,\langle\overline{\psi}\psi\rangle\\ &-\frac{i}{4d}x^2\bigg(\delta_{ij}+\frac{i}{d+2}mx^{\mu}(\gamma_{\mu})_{ji}\bigg)\,\langle\overline{\psi}\,\sigma_{\mu\nu}G^{\mu\nu}\psi\rangle\\ &+\frac{i}{288}x^2x^{\mu}(\gamma_{\mu})_{ji}\,g_s^2\Big\langle\overline{\psi}\,\gamma^{\rho}\frac{\lambda^a}{2}\psi\sum_C\overline{\psi}^C\gamma_{\rho}\frac{\lambda^a}{2}\psi^C\Big\rangle\Bigg].\end{aligned} \tag{2.137}$$

This expression contains all condensates up to dimension six, and is found in both [10] and [35]. However, as mentioned before, the six dimensional condensate involving four quark fields is a next to leading order in coupling constant correction ($O(\alpha_s^2)$), and as such, is beyond the scope of this calculation. The mixed condensate, however, has no such problem, and has a corresponding diagram that needs to be calculated.

The more common appearance of mixed condensate contributions stems from

$$\begin{aligned}\Big\langle :\overline{\psi}_i^{\alpha}(x)B_{\rho}(z)\psi_j^{\beta}(0):\Big\rangle = \frac{z^{\mu}}{96}\frac{\delta^{\alpha\beta}}{3}\Bigg[&\bigg(\sigma_{\mu\rho}-\frac{m}{2}\Big(x_{\mu}\gamma_{\rho}-x_{\rho}\gamma_{\mu}\Big)+i\frac{m}{2}x^{\nu}\sigma_{\mu\rho}\gamma_{\nu}\bigg)_{ji}\,\langle\overline{\psi}\,\sigma_{\omega\tau}G^{\omega\tau}\psi\rangle\\ &+\bigg(\frac{2i}{3}\Big(-z_{\mu}\gamma_{\rho}+z_{\rho}\gamma_{\mu}\Big)+\frac{1}{2}x^{\nu}\gamma_{\nu}\sigma_{\mu\rho}\bigg)_{ji}\\ &\times g_s^2\Big\langle\overline{\psi}\gamma^{\tau}\frac{\lambda^a}{2}\psi\sum_C\overline{\psi}^C\gamma_{\tau}\frac{\lambda^a}{2}\psi^C\Big\rangle\Bigg].\end{aligned} \tag{2.138}$$

The analagous expression involving the gluon field strength tensor rather than the gluon field itself is obtained through the relation

$$\begin{aligned}\Big\langle :\overline{\psi}_i^{\alpha}(x)G_{\mu\rho}(z)\psi_j^{\beta}(0):\Big\rangle = \frac{1}{48}\frac{\delta^{\alpha\beta}}{3}\Bigg[&\bigg(\sigma_{\mu\rho}-\frac{m}{2}\Big(x_{\mu}\gamma_{\rho}-x_{\rho}\gamma_{\mu}\Big)+i\frac{m}{2}x^{\nu}\sigma_{\mu\rho}\gamma_{\nu}\bigg)_{ji}\,\langle\overline{\psi}\,\sigma_{\omega\tau}G^{\omega\tau}\psi\rangle\\ &+\bigg(\frac{2i}{3}\Big(-z_{\mu}\gamma_{\rho}+z_{\rho}\gamma_{\mu}\Big)+\frac{1}{2}x^{\nu}\gamma_{\nu}\sigma_{\mu\rho}\bigg)_{ji}\\ &\times g_s^2\Big\langle\overline{\psi}\gamma^{\tau}\frac{\lambda^a}{2}\psi\sum_C\overline{\psi}^C\gamma_{\tau}\frac{\lambda^a}{2}\psi^C\Big\rangle\Bigg].\end{aligned} \tag{2.139}$$

Both of these expressions can be found in [35], and both of these hold for $d = 4$. As in (2.137), the four quark field condensate term enters as a next to leading order correction in

the strong coupling constant ($O(\alpha_s^2)$), and so it need not be considered at this order. To simplify how this VEV is used in calculations, we can break up the expansion (2.138) as follows:

$$\left\langle : \overline{\psi}_i^{\,\alpha}(x) B_\rho(z) \psi_j^\beta(0) : \right\rangle \;=\; \frac{z^\mu}{2}\Big(Y_{7ij,\,\mu\nu} - x^\rho\, m\, Y_{8ij,\,\mu\nu\rho} \Big) \left\langle \overline{\psi}\, \sigma_{\omega\tau} G^{\omega\tau} \psi \right\rangle , \tag{2.140}$$

$$\left\langle : \overline{\psi}_i^{\,\alpha}(0) B_\rho(z) \psi_j^\beta(x) : \right\rangle \;=\; \frac{z^\mu}{2}\Big(Y_{7ij,\,\mu\nu} + x^\rho\, m\, Y_{8ij,\,\mu\nu\rho} \Big) \left\langle \overline{\psi}\, \sigma_{\omega\tau} G^{\omega\tau} \psi \right\rangle . \tag{2.141}$$

Here we define, in d dimensions,

$$Y_{7ij,\mu\nu} = \frac{1}{4d(d-1)} \big(\sigma_{\mu\nu}\big)_{ji}, \tag{2.142}$$

$$Y_{8ij,\mu\nu\rho} = \frac{1}{4d(d-1)(d-2)} \big(g_{\rho\mu}\gamma_\nu - g_{\rho\nu}\gamma_\mu - i\sigma_{\mu\nu}\gamma_\rho\big)_{ji}. \tag{2.143}$$

The equations (2.140) and (2.141) hold only at this order of perturbation theory. This separation is convenient to split up the Dirac matrix structure by even and odd numbers of gamma matrices because they behave differently under traces.

2.7.2 Diagram VII

The first contribution to the mixed condensate arises from terms involving contractions of the form

$$\langle : \overline{\psi}_i^a(x) \underbrace{\psi_j^b(x) \overline{\psi}_k^c}(0) \psi_l^d(0) \underbrace{G^n_{\omega_1\omega_2}(x) G^m_{\omega_3\omega_4}}(0) : \rangle \,, \tag{2.144}$$

arising in the second and third terms of the Wick's Theorem expansion (2.13). The contraction of the gluon field strength tensors is more appropriately written

$$\begin{aligned} \underbrace{G^n_{\omega_1\omega_2}(x) G^m_{\omega_3\omega_4}}(0) =& \underline{G}^n_{\omega_1\omega_2}(x) \underline{G}^m_{\omega_3\omega_4}(0) + g f^{npq} \Big(B^p_{\omega_1}(x) \underbrace{B^q_{\omega_2}(x) \Big) \underline{G}^m_{\omega_3\omega_4}}(0) \\ &+ g f^{mpq} \underline{G}^n_{\omega_1\omega_2}(x) \Big(B^p_{\omega_3}(0) \underbrace{B^q_{\omega_4}}(0) \Big) \\ &+ g^2 f^{npq} f^{mrs} \Big(B^p_{\omega_1}(x) \underbrace{B^q_{\omega_2}(x) \Big) \Big(B^r_{\omega_3}(0) \underbrace{B^s_{\omega_4}}(0) \Big). \end{aligned} \tag{2.145}$$

with $\underline{G}^n_{\mu\nu}(x)$ defined in (1.18).

The last term in (2.145) contributes to a higher order in perturbation theory, so we leave it off; however, the second and third terms, by virtue of having an uncontracted field in them, contribute to the mixed condensate in (2.144). However, as a consequence of the fixed point gauge condition (2.56), we have

$$B_\mu(0) = 0. \tag{2.146}$$

Thus, for the mixed condensate contribution, we need only worry about contributions of the second term of (2.145), as the third yields zero contribution. A diagramatic representative of this form is given in Figure 2.8.

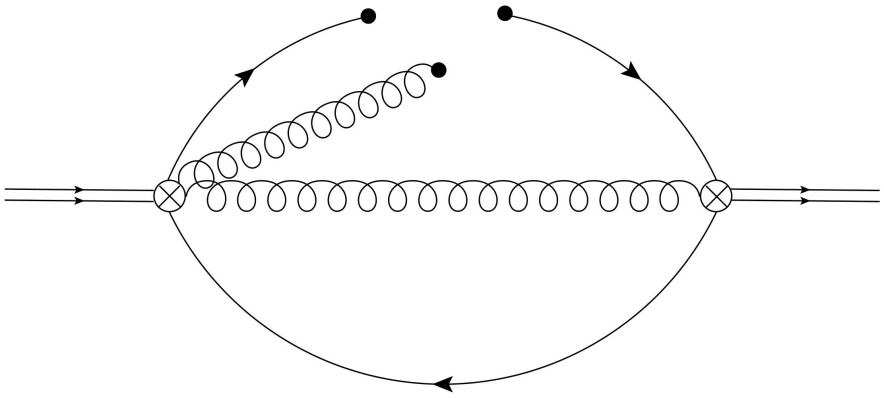

Figure 2.8: Diagram VII: The first contribution to the mixed condensate. There are two identical contributions of this type.

To account for all contributions to this diagram, we need to be careful about which contractions are identical and which are distinct. In splitting $G_{\mu\nu}$ into two pieces, when contracting $\underline{G}_{\rho\sigma}$ with either B_μ or B_ν in

$$\Big(B^a_\mu(x)\underbrace{B^b_\nu(x)\Big)\underline{G}^c_{\rho\sigma}}(0) = \underbrace{B^a_\mu(x)B^b_\nu(x)\underline{G}^c_{\rho\sigma}}(0) + B^a_\mu(x)\underbrace{B^b_\nu(x)\underline{G}^c_{\rho\sigma}}(0), \tag{2.147}$$

the two possibilities give rise to distinct contributions to the mixed condensate. However, the choice of fermion field contractions (one of which is given in (2.144)) does not matter. Thus, there are two distinct contributions to this diagram, and each contribution has a multiplicity of two, for a total of four. For the sake of simplicity, we show a calculation with only one choice of fermion field contractions; to obtain the final result for this diagram, we simply multiply the result of this calculation by two.

Before proceeding with the calculation, we introduce shorthand for a new type of gluon field contraction. As the gluon field contractions thus far have only appeared between gluon field strength tensors, this calculation is the first time where a field strength tensor explicitly is contracted with a gluon field on its own. We thus define this propagator via

$$\underbrace{G^n_{\mu\nu}(x)B^m_\rho}(y) = iH'^{nm}_{\mu\nu\rho}(x-y), \tag{2.148}$$

where

$$H'^{nm}_{\mu\nu\rho}(x-y) = i\delta^{nm}\int\frac{d^4p}{(2\pi)^4}\frac{1}{p^2}\big(p_\mu g_{\nu\rho} - p_\nu g_{\mu\rho}\big)e^{-ip(x-y)}. \tag{2.149}$$

While (2.149) is complicated in its own right, expressions involving it are handled via computer, and in defining (2.149) we avoid explicit derivatives in expressions arising from those contractions that give rise to the propagator $H'^{nm}_{\mu\nu\rho}(x-y)$.

Equipped with (2.148), one of the two contributions to the correlator under consideration is thus

$$\Pi^{\mu\nu(vii)}_{(\text{rep.})}(q) = \frac{i}{4}g^2\Delta_{\mu\rho\omega_1\omega_2}\Delta_{\nu\sigma\omega_3\omega_4}\lambda^n_{ab}\lambda^m_{cd}\Gamma^\rho_{ij}\Gamma^\sigma_{kl}f^{nrs}\int d^4x\, e^{iq\cdot x} \\ \langle :\overline{\psi}^a_i(x)\underbrace{\psi^b_j(x)\overline{\psi}^c_k}(0)\psi^d_l(0)\big(B^r_{\omega_1}(x)\underbrace{B^s_{\omega_2}(x)\big)G^m_{\omega_3\omega_4}}(0):\rangle\,. \tag{2.150}$$

The colour algebra is simplified using the identities in Appendix A.2, and we obtain an expression involving propagators and the mixed condensate,

$$\begin{aligned}\Pi^{\mu\nu(vii)}_{(\text{rep.})}(q) =& \frac{3}{4}g^2\Delta_{\mu\rho\omega_1\omega_2}\Delta_{\nu\sigma\omega_3\omega_4}\Gamma^\rho_{ij}\Gamma^\sigma_{kl}\left\langle\overline{\psi}\,\sigma G\psi\right\rangle\int d^4x\, e^{iq\cdot x}\Big[i\delta^{\beta\gamma}\widetilde{S}_{jk}(x)\Big] \\ &\times\Big\{\Big[i\widetilde{H'}^{rm}_{\omega_3\omega_4\omega_1}(x)\Big]\frac{x^\zeta}{2}\big(Y_{7li,\zeta\omega_2} - m\,x^\chi\,Y_{8li,\zeta\omega_2\chi}\big) \\ &\quad-\Big[i\widetilde{H'}^{sm}_{\omega_3\omega_4\omega_2}(x)\Big]\frac{x^\zeta}{2}\big(Y_{7li,\zeta\omega_1} - m\,x^\chi\,Y_{8li,\zeta\omega_1\chi}\big)\Big\}.\end{aligned} \tag{2.151}$$

With the expansion of the fermion propagators in mass, we have the final expression

$$\begin{aligned}\Pi^{\mu\nu(vii)}_{(\text{rep.})}(q) =&\frac{3}{8}g^2\Delta_{\mu\rho\omega_1\omega_2}\Delta_{\nu\sigma\omega_3\omega_4}m\left\langle\overline{\psi}\,\sigma G\psi\right\rangle\int\frac{d^4k}{(2\pi)^4}\\ &\Big\{\text{Tr}\Big[i\Gamma^\rho\Big(\widetilde{S}(q-k;0)^2\gamma^\zeta\widetilde{S}(q-k;0)+\widetilde{S}(q-k;0)\gamma^\zeta\widetilde{S}(q-k;0)^2\Big)\Gamma^\sigma Y_{7\zeta\omega_2}\\ &\quad+\Gamma^\rho\Big(\widetilde{S}(q-k;0)\gamma^\zeta\widetilde{S}(q-k;0)\gamma^\chi\widetilde{S}(q-k;0)\\ &\qquad+\widetilde{S}(q-k;0)\gamma^\chi\widetilde{S}(q-k;0)\gamma^\zeta\widetilde{S}(q-k;0)\Big)\Gamma^\sigma Y_{8\zeta\omega_2\chi}\Big]\widetilde{H'}_{\omega_3\omega_4\omega_1}(k)\\ &-\text{Tr}\Big[i\Gamma^\rho\Big(\widetilde{S}(q-k;0)^2\gamma^\zeta\widetilde{S}(q-k;0)+\widetilde{S}(q-k;0)\gamma^\zeta\widetilde{S}(q-k;0)^2\Big)\Gamma^\sigma Y_{7\zeta\omega_1}\\ &\quad+\Gamma^\rho\Big(\widetilde{S}(q-k;0)\gamma^\zeta\widetilde{S}(q-k;0)\gamma^\chi\widetilde{S}(q-k;0)\\ &\qquad+\widetilde{S}(q-k;0)\gamma^\chi\widetilde{S}(q-k;0)\gamma^\zeta\widetilde{S}(q-k;0)\Big)\Gamma^\sigma Y_{8\zeta\omega_1\chi}\Big]\widetilde{H'}_{\omega_3\omega_4\omega_2}(k)\Big\}.\end{aligned} \tag{2.152}$$

Then, we follow the usual procedure: perform the trace, simplify the integrals, and substitute the final results. Multiplying this result by two to take into account the multiplicity of the other choice of fermion propagator contraction, the scalar and vector projections for this diagram respectively are

$$\Pi^{(vii)}_S(q^2)=\frac{3}{64\pi}\frac{1}{\epsilon}\left\langle\overline{\psi}\,\sigma G\psi\right\rangle+\frac{3}{128\pi}\left\langle\overline{\psi}\,\sigma G\psi\right\rangle+\frac{3}{64\pi}\left\langle\overline{\psi}\,\sigma G\psi\right\rangle\log\left(\frac{-q^2}{\nu^2}\right), \tag{2.153}$$

$$\Pi^{(vii)}_V(q^2)=-\frac{3}{64\pi}\frac{1}{\epsilon}\left\langle\overline{\psi}\,\sigma G\psi\right\rangle-\frac{7}{128\pi}\left\langle\overline{\psi}\,\sigma G\psi\right\rangle-\frac{3}{64\pi}\left\langle\overline{\psi}\,\sigma G\psi\right\rangle\log\left(\frac{-q^2}{\nu^2}\right). \tag{2.154}$$

2.7.3 Diagram VIII

The mixed condensate contribution corresponding to Diagram VIII arises from two different kinds of gluon field contractions,

$$\langle:\overline{\psi}^a_i(x)\underbrace{\psi^b_j(x)\overline{\psi}^c_k}(0)\psi^d_l(0)\underbrace{G^n_{\omega_1\omega_2}(x)\underbrace{G^m_{\omega_3\omega_4}(0)G^p_{\eta\xi}(z)}B^\eta_u(z)}B^\xi_v(z):\rangle \tag{2.155}$$

and

$$\langle:\overline{\psi}^a_i(x)\underbrace{\psi^b_j(x)\overline{\psi}^c_k}(0)\psi^d_l(0)\underbrace{G^n_{\omega_1\omega_2}(x)\underbrace{G^m_{\omega_3\omega_4}(0)G^p_{\eta\xi}(z)B^\eta_u(z)}B^\xi_v(z)}:\rangle\,, \tag{2.156}$$

both of which arise in the application of Wick's Theorem to (2.25), involving the QCD interaction (1.16), with $p,u,v\in\{1,\ldots,8\}$.

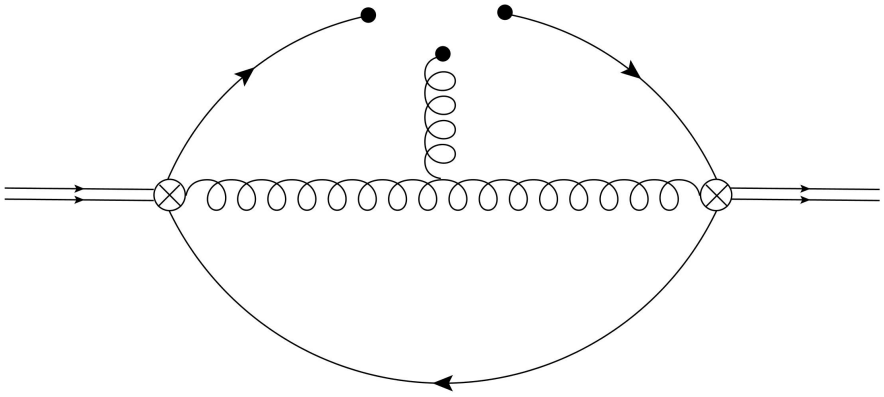

Figure 2.9: Diagram VIII: The second contribution to the mixed condensate. There are twelve contributions that have diagrams of this type, yet not all of them are equal.

A representative diagram for the sum of these contributions is given by Figure 2.9. There are four equal contributions of the type (2.155), and eight equal contributions of the type (2.156). However, since the expressions involved above have different contractions and VEVs, each type must be handled separately, and then summed after completion.

For the first case, a representative contribution is

$$\Pi^{\mu\nu(viii)}_{(\text{rep.})(1)}(q) = \frac{1}{8}g^3\Delta_{\mu\rho\omega_1\omega_2}\Delta_{\nu\sigma\omega_3\omega_4}\Gamma^{\rho}_{ij}\Gamma^{\sigma}_{kl}f_{rst}\lambda^n_{ab}\lambda^m_{cd}\int d^4x\, d^4z\, e^{iq\cdot x} \\ \langle :\overline{\psi}^a_i(x)\underbrace{\psi^b_j(x)\overline{\psi}^c_k}(0)\psi^d_l(0)\underbrace{G^n_{\omega_1\omega_2}(x)\underbrace{G^m_{\omega_3\omega_4}(0)G^p_{\eta\xi}(z)}B^{\eta}_u(z)}B^{\xi}_v(z):\rangle\,. \quad (2.157)$$

In terms of the propagators, (2.157) becomes

$$\Pi^{\mu\nu(viii)}_{(\text{rep.})(1)}(q) = -\frac{3}{8}g^3\Delta_{\mu\rho\omega_1\omega_2}\Delta_{\nu\sigma\omega_3\omega_4}\Gamma^{\rho}_{ij}\Gamma^{\sigma}_{kl}\left\langle\overline{\psi}\,\sigma G\psi\right\rangle\int d^4x\, d^4z\, e^{iq\cdot x}(Y_{7li,\eta\xi} - x^{\chi}\, m\, Y_{8li,\eta\xi\chi}) \\ \times\Big[S_{jk}(x)\Big]\Big[H'_{\omega_1\omega_2\xi}(x-z)\Big]\Big[H'_{\omega_3\omega_4\eta}(-z)\Big]. \quad (2.158)$$

Then, contracting on the relevant indices and expanding in the quark mass in the fermion propagators yields the expression

$$\Pi^{\mu\nu(viii)}_{(\text{rep.})(1)}(q) = \frac{3}{8}g^3\Delta_{\mu\rho\omega_1\omega_2}\Delta_{\nu\sigma\omega_3\omega_4}m\left\langle\overline{\psi}\,\sigma G\psi\right\rangle\int\frac{d^4k}{(2\pi)^4}\widetilde{H'}_{\omega_1\omega_2\xi}(k)\widetilde{H'}_{\omega_3\omega_4\eta}(k) \\ \text{Tr}\Big[\Gamma^{\rho}\widetilde{S}(q-k;0)^2\Gamma^{\sigma}Y_{7\eta\xi} - i\Big(\Gamma^{\rho}\widetilde{S}(q-k;0)\gamma^{\chi}\widetilde{S}(q-k;0)\Gamma^{\sigma}Y_{8\eta\xi\chi}\Big)\Big]. \quad (2.159)$$

This is then the expression that is fed to the computer for the usual procedure.

We need also compute the other contribution to Diagram VIII,

$$\Pi^{\mu\nu(viii)}_{(\text{rep.})(2)}(q) = \frac{1}{8}g^3\Delta_{\mu\rho\omega_1\omega_2}\Delta_{\nu\sigma\omega_3\omega_4}\Gamma^{\rho}_{ij}\Gamma^{\sigma}_{kl}f_{rst}\lambda^n_{ab}\lambda^m_{cd}\int d^4x\, d^4z\, e^{iq\cdot x}$$
$$\langle : \overline{\psi}^a_i(x)\underbrace{\psi^b_j(x)\overline{\psi}^c_k}(0)\psi^d_l(0)\underbrace{G^n_{\omega_1\omega_2}(x)\underbrace{G^m_{\omega_3\omega_4}(0)G^p_{\eta\xi}(z)B^{\eta}_u(z)}B^{\xi}_v(z)} : \rangle\,. \quad (2.160)$$

Then, we can convert this into an expression involving the propagators,

$$\Pi^{\mu\nu(viii)}_{(\text{rep.})(2)}(q) = \frac{3}{16}g^3\Delta_{\mu\rho\omega_1\omega_2}\Delta_{\nu\sigma\omega_3\omega_4}\Gamma^{\rho}_{ij}\Gamma^{\sigma}_{kl}\left\langle\overline{\psi}\,\sigma G\psi\right\rangle\int d^4x\, d^4z\, e^{iq\cdot x}\, z^{\tau}(Y_{7li,\tau\eta} - x^{\chi}\, m\, Y_{8li,\tau\eta\chi})$$
$$\times\Big[S_{jk}(x)\Big]\Big[H'_{\omega_1\omega_2\xi}(x-z)\Big]\Big[H_{\omega_3\omega_4\eta\xi}(-z)\Big]. \quad (2.161)$$

And finally, contracting on the indices, expanding the fermion propagators in the quark mass, forming the trace and integrating over momentum yields

$$\Pi^{\mu\nu(viii)}_{(\text{rep.})(2)}(q) = -\,i\frac{3}{16}g^3\Delta_{\mu\rho\omega_1\omega_2}\Delta_{\nu\sigma\omega_3\omega_4}\left\langle\overline{\psi}\,\sigma G\psi\right\rangle\int\frac{d^4k}{(2\pi)^4}\widetilde{H'}_{\omega_1\omega_2\xi}(k)\Big(\frac{\partial}{\partial k_{\tau}}\widetilde{H}_{\omega_3\omega_4\eta\xi}(k)\Big)$$
$$\text{Tr}\Big[\Gamma^{\rho}\widetilde{S}_{(}q-k;0)^2\Gamma^{\sigma}Y_{7\tau\eta} - i\Big(\Gamma^{\rho}\widetilde{S}_{(}q-k;0)\gamma^{\chi}\widetilde{S}_{(}q-k;0)\Gamma^{\sigma}Y_{8\tau\eta\chi}\Big)\Big]. \quad (2.162)$$

For the final result for Diagram VIII, we account for the multiplicity of each diagram and sum them. Hence our final contribution to the mixed condensate is

$$\Pi^{\mu\nu(viii)}(q) = 4\,\Pi^{\mu\nu(viii)}_{(1)}(q) + 8\,\Pi^{\mu\nu(viii)}_{(2)}(q). \quad (2.163)$$

Taking the two varieties of contributions into account with the appropriate weightings, we can project out the scalar and vector contributions to the correlator, and perform the traces and integrals via computer. The scalar and vector projections of Diagram VIII respectively are thus

$$\Pi^{(viii)}_S(q^2) = -\frac{3}{16\pi}\frac{1}{\epsilon}\left\langle\overline{\psi}\,\sigma G\psi\right\rangle - \frac{15}{64\pi}\left\langle\overline{\psi}\,\sigma G\psi\right\rangle - \frac{3}{16\pi}\left\langle\overline{\psi}\,\sigma G\psi\right\rangle\log\left(\frac{-q^2}{\nu^2}\right), \quad (2.164)$$

$$\Pi^{(viii)}_V(q^2) = \frac{3}{16\pi}\frac{1}{\epsilon}\left\langle\overline{\psi}\,\sigma G\psi\right\rangle - \frac{1}{64\pi}\left\langle\overline{\psi}\,\sigma G\psi\right\rangle + \frac{3}{16\pi}\left\langle\overline{\psi}\,\sigma G\psi\right\rangle\log\left(\frac{-q^2}{\nu^2}\right). \quad (2.165)$$

2.7.4 Diagram IX

For this contribution to the mixed condensate, there are two identical contributions; a representative diagram is given in Figure 2.10. Terms that correspond to this diagram arise in the application of Wick's Theorem to (2.24), involving the QCD interaction (1.15). One of these two terms is given by

$$\Pi^{\mu\nu(ix)}_{(\text{rep.})}(q) = -\frac{g^3}{8}\Delta_{\mu\rho\omega_1\omega_2}\Delta_{\nu\sigma\omega_3\omega_4}\Gamma^{\rho}_{ij}\Gamma^{\sigma}_{kl}\gamma^{\xi}_{rs}\lambda^{n}_{ab}\lambda^{m}_{cd}\lambda^{p}_{ef}\int d^4x\, d^4z\, e^{iq\cdot x}$$
$$\langle : \overline{\psi}^a_i(x)\underbrace{\psi^b_j(x)\overline{\psi}^c_k(0)}\psi^d_l(0)\underbrace{\overline{\psi}^e_r(z)\psi^f_s(z)}G^n_{\omega_1\omega_2}(x)G^m_{\omega_3\omega_4}(0)B^p_{\xi}(z) : \rangle\,. \qquad (2.166)$$

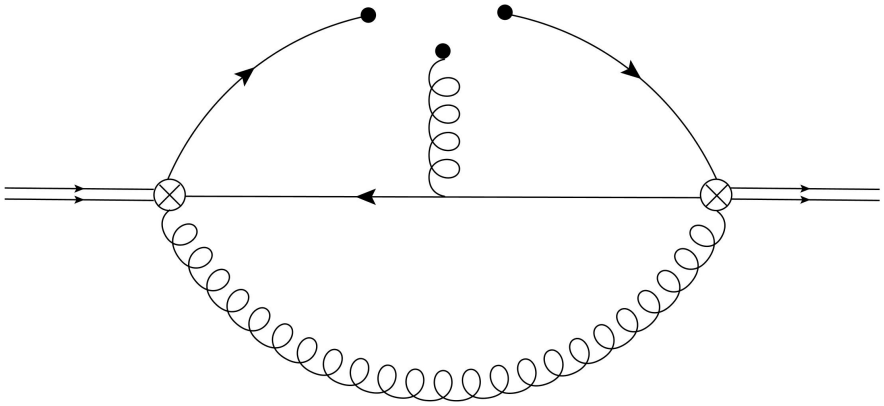

Figure 2.10: Diagram IX: The third contribution to the mixed condensate. There are two identical contributions of this type.

In terms of the propagators involved, (2.166) becomes

$$\Pi^{\mu\nu(ix)}_{(\text{rep.})}(q) = i\frac{g^3}{24}\Delta_{\mu\rho\omega_1\omega_2}\Delta_{\nu\sigma\omega_3\omega_4}\Gamma^{\rho}_{ij}\Gamma^{\sigma}_{kl}\gamma^{\xi}_{rs}\left\langle\overline{\psi}\,\sigma G\psi\right\rangle\int d^4x\, d^4z\, e^{iq\cdot x}$$
$$\Big[S_{sk}(z)\Big]\Big[S_{jr}(x-z)\Big]\Big[H_{\omega_1\omega_2\omega_3\omega_4}(x)\Big]z^{\zeta}\Big(Y_{7li,\zeta\xi} - x^{\chi}\,m\,Y_{8li,\zeta\xi\chi}\Big). \qquad (2.167)$$

From here, we can expand this out, and eliminate x and z using integration by parts. Expanding the fermion propagators in quark mass and keeping the lowest order nonzero terms

yields

$$\begin{aligned}\Pi^{\mu\nu(ix)}_{(\text{rep.})}(q) =& \frac{g^3}{24}\Delta_{\mu\rho\omega_1\omega_2}\Delta_{\nu\sigma\omega_3\omega_4} m \left\langle \overline{\psi}\, \sigma G \psi \right\rangle \int \frac{d^4k}{(2\pi)^4} \widetilde{H}_{\omega_1\omega_2\omega_3\omega_4}(k) \Big\{ \\ & \text{Tr}\Big[\Gamma^\rho \widetilde{S}(q-k;0)^2 \gamma^\xi \widetilde{S}(q-k;0) \gamma^\zeta \widetilde{S}(q-k;0) \Gamma^\sigma Y_{7\zeta\xi} \\ & \quad + \Gamma^\rho \widetilde{S}(q-k;0) \gamma^\xi \widetilde{S}(q-k;0)^2 \gamma^\zeta \widetilde{S}(q-k;0) \Gamma^\sigma Y_{7\zeta\xi} \\ & \quad + \Gamma^\rho \widetilde{S}(q-k;0) \gamma^\xi \widetilde{S}(q-k;0) \gamma^\zeta \widetilde{S}(q-k;0)^2 \Gamma^\sigma Y_{7\zeta\xi} \\ & \quad - i\Big(\Gamma^\rho \widetilde{S}(q-k;0) \gamma^\chi \widetilde{S}(q-k;0) \gamma^\xi \widetilde{S}(q-k;0) \gamma^\zeta \widetilde{S}(q-k;0) \Gamma^\sigma Y_{8\zeta\xi\chi} \\ & \qquad + \Gamma^\rho \widetilde{S}(q-k;0) \gamma^\xi \widetilde{S}(q-k;0) \gamma^\chi \widetilde{S}(q-k;0) \gamma^\zeta \widetilde{S}(q-k;0) \Gamma^\sigma Y_{8\zeta\xi\chi} \\ & \qquad + \Gamma^\rho \widetilde{S}(q-k;0) \gamma^\xi \widetilde{S}(q-k;0) \gamma^\zeta \widetilde{S}(q-k;0) \gamma^\chi \widetilde{S}(q-k;0) \Gamma^\sigma Y_{8\zeta\xi\chi} \Big) \Big] \Big\}. \end{aligned} \tag{2.168}$$

At this point, the computer carries out the rest of the calculation. The final result for this contribution is then multiplied by two to account for equivalent topologies, and the scalar and vector projections respectively for this diagram are

$$\Pi^{(ix)}_S(q^2) = -\frac{1}{192\pi}\frac{1}{\epsilon}\left\langle \overline{\psi}\, \sigma G \psi \right\rangle - \frac{1}{384\pi}\left\langle \overline{\psi}\, \sigma G \psi \right\rangle - \frac{1}{192\pi}\left\langle \overline{\psi}\, \sigma G \psi \right\rangle \log\left(\frac{-q^2}{\nu^2}\right), \tag{2.169}$$

$$\Pi^{(ix)}_V(q^2) = \frac{1}{192\pi}\frac{1}{\epsilon}\left\langle \overline{\psi}\, \sigma G \psi \right\rangle + \frac{23}{1152\pi}\left\langle \overline{\psi}\, \sigma G \psi \right\rangle + \frac{1}{192\pi}\left\langle \overline{\psi}\, \sigma G \psi \right\rangle \log\left(\frac{-q^2}{\nu^2}\right). \tag{2.170}$$

2.7.5 Diagram X

Diagram X has four equivalent topologies, one of which is given by Figure 2.11. A representative contribution to this diagram arises from the Wick's Theorem expansion of (2.24), involving the QCD interaction term (1.15):

$$\begin{aligned}\Pi^{\mu\nu(x)}_{(\text{rep.})}(q) = & -\frac{g^3}{8}\Delta_{\mu\rho\omega_1\omega_2}\Delta_{\nu\sigma\omega_3\omega_4}\Gamma^\rho_{ij}\Gamma^\sigma_{kl}\gamma^\xi_{rs}\lambda^n_{ab}\lambda^m_{cd}\lambda^p_{ef}\int d^4x\, d^4z\, e^{iq\cdot x} \\ & \left\langle : \underbrace{\overline{\psi}^a_i(x)\psi^b_j(x)\overline{\psi}^c_k}(0)\psi^d_l(0)\underbrace{\overline{\psi}^e_r(z)\psi^f_s}(z) G^n_{\omega_1\omega_2}(x)\underbrace{G^m_{\omega_3\omega_4}(0)}B^p_\xi(z) : \right\rangle. \end{aligned} \tag{2.171}$$

The calculation of this contribution is very similar to that in Section 2.7.4. In terms of propagators, (2.171) reads

$$\begin{aligned}\Pi^{\mu\nu(x)}_{(\text{rep.})}(q) = & -i\frac{g^3}{12}\Delta_{\mu\rho\omega_1\omega_2}\Delta_{\nu\sigma\omega_3\omega_4}\Gamma^\rho_{ij}\Gamma^\sigma_{kl}\int d^4x\, d^4z\, e^{iq\cdot x} \\ & \Big[S_{jk}(x)\Big]\Big[S_{si}(z-x)\Big]\Big[{H'}_{\omega_3\omega_4\xi}(-z)\Big]\Big(Y_{7lr,\omega_1\omega_2} - x^\zeta\, m\, Y_{8lr,\omega_1\omega_2\zeta}\Big). \end{aligned} \tag{2.172}$$

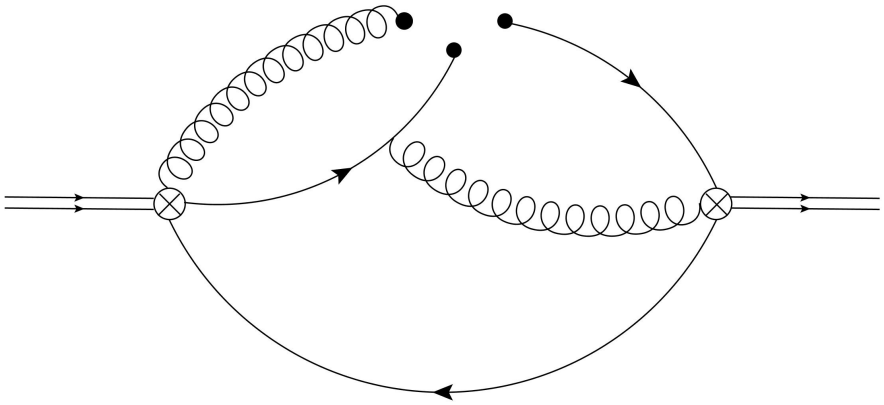

Figure 2.11: Diagram X: The fourth contribution to the mixed condensate. There are four identical contributions of this type.

Again, as in Section 2.7.4, we can separate out the terms in order to eliminate z via integration by parts, and expand out the fermion propagators in quark mass, keeping the lowest order nonzero terms, obtaining

$$\begin{aligned}\Pi^{\mu\nu(x)}_{(\text{rep.})}(q) =& i\frac{g^3}{12}\Delta_{\mu\rho\omega_1\omega_2}\Delta_{\nu\sigma\omega_3\omega_4} m\left\langle\overline{\psi}\,\sigma G\psi\right\rangle\int\frac{d^4k}{(2\pi)^4}\widetilde{H'}_{\omega_3\omega_4\xi}(k)\Big\{\\ &\text{Tr}\Big[\Gamma^\rho\widetilde{S}(q-k;0)^2\Gamma^\sigma Y_{7\omega_1\omega_2}\gamma^\xi\widetilde{S}(-k;0)\\ &+\Gamma^\rho\widetilde{S}(q-k;0)\Gamma^\sigma Y_{7\omega_1\omega_2}\gamma^\xi\widetilde{S}(-k;0)^2\\ &-i\Big(\Gamma^\rho\widetilde{S}(q-k;0)\gamma^\zeta\widetilde{S}(q-k;0)\Gamma^\sigma Y_{8\omega_1\omega_2\zeta}\gamma^\xi\widetilde{S}(-k;0)\\ &\quad+\Gamma^\rho\widetilde{S}(q-k;0)\Gamma^\sigma Y_{8\omega_1\omega_2\zeta}\gamma^\zeta\gamma^\xi\widetilde{S}(-k;0)\gamma^\zeta\widetilde{S}(-k;0)\Big)\Big]\Big\}. \end{aligned}\tag{2.173}$$

Multiplying the result of (2.173) by four to account for the equivalent topologies that arise from different possible contractions, the scalar and vector projections of this diagram are respectively

$$\Pi^{(x)}_S(q^2) = -\frac{1}{48\pi}\frac{1}{\epsilon}\left\langle\overline{\psi}\,\sigma G\psi\right\rangle - \frac{1}{96\pi}\left\langle\overline{\psi}\,\sigma G\psi\right\rangle - \frac{1}{48\pi}\left\langle\overline{\psi}\,\sigma G\psi\right\rangle\log\left(\frac{-q^2}{\nu^2}\right),\tag{2.174}$$

$$\Pi^{(x)}_V(q^2) = \frac{1}{48\pi}\frac{1}{\epsilon}\left\langle\overline{\psi}\,\sigma G\psi\right\rangle - \frac{1}{288\pi}\left\langle\overline{\psi}\,\sigma G\psi\right\rangle + \frac{1}{48\pi}\left\langle\overline{\psi}\,\sigma G\psi\right\rangle\log\left(\frac{-q^2}{\nu^2}\right).\tag{2.175}$$

2.7.6 Diagram XI

Diagram XI arises from terms of the form

$$\Pi^{\mu\nu(xi)}_{(\text{rep.})}(q) = -\frac{g^3}{8}\Delta_{\mu\rho\omega_1\omega_2}\Delta_{\nu\sigma\omega_3\omega_4}\Gamma^{\rho}_{ij}\Gamma^{\sigma}_{kl}\gamma^{\xi}_{rs}\lambda^{n}_{ab}\lambda^{m}_{cd}\lambda^{p}_{ef}\int d^4x\, d^4z\, e^{iq\cdot x}$$
$$\langle : \overline{\psi}^{\alpha}_{i}(x)\psi^{\beta}_{j}(x)\overline{\psi}^{\gamma}_{k}(0)\psi^{\delta}_{l}(0)\overline{\psi}^{a}_{r}(z)\psi^{b}_{s}(z)G^{n}_{\omega_1\omega_2}(x)G^{m}_{\omega_3\omega_4}(0)B^{p}_{\xi}(z) : \rangle\,. \quad (2.176)$$

which appear in the Wick's Theorem expansion of (2.24), involving the QCD interaction term (1.15). There are four equivalent topologies that appear, and a diagram representing these is given in Figure 2.12. Thus, we need only consider one of the terms from the Wick's Theorem expansion, and multiply the final result by four; the particular term we consider here is

$$\Pi^{\mu\nu(xi)}_{(\text{rep.})}(q) = i\frac{2g^3}{3}\Delta_{\mu\rho\omega_1\omega_2}\Delta_{\nu\sigma\omega_3\omega_4}\Gamma^{\rho}_{ij}\Gamma^{\sigma}_{kl}\gamma^{\xi}_{rs}\left\langle\overline{\psi}\,\sigma G\psi\right\rangle\int d^4x\, d^4z\, e^{iq\cdot x}$$
$$\Big[S_{si}(z-x)\Big]\Big[S_{jk}(x)\Big]\Big[H'_{\omega_1\omega_2\xi}(x-z)\Big]\Big(Y_{7lr,\omega_3\omega_4} - x^{\zeta}\, m\, Y_{8lr,\omega_3\omega_4\zeta}\Big). \quad (2.177)$$

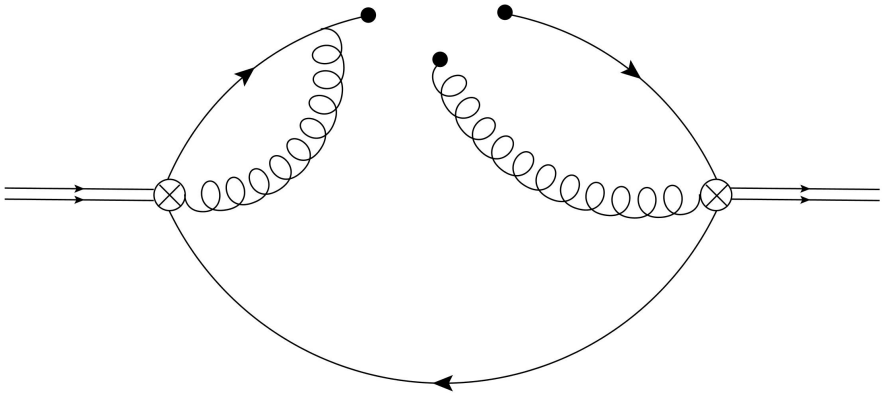

Figure 2.12: Diagram XI: The fifth contribution to the mixed condensate. There are four identical contributions with this topology.

The usual procedure can be followed here; we split the condensate pieces up to perform integration by parts on the second term, and then recombine to form a trace over the Dirac

indices and expand the integrand in the quark mass. This process yields

$$\begin{aligned}\Pi^{\mu\nu(xi)}_{(\text{rep.})}(q) =& i\frac{2g^3}{3}\Delta_{\mu\rho\omega_1\omega_2}\Delta_{\nu\sigma\omega_3\omega_4} m \left\langle \overline{\psi}\, \sigma G \psi \right\rangle \int \frac{d^4k}{(2\pi)^4} \widetilde{H'}_{\omega_1\omega_2\xi}(k) \Big\{ \\ & \text{Tr}\Big[\Gamma^\rho \widetilde{S}(q;0)^2 \Gamma^\sigma Y_{7\omega_3\omega_4} \gamma^\xi \widetilde{S}(k;0) \\ & + \Gamma^\rho \widetilde{S}(q;0) \Gamma^\sigma Y_{7\omega_3\omega_4} \gamma^\xi \widetilde{S}(k;0)^2 \\ & - i\Big(\Gamma^\rho \widetilde{S}(q;0) \gamma^\zeta \widetilde{S}(q;0) \Gamma^\sigma Y_{8\omega_3\omega_4\zeta} \gamma^\xi \widetilde{S}(k;0) \\ & \quad + \Gamma^\rho \widetilde{S}(q;0) \Gamma^\sigma Y_{8\omega_3\omega_4\zeta} \gamma^\xi \widetilde{S}(k;0) \gamma^\zeta \widetilde{S}(k;0) \Big) \Big] \Big\}. \end{aligned} \tag{2.178}$$

At this point, however, there is a problem with the propagators. In (2.178), the momentum integrals to be performed are of the form

$$\int \frac{d^dk}{(2\pi)^d} (k^2)^n \tag{2.179}$$

for various integer values of n. However, integrals of this form in the framework of dimensional regularization are zero [28]. As every term in (2.178) is proportional to an integral of the type (2.179) after projecting out the scalar and vector parts, this entire expression is zero. Thus, for Diagram XI,

$$\Pi^{(xi)}_S(q^2) = \Pi^{(xi)}_V(q^2) = 0. \tag{2.180}$$

2.7.7 Diagram XII

Diagram XII arises from the quark-quark-gluon QCD interaction (1.15). It has a multiplicity of four, and is given by contractions of the form

$$\begin{aligned}\Pi^{\mu\nu(xii)}_{(\text{rep.})}(q) = & -\frac{g^3}{8}\Delta_{\mu\rho\omega_1\omega_2}\Delta_{\nu\sigma\omega_3\omega_4}\Gamma^\rho_{ij}\Gamma^\sigma_{kl}\gamma^\xi_{rs}\lambda^n_{ab}\lambda^m_{cd}\lambda^p_{ef} \int d^4x\, d^4z\, e^{iq\cdot x} \\ & \langle : \overline{\psi}^a_i(x) \underbrace{\psi^b_j(x) \overline{\psi}^c_k(0) \psi^d_l(0) \overline{\psi}^e_r(z) \psi^f_s(z)} \underbrace{G^n_{\omega_1\omega_2}(x) G^m_{\omega_3\omega_4}(0)} B^p_\xi(z) : \rangle \,. \end{aligned} \tag{2.181}$$

which arises in the Wick's Theorem expansion of (2.24). A representative diagram of this type is given in Figure 2.13. In terms of the propagators involved, we have

$$\begin{aligned}\Pi^{\mu\nu(xii)}_{(\text{rep.})}(q) = & i\frac{2g^3}{3}\Delta_{\mu\rho\omega_1\omega_2}\Delta_{\nu\sigma\omega_3\omega_4}\Gamma^\rho_{ij}\Gamma^\sigma_{kl}\gamma^\xi_{rs} \left\langle \overline{\psi}\, \sigma G \psi \right\rangle \int d^4x\, d^4z\, e^{iq\cdot x} \\ & \Big[S_{jr}(x-z) \Big] \Big[S_{sk}(z) \Big] \Big[H'_{\omega_1\omega_2\xi}(x-z) \Big] \Big(Y_{7li,\omega_3\omega_4} - x^\chi\, m\, Y_{8li,\omega_3\omega_4\chi} \Big). \end{aligned} \tag{2.182}$$

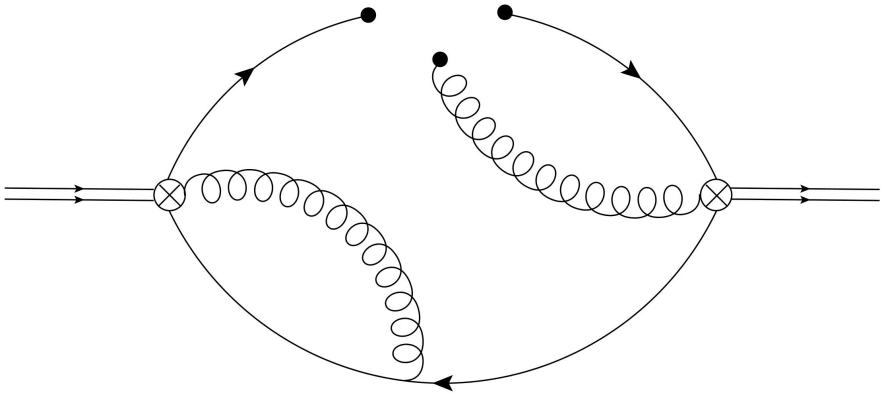

Figure 2.13: Diagram XII: The sixth contribution to the mixed condensate. There are four identical contributions to the correlation function of this type.

The calculations involved in taking (2.182) to an expression that the computer can interpret is standard at this point; we separate the condensate to handle the two VEV contributions, and recombine the result in terms of a trace over the Dirac indices to yield

$$\begin{aligned}\Pi^{\mu\nu(xii)}_{(\text{rep.})}(q) =& i\frac{2g^3}{3}\Delta_{\mu\rho\omega_1\omega_2}\Delta_{\nu\sigma\omega_3\omega_4} m\left\langle\overline{\psi}\,\sigma G\psi\right\rangle\int\frac{d^4k}{(2\pi)^4}\widetilde{H'}_{\omega_1\omega_2\xi}(k)\Big\{\\ &\text{Tr}\Big[\Gamma^\rho\widetilde{S}(q-k;0)^2\gamma^\xi\widetilde{S}(q;0)\Gamma^\sigma Y_{7\omega_3\omega_4}\\ &+\Gamma^\rho\widetilde{S}(q-k;0)\gamma^\xi\widetilde{S}(q;0)^2\Gamma^\sigma Y_{7\omega_3\omega_4}\\ &-i\Big(\Gamma^\rho\widetilde{S}(q-k;0)\gamma^\chi\widetilde{S}(q-k;0)\gamma^\xi\widetilde{S}(q;0)\Gamma^\sigma Y_{8\omega_3\omega_4\zeta}\\ &+\Gamma^\rho\widetilde{S}(q-k;0)\gamma^\xi\widetilde{S}(q-k;0)\gamma^\chi\widetilde{S}(q;0)\Gamma^\sigma Y_{8\omega_3\omega_4\zeta}\Big)\Big]\Big\}. \end{aligned}\tag{2.183}$$

To obtain the final result for this diagram, we multiply the result of (2.183) by four to account for the equivalent topologies. The scalar and vector projections of the correlator for this diagram are respectively

$$\Pi^{(xii)}_S(q^2) = \frac{1}{18\pi}\frac{1}{\epsilon}\left\langle\overline{\psi}\,\sigma G\psi\right\rangle + \frac{17}{108\pi}\left\langle\overline{\psi}\,\sigma G\psi\right\rangle + \frac{1}{18\pi}\left\langle\overline{\psi}\,\sigma G\psi\right\rangle\log\left(\frac{-q^2}{\nu^2}\right),\tag{2.184}$$

$$\Pi^{(xii)}_V(q^2) = \frac{1}{18\pi}\frac{1}{\epsilon}\left\langle\overline{\psi}\,\sigma G\psi\right\rangle - \frac{7}{108\pi}\left\langle\overline{\psi}\,\sigma G\psi\right\rangle + \frac{1}{18\pi}\left\langle\overline{\psi}\,\sigma G\psi\right\rangle\log\left(\frac{-q^2}{\nu^2}\right).\tag{2.185}$$

2.7.8 Diagram XIII

While the Wick's Theorem expansion of (2.24) yields terms of the form

$$\langle : \overline{\psi}_i^a(x)\psi_j^b(x)\overline{\psi}_k^c(0)\psi_l^d(0)\overline{\psi}_r^e(z)\psi_s^f(z)G^n_{\omega_1\omega_2}(x)G^m_{\omega_3\omega_4}(0)B^p_\xi(z) : \rangle \,, \tag{2.186}$$

perturbation theory does not make sense for this term; after expansion of the fermion propagator in quark mass, expressions of the form (2.186) have a zero momentum, massless propagator. We thus classify this diagram as an equation of motion diagram, and reinterpret it as a contribution arising from a term in the expansion of a lower order condensate (2.13). The expression that gives the reinterpretation of terms of the form (2.186) comes from the mixed condensate contribution from the expansion of the 4D quark condensate (2.137); the diagram that corresponds to this is given in Figure 2.14.

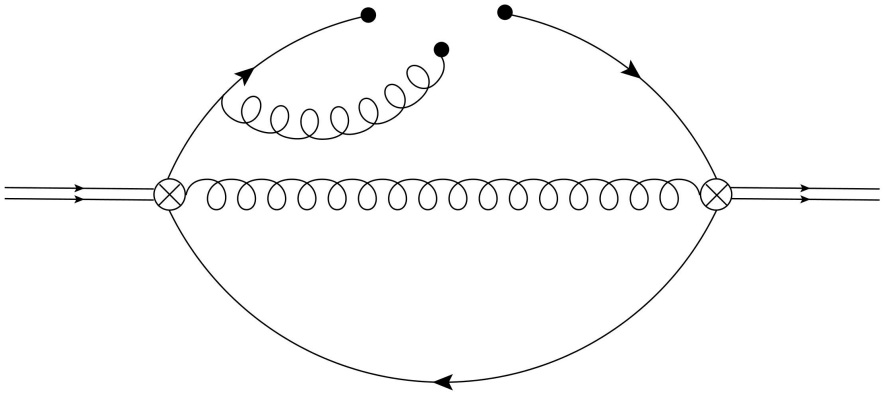

Figure 2.14: Diagram XIII: Due to the zero momentum quark line, this is an equation of motion diagram, which arises from the expansion in x of the quark condensate. There are two identical contributions of this type.

There are two identical contributions to the mixed condensate for Diagram XIII, one for each 4D quark condensate expansion, in the second and third terms of (2.13). However, since they yield identical contributions, we calculate one such contribution and multiply the result by two to obtain the final result for Diagram XIII. In terms of propagators, one contribution is

$$\Pi^{\mu\nu(xiii)}_{(\text{rep.})}(q) = -\frac{i}{12d}g^3\Delta_{\mu\rho\omega_1\omega_2}\Delta_{\nu\sigma\omega_3\omega_4}\Gamma^\rho_{ij}\Gamma^\sigma_{kl}\left\langle\overline{\psi}\,\sigma G\psi\right\rangle\int d^4x\, e^{iq\cdot x} \\ \Big[S_{jk}(x)\Big]\Big[H_{\omega_1\omega_2\omega_3\omega_4}(x)\Big]\Big[x^2\Big(\delta_{li}+\frac{i}{6}mx^\tau(\gamma_\tau)_{li}\Big)\Big]. \tag{2.187}$$

From the expression (2.187), the procedure is the usual one where we use integration by parts to eliminate factors of x, and reduce the expression to a trace over the Dirac indices. The result that gets passed to the computer is then

$$\begin{aligned}\Pi^{\mu\nu(xiii)}_{(\text{rep.})}(q) =& \frac{i}{12d} g^3 \Delta_{\mu\rho\omega_1\omega_2}\Delta_{\nu\sigma\omega_3\omega_4} g_{\alpha\beta} m \left\langle \overline{\psi}\,\sigma G\psi \right\rangle \int \frac{d^4k}{(2\pi)^4} \widetilde{H}_{\omega_1\omega_2\omega_3\omega_4}(k) \\ & \text{Tr}\Big[\Gamma^\rho \widetilde{S}(q-k;0)^2 \gamma^\alpha \widetilde{S}(q-k;0)\gamma^\beta \widetilde{S}(q-k;0)\Gamma^\sigma \\ & + \Gamma^\rho \widetilde{S}(q-k;0)\gamma^\alpha \widetilde{S}(q-k;0)^2\gamma^\beta \widetilde{S}(q-k;0)\Gamma^\sigma \\ & + \Gamma^\rho \widetilde{S}(q-k;0)\gamma^\alpha \widetilde{S}(q-k;0)\gamma^\beta \widetilde{S}(q-k;0)^2\Gamma^\sigma \\ & - \frac{1}{6}\Big\{\Gamma^\rho \widetilde{S}(q-k;0)\gamma^\tau \widetilde{S}(q-k;0)\gamma^\alpha \widetilde{S}(q-k;0)\gamma^\beta \widetilde{S}(q-k;0)\Gamma^\sigma\gamma_\tau \\ & \quad + \Gamma^\rho \widetilde{S}(q-k;0)\gamma^\alpha \widetilde{S}(q-k;0)\gamma^\tau \widetilde{S}(q-k;0)\gamma^\beta \widetilde{S}(q-k;0)\Gamma^\sigma\gamma_\tau \\ & \quad + \Gamma^\rho \widetilde{S}(q-k;0)\gamma^\alpha \widetilde{S}(q-k;0)\gamma^\beta \widetilde{S}(q-k;0)\gamma^\tau \widetilde{S}(q-k;0)\Gamma^\sigma\gamma_\tau \Big\}\Big]. \end{aligned} \tag{2.188}$$

The result of computing (2.188) is then multipled by two to account for the identical contributions of both quark field VEVs. The scalar and vector projections of Diagram XIII respectively are thus given by

$$\Pi^{(xiii)}_S(q^2) = -\frac{1}{24\pi}\frac{1}{\epsilon}\left\langle \overline{\psi}\,\sigma G\psi \right\rangle + \frac{13}{144\pi}\left\langle \overline{\psi}\,\sigma G\psi \right\rangle - \frac{1}{24\pi}\left\langle \overline{\psi}\,\sigma G\psi \right\rangle \log\left(\frac{-q^2}{\nu^2}\right), \tag{2.189}$$

$$\Pi^{(xiii)}_V(q^2) = \frac{1}{24\pi}\frac{1}{\epsilon}\left\langle \overline{\psi}\,\sigma G\psi \right\rangle + \frac{23}{144\pi}\left\langle \overline{\psi}\,\sigma G\psi \right\rangle + \frac{1}{24\pi}\left\langle \overline{\psi}\,\sigma G\psi \right\rangle \log\left(\frac{-q^2}{\nu^2}\right). \tag{2.190}$$

2.7.9 Diagram XIV

As in Section 2.7.8, the application of Wick's Theorem to the term (2.24) yields terms of the form

$$\langle : \overline{\psi}^a_i(x)\psi^b_j(x)\overline{\psi}^c_k(0)\psi^d_l(0)\overline{\psi}^e_r(z)\psi^f_s(z) G^n_{\omega_1\omega_2}(x) G^m_{\omega_3\omega_4}(0) B^p_\xi(z) : \rangle\,. \tag{2.191}$$

In this expression, however, it is a gluon propagator that carries zero momentum that renders perturbation theory meaningless. A diagram representing the contraction (2.191) is given in Figure 2.15. This is thus another example of an equation of motion diagram, and we need to reinterpret contributions to the mixed condensate of this type; following the same procedure

as Section 2.7.8, we reinterpret this diagram as arising from the expansion of a lower order condensate: the 4D gluon condensate.

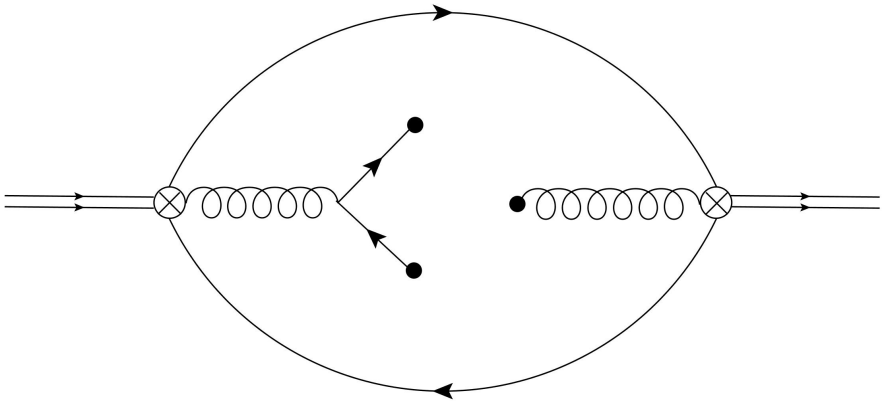

Figure 2.15: Diagram XIV: Due to the zero momentum gluon line, this diagram is interpreted as an equation of motion diagram. It arises from the expansion in x of the gluon condensate, which yields only one contribution of this type.

During the evaluation of (2.108), we left out dimension six terms that are proportional to g^2, as these terms contribute at next-to-leading order in perturbation theory and we are not considering contributions at that order. The terms left out are in fact those that would correspond to the reinterpretations of Figure 2.15; that is, terms proportional to the mixed condensate. As such, this diagram is then reinterpreted as zero at this order in perturbation theory, for both the scalar and vector projections, where contributions from this diagram arise only when considering higher order terms in the coupling constant expansion. Thus,

$$\Pi_S^{(xiv)}(q^2) = \Pi_V^{(xiv)}(q^2) = 0. \tag{2.192}$$

2.7.10 Mixed Condensate Conclusion

To obtain the contribution to the correlator proportional to the mixed condensate, we need to sum the results of the diagrams VII through XIV. As all of them have similar loop structure, all of the results of these diagrams have the same basic structure: a divergent $\frac{1}{\epsilon}$ term, a finite term, and a logarithmic term:

$$\Pi_{S,V}^{(\text{any mixed})}(q^2) = \left(C_1 \frac{1}{\epsilon} + C_2 + C_3 \log\left(\frac{-q^2}{\nu^2}\right) \right) \langle \overline{\psi}\, \sigma G \psi \rangle \,. \tag{2.193}$$

The divergent terms and logarithmic terms always have the matching coefficients ($C_1 = C_3$ in the above), so we omit the collection of the divergent coefficients for the sake of reducing redundancy.

	0^{++}	1^{-+}	0^{--}	1^{+-}	0^{-+}	1^{++}	0^{+-}	1^{--}
VII	$\frac{3}{64\pi}$	$-\frac{3}{64\pi}$	$-\frac{3}{64\pi}$	$\frac{3}{64\pi}$	$-\frac{3}{64\pi}$	$\frac{3}{64\pi}$	$\frac{3}{64\pi}$	$-\frac{3}{64\pi}$
VIII	$-\frac{3}{32\pi}$	$\frac{3}{32\pi}$	$\frac{3}{16\pi}$	$-\frac{3}{16\pi}$	$\frac{3}{32\pi}$	$-\frac{3}{32\pi}$	$-\frac{3}{16\pi}$	$\frac{3}{16\pi}$
IX	$-\frac{1}{192\pi}$	$\frac{1}{192\pi}$	$-\frac{1}{192\pi}$	$\frac{1}{192\pi}$	$-\frac{1}{192\pi}$	$\frac{1}{192\pi}$	$-\frac{1}{192\pi}$	$\frac{1}{192\pi}$
X	$\frac{1}{96\pi}$	$-\frac{1}{96\pi}$	$\frac{1}{32\pi}$	$-\frac{1}{32\pi}$	0	0	$-\frac{1}{48\pi}$	$\frac{1}{48\pi}$
XI	0	0	0	0	0	0	0	0
XII	$\frac{7}{36\pi}$	$-\frac{1}{12\pi}$	$\frac{1}{36\pi}$	$-\frac{5}{36\pi}$	$-\frac{1}{9\pi}$	0	$\frac{1}{18\pi}$	$\frac{1}{18\pi}$
XIII	$-\frac{1}{24\pi}$	$\frac{1}{24\pi}$	$-\frac{1}{24\pi}$	$\frac{1}{24\pi}$	$-\frac{1}{24\pi}$	$\frac{1}{24\pi}$	$-\frac{1}{24\pi}$	$\frac{1}{24\pi}$
XIV	0	0	0	0	0	0	0	0
Sum	$\frac{1}{9\pi}$	0	$\frac{11}{72\pi}$	$-\frac{19}{72\pi}$	$-\frac{1}{9\pi}$	0	$-\frac{11}{72\pi}$	$\frac{19}{72\pi}$

Table 2.2: Collection of all of the various mixed condensate contributions to the logarithmic coefficient (as well as the divergent coefficient). The final row is the the sum of the individual columns. This coefficient of the mixed condensate is what is necessary for a sum-rule analysis.

In Table 2.2, we collect the coefficients proportional to the logarithms in each of the mixed condensate calculations. While the sum of all these contributions is the quantity that we are interested in, due to the complicated nature of the mixed condensate calculations, we collect the values for all choices of J^{PC} for $J = 0, 1$ for use in future consistency checks. In Table 2.3, we collect all of the finite coefficients of the mixed condensate in the same way as we did in Table 2.2.

Of particular note in Table 2.2, for $J^{PC} = 1^{-+}$ and 1^{++}, the mixed condensate coefficient for the logarithmic and divergent terms are zero. This, in conjunction with zero coefficient of the logarithmic and divergent terms of both the 6D quark and gluon condensates, implies that we have no 6D condensate contribution to the correlation function. This has ramifications that will be elaborated upon in the conclusion.

	0^{++}	1^{-+}	0^{--}	1^{+-}	0^{-+}	1^{++}	0^{+-}	1^{--}
VII	$-\frac{9}{128\pi}$	$\frac{5}{128\pi}$	$\frac{9}{128\pi}$	$-\frac{5}{128\pi}$	$-\frac{3}{128\pi}$	$\frac{7}{128\pi}$	$\frac{3}{128\pi}$	$-\frac{7}{128\pi}$
VIII	$\frac{9}{32\pi}$	$-\frac{7}{32\pi}$	$-\frac{33}{64\pi}$	$\frac{17}{64\pi}$	$-\frac{3}{32\pi}$	$\frac{1}{32\pi}$	$-\frac{15}{64\pi}$	$-\frac{1}{64\pi}$
IX	$-\frac{3}{128\pi}$	$-\frac{1}{1152\pi}$	$\frac{1}{128\pi}$	$\frac{11}{1152\pi}$	$-\frac{13}{384\pi}$	$\frac{11}{1152\pi}$	$-\frac{1}{384\pi}$	$\frac{23}{1152\pi}$
X	$\frac{1}{64\pi}$	$\frac{1}{192\pi}$	$-\frac{1}{64\pi}$	$\frac{13}{576\pi}$	0	0	$-\frac{1}{96\pi}$	$-\frac{1}{288\pi}$
XI	0	0	0	0	0	0	0	0
XII	$-\frac{85}{216\pi}$	$\frac{29}{216\pi}$	$-\frac{31}{216\pi}$	$\frac{55}{216\pi}$	$\frac{5}{27\pi}$	$-\frac{1}{54\pi}$	$\frac{17}{108\pi}$	$-\frac{7}{108\pi}$
XIII	$-\frac{11}{144\pi}$	$-\frac{1}{144\pi}$	$\frac{25}{144\pi}$	$\frac{11}{144\pi}$	$-\frac{23}{144\pi}$	$\frac{11}{144\pi}$	$\frac{13}{144\pi}$	$\frac{23}{144\pi}$
XIV	0	0	0	0	0	0	0	0
Sum	$-\frac{461}{1728\pi}$	$-\frac{83}{1728\pi}$	$-\frac{731}{1728\pi}$	$\frac{1019}{1728\pi}$	$-\frac{217}{1728\pi}$	$\frac{265}{1728\pi}$	$\frac{41}{1728\pi}$	$\frac{71}{1728\pi}$

Table 2.3: Collection of all of the various mixed condensate contributions to the finite coefficient. While these will typically be irrelevant for a sum-rule analysis, we can collect the coefficients for use as a consistency check. Case in point, the first four columns in this table agree with [1] on a diagram by diagram basis.

Chapter 3

Conclusion

Regardless of the quantum numbers under consideration (corresponding to the choices of $\Delta_{\mu\nu\rho\sigma}$ and Γ_μ) the correlator is the sum of the diagrams arising from the Wick's Theorem expansion,

$$\Pi(q^2) = \sum_n \Pi^{(n)}(q^2). \tag{3.1}$$

This sum runs from Diagram I to XIV. Because the final result for each of the diagrams has the same structure regardless of the choice of $\Delta_{\mu\nu\rho\sigma}$ and Γ_μ, we have, in general, a correlator of the form

$$\begin{aligned}
\Pi(q^2) =& \Big(A_1 q^6 + A_2 m^2 q^4\Big) \left\{ \log\left(\frac{-q^2}{\nu^2}\right) + \frac{1}{2\epsilon} \right\} \\
&+ \Big(A_3 q^2 \, m\langle\overline{\psi}\psi\rangle + A_4 q^2 \left\langle \alpha G^2 \right\rangle + A_5 \left\langle \overline{\psi}\psi \right\rangle^2 + A_6 \left\langle G^3 \right\rangle + A_7 \, m\langle \overline{\psi}\, \sigma_{\mu\nu} F^{\mu\nu} \psi \rangle \Big) \\
&\quad \times \left\{ \log\left(\frac{-q^2}{\nu^2}\right) + \frac{1}{\epsilon} \right\} \\
&+ B_1 q^6 + A_2 m^2 q^4 + B_3 q^2 \, m\langle\overline{\psi}\psi\rangle + B_4 q^2 \left\langle \alpha G^2 \right\rangle \\
&+ B_5 \left\langle \overline{\psi}\psi \right\rangle^2 + B_6 \left\langle G^3 \right\rangle + B_7 \, m\langle \overline{\psi}\, \sigma_{\mu\nu} F^{\mu\nu} \psi \rangle \, .
\end{aligned} \tag{3.2}$$

The analysis performed on the computer is largely independent of the choice of $\Delta_{\mu\nu\rho\sigma}$ and Γ_μ. As such, while we illustrated the calculation of the coefficients for $J^{PC} = 0^{+-}$ and 1^{--}, we can generate a table of the coefficients for all eight combinations of quantum numbers under consideration.

In Table 3.1, we list all of the coefficients that correspond to the terms proportional to the logarithm in (3.2), and in Table 3.2, those coefficients that correspond to the finite contributions. While the terms proportional to logarithms play an important role in the sum-rule analysis, most of the finite terms end up being irrelevant; however, Table 3.2 may

	0^{++}	1^{-+}	0^{--}	1^{+-}	0^{-+}	1^{++}	0^{+-}	1^{--}
A_1	$-\frac{1}{480\pi^3}$	$-\frac{1}{240\pi^3}$	$-\frac{1}{480\pi^3}$	$-\frac{1}{240\pi^3}$	$-\frac{1}{480\pi^3}$	$-\frac{1}{240\pi^3}$	$-\frac{1}{480\pi^3}$	$-\frac{1}{240\pi^3}$
A_2	0	$\frac{1}{12\pi^3}$	$\frac{1}{16\pi^3}$	$\frac{5}{48\pi^3}$	0	$\frac{1}{12\pi^3}$	$\frac{1}{16\pi^3}$	$\frac{5}{48\pi^3}$
A_3	$\frac{1}{3\pi}$	$-\frac{2}{9\pi}$	$-\frac{1}{3\pi}$	$-\frac{4}{9\pi}$	$\frac{1}{3\pi}$	$-\frac{2}{9\pi}$	$-\frac{1}{3\pi}$	$-\frac{4}{9\pi}$
A_4	$\frac{1}{24\pi}$	$-\frac{1}{36\pi}$	$\frac{1}{24\pi}$	$-\frac{1}{36\pi}$	$-\frac{1}{24\pi}$	$\frac{1}{36\pi}$	$-\frac{1}{24\pi}$	$\frac{1}{36\pi}$
A_5	0	0	0	0	0	0	0	0
A_6	0	0	0	0	0	0	0	0
A_7	$\frac{1}{9\pi}$	0	$\frac{11}{72\pi}$	$-\frac{19}{72\pi}$	$-\frac{1}{9\pi}$	0	$-\frac{11}{72\pi}$	$\frac{19}{72\pi}$

Table 3.1: Coefficients of the logarithmic and divergent terms of the perturbative and condensate contributions to the correlation function for all values of J^{PC} under consideration.

serve as a useful benchmark for other calculations of this type. In particular, the results for $J^{PC} = 0^{++}, 1^{-+}, 0^{--}, 1^{+-}$ agree with the results of [1].

The results of Tables 3.1 and 3.2 could, in principle, be used to perform a sum-rules analysis for hybrids of various quantum numbers with light quarks. While an analysis can be performed for any of the channels, the more interesting ones would be those with exotic quantum numbers (ie. $J^{PC} = 0^{+-}, 0^{--}, 1^{-+}$), as these channels correspond to particles that cannot exist within the quark model. This is a reason that throughout this thesis we have focused specifically on the $J^{PC} = 0^{+-}$ results.

For all channels, the logarithmic and divergent terms have zero coefficient for the 6D quark and gluon condensates, while the mixed condensate coefficients are non-zero for the majority of the channels under consideration. It is currently unclear whether or not the divergence associated with the mixed condensate is an artifact of expanding in the quark mass before the integrals are performed. In the future, an analysis containing the quark masses to all orders can be performed, and these results compared to the results presented here.

However, there are complications going forward that have yet to be worked out. In forming sum-rules, one eliminates the divergences appearing in the correlator (3.2) by introducing a

	0^{++}	1^{-+}	0^{--}	1^{+-}	0^{-+}	1^{++}	0^{+-}	1^{--}
B_1	$\frac{97}{19200\pi^3}$	$\frac{39}{3200\pi^3}$	$\frac{97}{19200\pi^3}$	$\frac{39}{3200\pi^3}$	$\frac{19}{6400\pi^3}$	$\frac{77}{9600\pi^3}$	$\frac{19}{6400\pi^3}$	$\frac{77}{9600\pi^3}$
B_2	$\frac{1}{32\pi^3}$	$-\frac{7}{32\pi^3}$	$-\frac{55}{384\pi^3}$	$-\frac{109}{384\pi^3}$	$\frac{1}{32\pi^3}$	$-\frac{13}{96\pi^3}$	$-\frac{31}{384\pi^3}$	$-\frac{23}{128\pi^3}$
B_3	$-\frac{1}{2\pi}$	$\frac{7}{27\pi}$	$\frac{1}{6\pi}$	$\frac{17}{27\pi}$	$\frac{1}{6\pi}$	$-\frac{5}{27\pi}$	$-\frac{1}{2\pi}$	$-\frac{7}{27\pi}$
B_4	$-\frac{13}{144\pi}$	$\frac{11}{216\pi}$	$-\frac{13}{144\pi}$	$\frac{11}{216\pi}$	$-\frac{5}{144\pi}$	$\frac{7}{216\pi}$	$-\frac{5}{144\pi}$	$\frac{7}{216\pi}$
B_5	$-\frac{4\pi}{3}$	$\frac{4\pi}{9}$	$\frac{4\pi}{3}$	$-\frac{4\pi}{9}$	0	$-\frac{8\pi}{9}$	0	$\frac{8\pi}{9}$
B_6	$-\frac{1}{192\pi^2}$	$\frac{1}{192\pi^2}$	$-\frac{1}{192\pi^2}$	$\frac{1}{192\pi^2}$	$\frac{5}{192\pi^2}$	$-\frac{5}{192\pi^2}$	$\frac{5}{192\pi^2}$	$-\frac{5}{192\pi^2}$
B_7	$-\frac{461}{1728\pi}$	$-\frac{83}{1728\pi}$	$-\frac{731}{1728\pi}$	$\frac{1019}{1728\pi}$	$-\frac{217}{1728\pi}$	$\frac{265}{1728\pi}$	$\frac{41}{1728}$	$\frac{71}{1728\pi}$

Table 3.2: Coefficients of the finite terms of the perturbative and condensate contributions to the correlation function for all values of J^{PC} under consideration.

transform, known as the Borel transform:

$$\widehat{B} \equiv \lim_{\substack{N,Q^2\to\infty \\ N/Q^2\equiv\tau}} \frac{(-Q^2)^N}{\Gamma(N)} \left(\frac{d}{dQ^2}\right)^N. \tag{3.3}$$

The derivatives in this expression cause polynomials in q^2 to vanish:

$$\widehat{B}\left[a_0 + a_1 Q^2 + \cdots + a_n Q^{2n}\right] = 0 \qquad (n \text{ finite}). \tag{3.4}$$

This transform can be used to form a family of Laplace sum-rules $\mathscr{L}_k(\tau)$ for various integer values of k by

$$\mathscr{L}_k(\tau) = \frac{1}{\tau}\widehat{B}\Big[(-Q^2)^k\,\Pi(Q^2)\Big], \tag{3.5}$$

where $Q^2 = -q^2$, and $\Pi(Q^2)$ is a hybrid correlation function for a particular choice of J^{PC}.

We can obtain a minimum value of k for which (3.5) is defined. Should a power of q^2 appear in the denominator of any of the divergent terms in the correlation function (1.43), the Borel transform cannot eliminate that term. As the divergence cannot be removed in this way, the Laplace sum-rules would be ill-defined. For the correlation function (1.43), the six dimensional condensates have no momentum dependence in their divergent terms; division by any power of q^2 will cause the situation outlined above to occur, and so in general, the smallest value k for which the Laplace sum-rules would be defined is $k = 0$.

In constructing a family of Laplace sum-rules for our correlation function (1.43), in general, we are restricted to $k > 0$. However, the J^{PC} values 1^{-+} and 1^{++} both have zero as coefficients of the divergent terms of all the dimension six condensates. Due to this, we are free to divide the correlation function (1.43) by q^2, and still have no factors of q^2 in the denominators of the divergent terms. So, for the J^{PC} values 1^{-+} and 1^{++}, we can construct a sum-rule for $k = -1$ without issue. In constructing this sum-rule, however, we gain contributions from the finite coefficients of the six dimensional condensates, as the gain a pole structure for these terms. This allows us to retain more information from the correlation function for these two choices of J^{PC}, but is unique to these two channels.

The multiplication by higher weights of q^{2k} effectively washes out more information in the sum-rules, and so analysis focuses on the lowest weight sum-rules possible. As most of the channels forbid forming sum-rules with multiplication of the correlator by $\frac{1}{q^2}$, we lose the information contained within the finite contributions. This can cause the information extracted from the sum-rules to be poor or unreliable; since this comes down to numerics, it remains to be seen whether or not the predictions that can be made for all channels is reasonable, and under what general conditions are satisfactory to generate reliable predictions. Should the information extracted via the sum-rules analysis prove to be poor, it may be necessary to consider next to leading order terms in α_s (ie. terms proportional to α_s^2), or a different type of family of sum-rules be constructed in order to extract information in a different way.

Despite the above complexities, the calculations outlined throughout this thesis provide the foundation for future study of light quarkonium and strangeonium hybrids with a sum-rule approach. In particular, a comprehensive analysis for all J^{PC} for $J = 0, 1$, similar to that of [8] is envisioned.

Bibliography

[1] J. Latorre, P. Pascual, and S. Narison, Z. Phys. **C34**, 347 (1987).

[2] M. Gell-Mann, Phys. Lett. **8**, 214 (1964).

[3] G. Zweig, CERN-TH-412:80 pp. 22–101 (1964).

[4] O. Greenberg, Phys. Rev. Lett. **13**, 598 (1964).

[5] S. Narison, *QCD as a Theory of Hadrons* (Cambridge University Press, 2004).

[6] GlueX Homepage http://www.gluex.org/GlueX/Home.html.

[7] PANDA Collaboration http://www-panda.gsi.de/.

[8] D. Harnett, R. Berg, R. Kleiv, and T. Steele, Nucl. Phys. Proc. Suppl. **234**, 154 (2013), 1209.4102.

[9] M. E. Peskin and D. V. Schroeder, *An Introduction to Quantum Field Theory* (Westview Press, 1995).

[10] P. Pascual and R. Tarrach, *QCD: Renormalization for the Practitioner* (Springer-Verlag, 1984).

[11] M. Srednicki, *Quantum Field Theory* (Cambridge University Press, 2007).

[12] K. G. Wilson, Phys. Rev. **179**, 1499 (1969).

[13] Y. Nambu, Phys. Rev. Lett. **4**, 380 (1960).

[14] J. Goldstone, Nuovo Cim. **19**, 154 (1961).

[15] J. Goldstone, A. Salam, and S. Weinberg, Phys. Rev. **127**, 965 (1962).

[16] M. A. Shifman, A. Vainshtein, and V. I. Zakharov, Nucl. Phys. **B147**, 385 (1979).

[17] J. Govaerts, L. Reinders, H. Rubinstein, and J. Weyers, Nucl. Phys. **B258**, 215 (1985).

[18] M. Gell-Mann, R. Oakes, and B. Renner, Phys. Rev. **175**, 2195 (1968).

[19] J. Beringer, J. F. Arguin, R. M. Barnett, K. Copic, O. Dahl, D. E. Groom, C. J. Lin, J. Lys, H. Murayama, C. G. Wohl, et al. (Particle Data Group), Phys. Rev. D **86**, 010001 (2012).

[20] S. Narison, Phys. Lett. B **210**, 238 (1988).

[21] H. Dosch, M. Jamin, and S. Narison, Phys. Lett. B **220**, 251 (1989).

[22] S. Narison, Phys. Lett. **B626**, 101 (2005), `hep-ph/0501208`.

[23] S. Narison, Phys. Lett. **B693**, 559 (2010), `1004.5333`.

[24] D. Binosi and L. Theussl, Comput. Phys. Commun. **161**, 76 (2004), `hep-ph/0309015`.

[25] D. Binosi, J. Collins, C. Kaufhold, and L. Theussl, Comput. Phys. Commun. **180**, 1709 (2009), `0811.4113`.

[26] G. t Hooft and M. Veltman, Nucl. Phys. B **44**, 189 (1972).

[27] C. Bollini and J. Giambiagi, Nuovo Cim. **12**, 20 (1972).

[28] J. C. Collins, *Renormalization* (Cambridge University Press, 1984).

[29] O. Tarasov, Nucl. Phys. **B502**, 455 (1997), `hep-ph/9703319`.

[30] O. Tarasov, Phys. Rev. D **54**, 6479 (1996).

[31] R. Mertig and R. Scharf, Comput. Phys. Commun. **111**, 265 (1998), `hep-ph/9801383`.

[32] J. S. Schwinger, *Particles, sources, and fields* (Perseus, 1998).

[33] C. Cronström, Phys. Lett. B **90**, 267 (1980).

[34] E. Bagan, M. Ahmady, V. Elias, and T. G. Steele, Z. Phys. **C61**, 157 (1994).

[35] V. Elias, T. G. Steele, and M. Scadron, Phys. Rev. **D38**, 1584 (1988).

[36] L. Reinders, H. Rubinstein, and S. Yazaki, Phys. Rept. **127**, 1 (1985).

Appendix A

Conventions

A.1 Units

As is conventional in theoretical particle physics, through this thesis we choose units such that $\hbar = c = 1$. Dimensional analysis can be performed to restore factors of $\hbar$ and c where appropriate.

A.2 Dirac and Colour Algebra

The metric for flat spacetime used throughout the thesis is given by

$$\left(g_{\mu\nu}\right) = \begin{pmatrix} +1 & 0 & 0 & 0 \\ 0 & -1 & 0 & 0 \\ 0 & 0 & -1 & 0 \\ 0 & 0 & 0 & -1 \end{pmatrix}. \tag{A.1}$$

However, in use of dimensional regularization, we extend this to d dimensions, where the metric becomes

$$(g_{\mu\nu}) = \mathrm{diag}(+1, \underbrace{-1, \ldots, -1}_{\text{d-1 entries}}), \tag{A.2}$$

such that

$$g^{\mu}_{\mu} = d. \tag{A.3}$$

For the γ matrices, we follow the conventions used in in [9]. As we use dimensional regularization in the evaluation of integrals, we need the d dimensional identities for the γ matrices, defined by

$$\{\gamma_\mu, \gamma_\nu\} = \gamma_\mu\gamma_\nu + \gamma_\nu\gamma_\mu = 2g_{\mu\nu} \tag{A.4}$$

$$\gamma_\mu\gamma^\mu = d \tag{A.5}$$

In the previous expressions, there is an implied 4 by 4 identity matrix, $I_{4\text{x}4}$, such that the expressions make sense as matrix equality. We define γ_5 via

$$[\gamma_\mu, \gamma_5] = 0_{4\text{x}4} \tag{A.6}$$

$$(\gamma_5)^2 = 1. \tag{A.7}$$

Lastly, we have the trace identities

$$\mathrm{Tr}\,(1) = \mathrm{Tr}\,(I_{4\mathrm{x}4}) = 4 \tag{A.8}$$

$$\mathrm{Tr}\,(\text{any odd number of } \gamma \text{ matrices}) = 0 \tag{A.9}$$

$$\mathrm{Tr}\,(\gamma_\mu \gamma_\nu) = 4 g_{\mu\nu}. \tag{A.10}$$

All traces of greater numbers of γ matrices can be reduced to traces over a reduced number of γ matrices, and thus these are the only identites needed.

For the particulars of the $SU(3)$ colour algebra, we follow the conventions layed out in [10]. In particular, we choose the representation for the $SU(3)$ $t_a = \lambda_a/2$, where λ_a are the Gell-Mann matrices, satisfying

$$[\lambda_n, \lambda_m] = 2i f_{nml} \lambda_l. \tag{A.11}$$

The most important identities involving λ_a for the calculations involving the condensates are

$$f^{nml} \lambda^m \lambda^l = 3i\lambda^n \tag{A.12}$$

$$\mathrm{Tr}(\lambda^n) = 0 \tag{A.13}$$

$$\mathrm{Tr}(\lambda^n \lambda^m) = 2\delta^{nm} \tag{A.14}$$

$$\mathrm{Tr}(\lambda^n \lambda^m \lambda^l) = 2\big(d^{nml} + i f^{nml}\big). \tag{A.15}$$

Here, f^{nml} is defined to be totally antisymmetric in its indices, while d^{nml} is totally symmetric. Additional details on the $SU(3)$ colour algebra can be found in [10].

Appendix B

Mathematica Code

There are two Mathematica worksheets included here. The first of these, titled Special Relativity Identities and Contractions, contains the code used to simplify all of the products of four-vectors and Dirac matrices used in the calculations outlined throughout the thesis. The diracTrace function performs the neccessary traces noted throughout the thesis, returning expressions that depend only on four-vectors.

The second Mathematica worksheet, titled TARCER Converter, takes as input expressions involving four-vectors using the notation from the previous worksheet, and the specification of an external momentum. It then determines the momenta to be integrated over, and outputs the related TFI form, as outlined in [29, 31]. These expressions are then easily passed into TARCER, which allows the evaluation of the integrals appearing throughout this thesis. In this worksheet, the line

$$<< tarcer06.mx \tag{B.1}$$

is the loading of the TARCER program.

Special Relativity Identities and Contactions

```
metric[μ, ν];
fourvector[p, μ];
lorentzdot[p, q];
epsilon[υ, ν, ρ, σ];
dirac[γ[μ]]; dirac[γ[5]]; dirac[1];
```

Metric Tensor

```
Clear[metric]

SetAttributes[metric, Orderless];

metric[μ_, μ_] = D;
metric /: metric[μ_, ν_]^2 = D;
metric /: metric[μ_, ν_] metric[ν_, ρ_] = metric[μ, ρ];
metric /: metric[μ_, ν_] metric[μ_, ν_] = metric[μ, μ];
Format[metric[μ_, ν_], TraditionalForm] := Subscript[g, μ ν]
```

4-Vector

```
Clear[fourvector]

metric /: metric[μ_, ν_] fourvector[p_, μ_] = fourvector[p, ν];

fourvector[p_ + q_, μ_] := fourvector[p, μ] + fourvector[q, μ];

fourvector[a_?NumberQ p_, μ_] := a fourvector[p, μ]

Format[fourvector[p_?AtomQ, μ_], TraditionalForm] := Subscript[p, μ]
```

4-Dot Product

```
Clear[lorentzdot]
SetAttributes[lorentzdot, Orderless];

fourvector /: fourvector[p_, μ_] fourvector[q_, μ_] = lorentzdot[p, q];
```

```
fourvector /: Power[fourvector[p_, μ_], 2] := lorentzdot[p, p]

lorentzdot /: lorentzdot[-p_, -p_] := lorentzdot[p, p];
lorentzdot /: lorentzdot[-a_, b_] := -lorentzdot[a, b];

Format[lorentzdot[p_, q_], TraditionalForm] := CenterDot[p, q]
```

Levi-Civita Permutation Symbol

```
Clear[epsilon]

Format[epsilon[μ, ν, ρ, σ], TraditionalForm] := Subscript[ϵ, μ ν ρ σ]

epsilon /: epsilon[a_, b_, c_, d_] epsilon[i_, j_, k_, l_] :=
 -Apply[Plus, Map[Apply[Times, #] &, Map[metric[#[[1]], #[[2]]] &,
      Map[Times[#, {a, b, c, d}] &, Permutations[{i, j, k, l}]], {2}]] *
    Map[Signature, Permutations[{i, j, k, l}]]]
```

Derivatives

```
Clear[fourderivative]

fourderivative[a_ + b_, c_] := fourderivative[a, c] + fourderivative[b, c];
fourderivative[a_ b_, c_] :=
  a fourderivative[b, c] /; FreeQ[a, fourvector] && FreeQ[a, lorentzdot];
fourderivative[a_ b_, c_] := b fourderivative[a, c] + a fourderivative[b, c];
fourderivative[lorentzdot[a_, b_]^c_, d_] :=
 c lorentzdot[a, b]^(c-1) fourderivative[lorentzdot[a, b], d]

fourderivative /:
 fourderivative[fourvector[p_, μ_], fourvector[q_, ν_]] := 0 /; p =!= q
fourderivative /: fourderivative[fourvector[p_, μ_], fourvector[q_, ν_]] :=
 metric[μ, ν] /; p == q
fourderivative /: fourderivative[lorentzdot[p_, q_], fourvector[k_, μ_]] := Which[
  SameQ[p, k] && SameQ[q, k], 2 fourvector[k, μ],
  SameQ[p, k] && UnsameQ[q, k], fourvector[q, μ],
  SameQ[q, k] && UnsameQ[p, k], fourvector[p, μ],
  UnsameQ[p, k] && UnsameQ[q, k], 0
 ]
```

Dirac Algebra

```
Clear[dirac, diracTrace, diracslash, tracer]
```

```
Format[dirac[γ[μ_]], TraditionalForm] := Subscript[γ, μ]
Format[dirac[γ[5]], TraditionalForm] := Subscript[γ, 5]
Format[dirac[1], TraditionalForm] := Subscript["I", 4]

dirac /: dirac[γ[μ_]] ** dirac[γ[5]] := -dirac[γ[5]] ** dirac[γ[μ]] /; μ =!= 5
dirac /: dirac[1] ** dirac[γ[μ_]] := dirac[γ[μ]]
dirac /: dirac[γ[μ_]] ** dirac[1] := dirac[γ[μ]]
dirac /: dirac[γ[5]] ** dirac[γ[5]] := dirac[1]

dirac[σ[μ_, ν_]] := I/2 dirac[γ[μ]] ** dirac[γ[ν]] - I/2 dirac[γ[ν]] ** dirac[γ[μ]];

tracer[NonCommutativeMultiply[]] = 4;
tracer[in_] := 0 /; (OddQ[Length[in]] == True || Length[in] == 0);
tracer[in : NonCommutativeMultiply[dirac[γ[_]] ..]] :=
 Expand[Sum[(-1)^n metricise[in[[1]], in[[n]]] *
    tracer[Delete[in, {{1}, {n}}]], {n, 2, Length[in]}]]
metricise[dirac[γ[μ_]], dirac[γ[ν_]]] := metric[μ, ν]

diracTrace[x_ + y_] := diracTrace[x] + diracTrace[y];

diracTrace[x_ y_] := Distribute[x diracTrace[y]] /; FreeQ[x, dirac]

diracTrace[x_] := Module[{tmp, out},
  tmp = Distribute[Numerator[x]];
  tmp = tracer[tmp];
  out = Distribute[tmp]/Denominator[x]
 ]

Unprotect[NonCommutativeMultiply];
NonCommutativeMultiply[x___, a_ b_, y___] :=
 a NonCommutativeMultiply[x, b, y] /; FreeQ[a, dirac]
NonCommutativeMultiply[a_, b_ + c_] :=
  NonCommutativeMultiply[a, b] + NonCommutativeMultiply[a, c];
NonCommutativeMultiply[a_ + b_, c_] :=
  NonCommutativeMultiply[a, c] + NonCommutativeMultiply[b, c];
Protect[NonCommutativeMultiply];

diracslash[fourvector[p_]] := Module[{μ = Unique["μ"]},
  fourvector[p, μ] dirac[γ[μ]]
 ]

transverseprojector = 1/(D - 1) (fourvector[q, μ] fourvector[q, ν]/lorentzdot[q, q] - metric[μ, ν]);

longitudinalprojector = fourvector[q, μ] fourvector[q, ν]/lorentzdot[q, q];
```

Momentum Space Propagators

Spin-0 Boson Propagator

```
Δ[k_, m_] := 1 / (lorentzdot[k, k] - m^2)
```

Spin-1 Boson Propagator

```
A[k_, m_, μ_, ν_] := -metric[μ, ν] Δ[k, m]
```

Fermion Propagator

```
s[k_, m_] := (diracslash[fourvector[k]] + m dirac[1]) / (lorentzdot[k, k] - m^2)

s[k_, m_, α_, β_] := delta[α, β] s[k, m];
```

Gluon Field Strength Propagator

```
d[k_, a_, b_, c_, d_] :=
 -1 / lorentzdot[k, k] Expand[(metric[b, d] fourvector[k, a] fourvector[k, c] -
     metric[b, c] fourvector[k, a] fourvector[k, d] - metric[a, d] fourvector[k, b]
      fourvector[k, c] + metric[a, c] fourvector[k, b] fourvector[k, d])]

d1[k_, a_, b_, c_] :=
 I / lorentzdot[k, k] Expand[fourvector[k, a] metric[b, c] - fourvector[k, b] metric[a, c]]

gluonTensorStructure1[a_, b_, c_, d_] :=
  metric[a, c] metric[b, d] - metric[a, d] metric[b, c];

gluonTensorStructure2[μ_, ν_, ω1_, ω2_, λ1_, λ2_] :=
 2 metric[μ, ν] (metric[ω1, λ1] metric[ω2, λ2] - metric[ω2, λ1] metric[ω1, λ2]) +
  metric[ν, λ2] (metric[ω1, λ1] metric[ω2, μ] - metric[ω2, λ1] metric[ω1, μ]) -
  metric[ν, λ1] (metric[ω1, λ2] metric[ω2, μ] - metric[ω2, λ2] metric[ω1, μ]) -
  3 / (D - 1) (metric[μ, λ2] (metric[ω1, λ1] metric[ω2, ν] - metric[ω2, λ1] metric[ω1, ν]) -
     metric[μ, λ1] (metric[ω1, λ2] metric[ω2, ν] - metric[ω2, λ2] metric[ω1, ν]))
```

```
gluonTensorStructure3[ω1_, ω2_, λ1_, λ2_, ξ1_, ξ2_] :=
 ((metric[ω1, λ1] metric[ω2, ξ1] metric[λ2, ξ2] -
      metric[ω2, λ1] metric[ω1, ξ1] metric[λ2, ξ2]) - (metric[ω1, λ2] metric[ω2, ξ1]
       metric[λ1, ξ2] - metric[ω2, λ2] metric[ω1, ξ1] metric[λ1, ξ2])) -
  ((metric[ω1, λ1] metric[ω2, ξ2] metric[λ2, ξ1] - metric[ω2, λ1] metric[ω1, ξ2]
       metric[λ2, ξ1]) - (metric[ω1, λ2] metric[ω2, ξ2] metric[λ1, ξ1] -
      metric[ω2, λ2] metric[ω1, ξ2] metric[λ1, ξ1]))

tensorStructure4[μ_, ν_, η_] :=
 dirac[γ[μ]] metric[ν, η] - dirac[γ[ν]] metric[μ, η] + I dirac[σ[μ, ν]] ** dirac[γ[η]]

dprime[p_, a_, b_, c_, e_, f_] := fourderivative[d[p, a, b, c, e], fourvector[p, f]]
```

TARCER Converter

```
Clear[momentumSearch, minElim, lineWeight, toTARCER]

<< tarcer06.mx

SetAttributes[lorentzdot, Orderless]

minElim[-x_] := x
minElim[x_] := x;

momentumSearch[Plus[lorentzdot[Plus[x_, u_.], Plus[y_, v_.]], _.]^-] :=
  DeleteCases[DeleteDuplicates[Map[minElim, {x, u, y, v}]], 0];

lineWeight[Plus[lorentzdot[z_, z_], m_.]^Y_-] := If[m === 0, {v, 0},
  {v, Simplify[Simplify[√(-m), -m > 0], Simplify[√(-m), -m > 0][[1]] > 0]} ]

toTARCER[x_ + y_, q_] := toTARCER[x, q] + toTARCER[y, q];
toTARCER[in_, q_] := Module[{total, lorentzFactors, preFactorList, preFactors,
    tmp, momentumList, internalMomentum1, internalMomentum2, tfiOut, lineFind},

   total = Apply[List, in];
   preFactorList = {};

   Do[
    tmp = total[[i]];
    If[
     MatchQ[tmp, Plus[lorentzdot[a_, b_], _.]^- /; ((a =!= q) || (b =!= q))] == False,
     AppendTo[preFactorList, tmp]
    ];,
    {i, 1, Length[total]}
   ];

   lorentzFactors =
    DeleteCases[total, x_ /; MatchQ[x, Plus[lorentzdot[_, _], _.]^-] == False];
   preFactors = Apply[Times, preFactorList];
   momentumList = DeleteCases[
     DeleteDuplicates[Flatten[Map[momentumSearch, lorentzFactors]]], q];

   lineFind[z_] :=
    If[FreeQ[Denominator[lorentzFactors], Plus[lorentzdot[z, z], _.]^-] == True,
     0,
     lineWeight[Denominator[lorentzFactors[[ Apply[Times, Flatten@Position[
           Denominator[lorentzFactors], Plus[lorentzdot[z, z], _.]^-, 1] ]  ]] ] ]
    ];

   Which[
```

```
  Length[momentumList] == 1,

  internalMomentum1 = momentumList[[1]];
  tfiOut = 1/((4 π)^(D/2) TAI[D, 0, {{1, M}}]) * TFI[D, lorentzdot[q, q],
     {Exponent[Numerator[in], lorentzdot[internalMomentum1, internalMomentum1]],
      0,
      Exponent[Numerator[in], lorentzdot[q, internalMomentum1]],
      0,
      0},
     {lineFind[internalMomentum1],
      {1, M},
      lineFind[internalMomentum1 - q] + lineFind[q - internalMomentum1],
      0,
      0}
    ];,

  Length[momentumList] == 2,

  internalMomentum1 = momentumList[[1]];
  internalMomentum2 = momentumList[[2]];
  tfiOut = 1/((4 π)^D) * TFI[D, lorentzdot[q, q],
     {Exponent[Numerator[in], lorentzdot[internalMomentum1, internalMomentum1]],
      Exponent[Numerator[in],
       lorentzdot[internalMomentum2, internalMomentum2]],
      Exponent[Numerator[in], lorentzdot[q, internalMomentum1]],
      Exponent[Numerator[in], lorentzdot[q, internalMomentum2]],
      Exponent[Numerator[in],
       lorentzdot[internalMomentum1, internalMomentum2]]},
     {lineFind[internalMomentum1],
      lineFind[internalMomentum2],
      lineFind[internalMomentum1 - q] + lineFind[q - internalMomentum1],
      lineFind[internalMomentum2 - q] + lineFind[q - internalMomentum2],
      lineFind[internalMomentum1 - internalMomentum2] +
       lineFind[internalMomentum2 - internalMomentum1]}
    ];
 ];
 preFactors * tfiOut
];
```